



Target Identification of anti-mycobacterial Substances

Dissertation zur Erlangung des Doktorgrades
Technischen Universität München
Fakultät für Chemie



Lehrstuhl für Organische Chemie II

von Johannes Lehmann
geboren am 25.09.1987
in Halle (Saale)



TECHNISCHE UNIVERSITÄT MÜNCHEN
FAKULTÄT CHEMIE
LEHRSTUHL FÜR ORGANISCHE CHEMIE II

Target Identification of anti-mycobacterial Substances

Johannes Lehmann

Vollständiger Abdruck der von der Fakultät für Chemie der Technischen Universität München zur Erlangung des akademischen Grades eines

Doktors der Naturwissenschaften (Dr. rer. nat)

genehmigten Dissertation.

Vorsitzender: Prof. Dr. Tobias A. M. Gulder
Prüfer der Dissertation: 1. Prof. Dr. Stephan A. Sieber
2. apl. Prof. Dr. Wolfgang Eisenreich

Die Dissertation wurde am 26.10.2016 bei der Technischen Universität München eingereicht und durch die Fakultät für Chemie am 24.11.2016 angenommen.

“An expert is someone who has made every possible mistake
that can be made in a very narrow field.”

~Niels Bohr

Danksagung

Zuallererst möchte ich bei meinem Mentor und Betreuer Prof. Dr. Stephan A. Sieber für die Aufnahme in seinen Arbeitskreis und die Bereitstellung von exzellenten Arbeitsbedingungen bedanken. Sowohl in der Wahl der Thematik, als auch in deren Bearbeitung wurde durch die interdisziplinäre Arbeitsweise einiges an Freiraum gewährt, das ich sehr zu schätzen weiß. Wir hatten viele tiefgehende und nachhaltige Diskussionen, wobei er trotz ausgebuchten Kalenders immer Zeit für mich hatte. Auch möchte ich mich für die Möglichkeit bedanken Teile dieser Arbeit in Boston an einem S3-Labor ausführen zu können.

Prof. Dr. Dr. Eric J. Rubin danke ich für die Aufnahme und Betreuung in seinem Labor während meiner Zeit in Boston an der Harvard School of Public Health. Ich schätze sein detailliertes Wissen im Bereich der Medizin und der Forschung an Tuberkulose, sowie seine offenerzige Art mit Menschen umzugehen.

Weiterer Dank gilt meinem langjährigen Mentor Dr. Rainer Martin, der sich immer Zeit für meine Anliegen genommen hat und mit wertvollen Tipps und Ideen an meiner Seite stand, vor allem wenn Dinge nicht liefen wie sie sollten.

Ich möchte dem Prüfungskomitee danken, sich die Zeit für meine Arbeit zu nehmen und meine Prüfung zu evaluieren.

Wenn es um Angelegenheiten im Labor geht, kann ich mir niemand besseren vorstellen als Frau Mona Wolff und Frau Katja Bäuml, die mit einer Hingabe und einem Einsatz arbeiten, der seinesgleichen sucht. Die Unterstützung im alltäglichen Laborchaos war eine unverzichtbare Hilfe!

Ich möchte all meinen Kollegen, sowohl den jetzigen Doktoranten des AK Sieber und der Rubingruppe, sowie den ehemaligen Mitarbeitern, danken für eine unvergleichliche Arbeitsatmosphäre über die fast vier Jahre hinweg. Mit euch habe ich die glücklichsten und die schwierigsten Situationen gemeistert, während der Arbeitszeit und auch im Privatleben.

Des Weiteren möchte ich mich bei all meinen Praktikanten bedanken für die Arbeit, die für mich erledigt wurde. Ich hoffe, ich konnte euch etwas mitgeben.

Letztendlich danke ich meinen Freunden und meiner Familie für die langjährige Unterstützung in einer nicht immer einfachen Zeit. Ganz besonders möchte ich meine Frau hervorheben, weil du mit mir alle Höhen und Tiefen teilst.

Introductory Remarks

This doctoral dissertation was carried out between December 2012 and October 2016 under supervision of Prof. Dr. Stephan A. Sieber at the Chair of Organic Chemistry II of the Technische Universität München. Parts of the accomplished work have been carried out between January 2016 and June 2016 under supervision of Prof. Dr. Dr. Eric J. Rubin at the Department of Immunology and Infectious Diseases of the Harvard School of Public Health.

Parts of this thesis are based on the following publications and manuscripts in preparation for publication:

Chapter 1

“Making a Long Journey Short: Alkyne Functionalization of Natural Product Scaffolds.”

Lehmann J, Wright MH, Sieber SA.

Chem. Eur. J., **2016**, *22*, 4666. (Concept)

Chapter 2

“Synthesis of Ramariolide Natural Products and Discovery of their Targets in Mycobacteria”

Lehmann J, Richers J, Pöthig A, Sieber SA.

Chem. Comm., **2016**, *submitted* (Communication)

Chapter 4

“Human lysosomal acid lipase inhibitor Ialostatat impairs *Mycobacterium tuberculosis* growth by targeting bacterial hydrolases”

Lehmann J, Vomacka J, Esser K, Nodwell M, Kolbe K, Rämmer P, Protzer U, Reiling N, Sieber SA.

Med. Chem. Comm., **2016**, *7*, 1797. (Communication)

“Means and Methods for Treating Mycobacterial Diseases”

Esser K, Vomacka J, **Lehmann J**, Nodwell M, Kolbe K, Rämmer P, Protzer U, Reiling N, Sieber SA.

European Patent Application, **2016**, EP16169499.7. (Patent)

Summary

Mycobacteria present a unique class of Gram-positive prokaryotes bearing an exclusive outer membrane. Their existence on this planet is dated far longer than most other bacterial species. Surviving for eons mycobacteria can be considered as bacterial reptiles, and just like those mycobacteria are slow in terms of motility, growth and cellular division. Taking this analogy to the next level, just like reptiles they comprise a very thick “skin” made up of special lipids only found amongst Actinobacteria. They outlived ice ages and dinosaurs and might as well withstand global warming and mankind. Still, some species present a major threat for dangerous infections. *Mycobacterium tuberculosis*, *leprae* and *avium* are the causes of infectious diseases as tuberculosis, leprosy and others. Considering modern times access to antibiotics is available to almost everyone and almost every sickness is curable, the fact that one third of the world’s population is latently infected with tuberculosis is frightening. And it gets worse: The improper use of antibiotics in agriculture and public health leads to a significant increase of (multidrug-) resistance. The number of multidrug-resistant tuberculosis (MDR-TB) is estimated around half a million incidents annually. Taking a look at treatment options is also alarming. Currently tuberculosis is medicated by the combination of four different antibiotics, of which the latest dates from the 1960’s. In the past four decades only a single drug for tuberculosis indication was marketed, predominantly due to the impermeability of mycobacterial cell walls.

With these facts in mind it is time for a change. Natural products comprise an enormous potential for antibacterial substances and serve as drug leads. New structural features have to be explored in order to find novel treatment strategies. The recent discovery of teixobactin is an excellent example for circumvent resistance. In order to take the long way of pharmaceutical research and clinical trials it is necessary to determine cellular targets of small molecules. Activity-based protein profiling (ABPP) is a mature technique to find protein targets reliably. The work presented here focuses on various kinds of novel molecular features based on and inspired by natural products with anti-mycobacterial activity. ABPP is used to reveal their protein targets as well as new pathways to interfere with. Interestingly, disruption of mycobacterial lipid metabolism could be shown as a successful tool to contain cellular growth.

Zusammenfassung

Mykobakterien stellen, durch ihre besondere Außenmembran, eine einzigartige Klasse an Gram-positiven Prokaryoten dar, deren Existenz auf diesem Planeten weit länger andauert, als von vielen anderen Bakterienarten. Dass sie bereits mehrere Erdzeitalter durchlebt haben legt den Vergleich zu Reptilien nahe, denn genauso wie sie bewegen, wachsen und reproduzieren sie sich langsam. Will man diese Analogie auf die Spitze treiben, vergleicht man die dicke Haut von Reptilien mit der enorm hydrophoben Zellwand der Actinobakterien. Diese haben bereits Eiszeiten und die Dinosaurier überlebt und werden wohl auch die Erderwärmung und eventuell die menschliche Rasse überdauern. Dennoch stellen einige Spezies eine enorme Gefahr durch Infektionen dar. *Mycobacterium tuberculosis*, *leprae* und *avium* sind die Erreger von Tuberkulose, Lepra und anderen Infektionskrankheiten. Bedenkt man, dass in der heutigen Zeit Antibiotika überall und für fast jeden verfügbar sind und damit fast jede Krankheit behandelbar, macht es einem Angst, dass ein Drittel der Weltbevölkerung an latenter Tuberkulose leidet. Aber es kommt noch schlimmer: Der unsachgemäße Einsatz von Antibiotika in der Landwirtschaft und im Gesundheitswesen führen zum stetigen Wachstum von (Multi-)Resistenzen. Die Zahl der Multiresistenten Tuberkuloseinfektionen wird jährlich auf ca. eine halbe Million Fälle gerechnet. Auch ein Blick auf die Behandlungsmöglichkeiten sind alarmierend: So wird Tuberkulose derzeit durch den teilweise gleichzeitigen Einsatz von vier Antibiotika behandelt, von denen das neuste aus den 1960er Jahren stammt. In den letzten vier Jahrzehnten wurde genau ein Tuberkulosemedikament zugelassen, was vor allem an der undurchlässigen Zellmembran liegt.

Aufgrund dieser Tatsachen muss etwas passieren. Naturstoffe tragen ein enormes Potenzial für antibakterielle Substanzen und dienen häufig als Vorläufer von Medikamenten. Neuartige Strukturen müssen gefunden werden um neue Behandlungsstrategien zu entwickeln. Die kürzliche Entdeckung von Teixobactin ist ein herausragendes Beispiel, um Resistenzen zu trotzen. Um den schweren Weg pharmazeutischer Forschung und klinischer Studien zu gehen, ist es nötig die zellulären Ziele der Moleküle zu kennen. Aktivitätsbasierte proteomische Studien sind eine ausgereifte Methode um proteinogene Ziele zu identifizieren. Diese Arbeit beschäftigt sich mit verschiedenen neuartigen Strukturen auf der Basis von oder inspiriert durch Naturstoffe. Es werden neue zelluläre Ziele und Stoffwechselwege gefunden, die als Anhaltspunkt zur Tuberkulosebekämpfung dienlich sein können. Interessanter Weise kann die Störung der mykobakteriellen Fettsäuresynthese ein aufs andere Mal erfolgreich als Wachstumsinhibitor gezeigt werden.

List of Abbreviations

ABPP	Activity-based protein profiling	EDCI	1-Ethyl-3-(3-dimethylamino-4-propyl)carbodiimide
Ac	Acyl	EDTA	Ethylenediaminetetra-acetic acid
ACN	Acetonitrile	ee	Enantiomeric excess
Ag85	Antigen 85	eq	Equivalent
Ala	Alanine	ESI	Electrospray ionization
Amp	Ampicillin	Et	Ethyl
Asc	Ascorbate	g	Gram
Boc	<i>tert</i> -Butoxycarbonyl	H	Hexane
bp	Basepairs	h	Hour
br	Broad	HEPES	4-(2-Hydroxyethyl)-1-piperazine-ethanesulfonic acid
BSA	Bovine Serum Albumin	HMBC	Heteronuclear multiple-bond correlation spectroscopy
Bt	Benzotriazole	HPLC	High Performance Liquid Chromatography
Bu	Butyl	HSQC	Heteronuclear single-quantum correlation spectroscopy
calc.	Calculated	Hz	Hertz
CoA	Coenzyme A	IAA	2-Iodacetamide
COSY	Correlation spectroscopy	<i>i</i> -Pr	<i>iso</i> -Propyl
CSA	Camphorsulfonic acid	IPTG	Isopropyl β -D-1-thiogalactopyranoside
Cys	Cysteine	L	Liter
d	Doublet	LDA	Lithium diisopropylamide
Da	Dalton (g/mole)	M	Molar
DIPEA	Diisopropylamine	m	Multiplett
DIPT	Diisopropyl tartrate	<i>m</i> -CPBA	<i>meta</i> -Chloroperoxy-benzoic acid
DMAP	<i>N,N</i> -Dimethylaminopyridine	Me	Methyl
DMDO	Dimethyldioxirane	MIC	Minimal inhibitory concentration
DMF	<i>N,N</i> -Dimethylformamide	min	Minutes
DMP	Dess-Martin Periodane		
DMSO	Dimethylsulfoxide		
DNA	Deoxynucleic acid		
dNTP	Deoxyribonucleotide triphosphate		
dr	Diastereomeric ratio		
DTT	Dithiothreitol		
e.g.	Exempli gratia		

Msmeg	<i>Mycobacterium smegmatis</i>	rt	Room temperature
Mtb	<i>Mycobacterium tuberculosis</i>	s	Singulett
MW	Molecular Weight	SDS	Sodium Dodecyl Sulfate
NADH	Nicotinamide adenine dinucleotide	sec	Seconds
NMR	Nuclear Magnetic Resonance	t	Triplett
		TAMRA	Carboxy-tetramethyl-rhodamine
NOESY	Nuclear Overhasuer effect spectroscopy	TBTA	Tris-(5-benzyl-1H-triazole-4-yl)-methanamine
PAGE	Polyacrylamide gel electrophoresis	TCEP	Tris-(2-carboxyethyl)phosphine
Ph	Phenyl	TFA	Triflouroacetic acid
Pks	Polyketide synthase	THF	Tetrahydrofuran
q	Quartett	TLC	Thin-layer Chromatography
Rh	Rhodamine	TMS	Trimethylsilane
RP	Reverse Phase	Vol	Volume
<i>t</i> -Bu	<i>tert</i> -Butyl		

Table of Contents

CHAPTER 1 INTRODUCTION	1
1.1 MYCOBACTERIA	1
1.2 MYCOBACTERIAL MEMBRANE STRUCTURE	2
1.3 NATURAL PRODUCTS AS LEADS FOR DRUG DESIGN.....	4
1.4 ACTIVITY-BASED PROTEIN PROFILING	6
1.5 OBJECTIVE	9
CHAPTER 2 RAMARIOLIDES	11
2.1 BACKGROUND AND SYNTHETIC ANALYSIS.....	11
2.2 SYNTHESIS OF RAMARIOLIDES A-D	11
2.3 BIOACTIVE RAMARIOLIDE ABPP PROBES FOR TARGET IDENTIFICATION.....	18
2.4 PROTEOME ANALYSIS AND TARGET VALIDATION	20
2.5 CONCLUSION	24
CHAPTER 3 MYCOBACTERIAL TARGETS OF β-LACTONES	25
3.1 β -LACTONES IN NATURAL PRODUCTS AS ENZYME INHIBITORS.....	25
3.2 MYCOBACTERIAL TARGETS OF EZ120.....	27
3.3 TARGET VALIDATION OF PKS13.....	29
3.4 TARGET VALIDATION OF AG85-FAMILY.....	32
3.5 EFFECT OF EZ120 ON MYCOLIC ACID SYNTHESIS.....	34
3.6 CONCLUSION	37
CHAPTER 4 LALISTAT	38
4.1 LIPID METABOLISM IN MYCOBACTERIA.....	38
4.2 MYCOBACTERIAL HYDROLASES	38
4.3 SYNTHESIS OF LALISTAT AND ABPP PROBE.....	41
4.4 BIOACTIVITY	42
4.5 TARGET IDENTIFICATION.....	44
4.6 TARGET VALIDATION.....	47
4.7 CONCLUSION	47
CHAPTER 5 EXPERIMENTAL SECTION	48
5.1 ORGANIC CHEMISTRY	48
5.1.1 <i>General Methods and Material</i>	48
5.1.2 <i>Synthesis</i>	50
5.1.2.1 General procedure for α -bromo ketones ^{85, 86}	50
5.1.2.2 General procedure for 5-(2-Oxododecylidene)furan-2(5H)-ones ^{79, 87, 89}	51
5.1.2.3 General procedure for 5-(2-Hydroxydodecylidene)furan-2(5H)-ones ⁹⁰	53
5.1.2.4 General procedure for 1-Hydroxyundecyl)-1,4-dioxaspiro[2.4]hept-6-en-5-ones ^{91, 92}	55
5.1.2.5 (2S*,3R*)-2-((R*)-1-Hydroxyundecyl)-1,4-dioxaspiro[2.4]hept-6-en-5-one (2.9)	57
5.1.2.6 General procedure for (S)-1-((2S,3S)-5-Oxo-1,4-dioxaspiro[2.4.]hept-6-en-2-yl)undecyloates ⁷⁹	57
5.1.2.7 (2S*,3R*)-2-Undecanoyl-1,4-dioxaspiro[2.4]hept-6-en-5-one (2.21)	59
5.1.2.8 (2S*,3R*)-2-((S*)-1-Hydroxyundecyl)-1,4-dioxaspiro[2.4]hept-6-en-5-one (2.11) ⁹⁵	59
5.1.2.9 (\pm)-Ramariolide B (2.2) ⁹⁴	60
5.1.2.10 4-(N,N-Dimethylamino)-N'-(6-hydroxyhexyl)benzamide.....	61
5.1.2.11 4-(N,N-Dimethylamino)-N'-(6-oxohexyl)benzamide	61
5.1.2.12 General procedure for S-(Pyridin-2-yl) thiolates.....	62
5.1.2.13 General procedure for (3R*,4R*) oxetan-2-ones ¹¹⁶	63
5.1.2.14 3-Piperidinyl-4-chloro-1,2,5-thiadiazol.....	65
5.1.2.15 3-Hydroxy-4-piperidinyl-1,2,5-thiadiazole (4.4) ¹²⁷	65
5.1.2.16 Lalistat (La-0)(4.1) ¹²⁷	66

5.1.2.17	tert-Butyl 4-ethynylpiperidine-1-carboxylate ¹⁵⁶	66
5.1.2.18	4-Ethynylpiperidine (4.6) ¹⁵⁶	67
5.1.2.19	4-(Piperidin-1-yl)-1,2,5-thiadiazol-3-yl 4-ethynylpiperidine-1-carboxylate (4.2)	67
5.2	BIOCHEMISTRY	69
5.2.1	<i>Microbiology</i>	69
5.2.1.1	Material	69
5.2.1.1.1	Bacteria	69
5.2.1.1.2	Media	69
5.2.1.2	Methods	70
5.2.1.2.1	Over-night cultures	70
5.2.1.2.2	Cryostocks	70
5.2.1.2.3	Competent cells	71
5.2.1.2.4	Minimal Inhibitory Concentration (MIC) Assay	71
5.2.1.2.5	FICI determination	72
5.2.1.2.6	Analysis of mycobacterial lipids	72
5.2.1.2.7	Mycobacterium tuberculosis Growth Analysis	72
5.2.1.2.8	Analysis of M. tuberculosis growth in human macrophages	72
5.2.2	<i>Genomics</i>	74
5.2.2.1	Materials	74
5.2.2.1.1	Buffers	74
5.2.2.1.2	Plasmids	74
5.2.2.1.3	Primers	74
5.2.2.2	Methods	75
5.2.2.2.1	Extraction of DNA	75
5.2.2.2.2	Polymerase Chain Reaction (PCR)	75
5.2.2.2.3	Agarose gel electrophoresis	77
5.2.2.2.4	Gateway Cloning	77
5.2.2.2.5	Transformation.....	78
5.2.3	<i>Proteomics</i>	79
5.2.3.1	Material	79
5.2.3.1.1	Buffers	79
5.2.3.2	Methods	80
5.2.3.2.1	Activity based protein profiling (ABPP)	80
5.2.3.2.2	SDS-Polyacrylamide gel electrophoresis (SDS-PAGE)	82
5.2.3.2.3	In-gel digest	82
5.2.3.2.4	Gel free protein profiling	83
5.2.3.2.5	Column-based dimethyl labeling.....	83
5.2.3.2.6	Sample preparation and statistical evaluation	84
5.2.3.2.7	Overexpression and purification of recombinant proteins	85
5.2.3.2.8	In-situ labeling	85
5.2.3.2.9	Western Blot	86
CHAPTER 6	APPENDIX	87
CHAPTER 7	REFERENCES	89

Chapter 1 Introduction

1.1 Mycobacteria

The class of Actinobacteria includes Corynebacteria and Mycobacteria hallmarked by a unique membrane structure (as described in 1.2.), which leads to the development of special characteristics for these prokaryotes.¹ The incorporation of branched long-chain fatty acids, so-called mycolic acids, besides usual triacylglycerides creates an almost impermeable surface.² These lipids are unique for Actinobacteria and associated for pathology, forming the most outer layer of the bacterial membrane creating extensions (cord-factor) comparable to molds when grown on solid medium, which led to the Greek prefix *myco-* meaning “fungus”.^{3, 4} Mycobacteria are characteristically Gram-positive, aerobic bacteria with a long doubling time compared to other bacterial species.⁵ Generally mycobacteria can give rise to severe infections in humans and other animals. The complex of *M. tuberculosis* (Mtb), *M. africanum*, *M. microti* and *M. bovis* causes tuberculosis.⁶ Infection with *M. leprae* can lead to Hansen’s disease (leprosy) and also *M. avium* presents a major threat to immunocompromised humans.

Robert Koch was the first person to isolate a culture of Mtb and to characterize it as the etiologic agent of tuberculosis in 1882.⁷ Nowadays, it is still responsible for the largest number of tuberculosis infections, causing over 1.5 million deadly incidences and almost 10 million newly reported cases annually.⁸ Being spread by aerosols, it enters human macrophages in the respiratory tract and withstands the immune response by hiding intracellularly. After infection Mtb is difficult to treat using standard antibiotics as these bacteria are able to switch between an active (reproductive) and a latent (steady) state inside the host. In latent stage key metabolic processes are reduced to a minimum rendering most anti-tuberculosis agents ineffective.⁹ Bacteria are able to survive within the host for years and become prevalent upon immune deficiency (i.e. HIV-infection). Current treatment involves a combination of four different antibiotics, namely isoniazid, rifampicin, ethambutol and pyrazinamide, over a period of six months. Only a few second-line drugs are available (Table 1.1). Unfortunately, the number of (multidrug)-resistant tuberculosis (MDR-TB) is steadily rising¹⁰ and novel drugs rarely pass clinical phases causing a need for new pharmaceutical compounds, therapeutic strategies and cellular targets.¹¹ With a timely gap of more than 40 years the latest approved drug selectively targeting tuberculosis is bedaquiline, a diarylquinoline inhibiting the F_1F_0 -ATPase.^{12, 13} Efforts to develop anti mycobacterial compounds are additionally challenged by the uptake of small molecules being able to cross the highly hydrophobic mycomembrane and still act at their designated target.^{14, 15}

Table 1.1: First- and second-line drugs used against tuberculosis.

	Drug (year discovered)	Mechanism of Action
First-Line Drugs	Isoniazid (1952)	Inhibition of mycolic acid synthesis
	Rifampicin (1966)	Inhibition of RNA synthesis
	Pyrazinamide (1952)	Inhibition of fatty acid synthesis
	Ethambutol (1961)	Inhibition of arabinogalactan synthesis
	Bedaquiline (2004)	Inhibition of the F ₁ F ₀ -ATPase
Second-Line Drugs	Streptomycin (1944)	Inhibition of protein synthesis
	Kanamycin (1957)	Inhibition of protein synthesis
	Capreomycin (1960)	Inhibition of protein synthesis
	Quinolones (1963)	Inhibition of DNA gyrase
	Ethionamide (1956)	Inhibition of mycolic acid synthesis
	p-Aminosalicylat (1946)	Inhibition of folic acid and iron metabolism

As working with virulent Mtb is more dangerous than using other (opportunistic)-pathogens and more time intensive due to its long doubling time *Mycobacterium smegmatis* (Msmeg) is commonly used as a model organism.¹⁶ Both strains possess high DNA-sequence identity as well as high amino acid similarity. Msmeg is a non-toxic, fast growing bacterium (doubling time ~3h) that displays similar microbial features to Mtb in terms of cell wall permeability, protein expression and growth conditions.¹⁷ General screens can be performed in Msmeg and transferred to Mtb.

1.2 Mycobacterial membrane structure

One of the major difficulties to treat mycobacterial infections is their unusual cellular envelope composition. The typical motive of Gram-positive bacteria is an enclosed cytosolic compartment surrounded by a lipid bilayer mainly consisting of triacylglycerides (TAGs). Attached to this membrane are multiple layers of peptidoglycan (murein), a polymer of sugars interconnected by amino acids. Mycobacteria share these structural features despite differing in their interconnectivity of the peptidoglycan to other bacteria.¹⁸ Furthermore a second polymer consisting of arabinose- and galactose-sugars, the arabinogalactan layer (AG), is attached on top. The outer surface of the AG is covalently linked to mycobacterial fatty acids (mycolic acids), which form a second membrane together with glycolipids (cord-factor) around the bacterium for protection from environmental influences.^{1, 19}

Mycolic acids are exclusively found in Actinobacteria. They present an essential feature for bacterial survival and pathogenesis.²⁰ In contrast to TAGs, which are generally used to assemble biological membranes, mycolic acids are branched long chain β -hydroxy fatty acids.²¹ Their structure consists of an α -chain with 24 to 26 carbon atoms and a mero-chain of up to 60 carbons making them significantly more hydrophobic than other lipids. Each

chain is synthesized individually starting with acetyl-coenzyme A (Ac-CoA) using fatty acid synthase complexes (FAS) to perform chain elongation (Fig. 1.1).²² The α -branch commonly consists of a completely saturated carbon chain only carboxylated in α -position prior to condensation of chains to present a strong nucleophile. In comparison mero-chains usually possess several different modifications like unsaturations, vinylic substitution or cyclopropylation that influence their “secondary structure” (Appendix Fig. 6.1).²³ Especially chain length and the kind of modification within the mero-chain are specific to each bacterial species. Finally processed mero-chain molecules are activated as adenosine mono phosphate (AMP) esters and serve as electrophiles in a hetero-*Claisen* condensation. This reaction is catalyzed by the polyketide synthase 13 (PKS13), a multi-domain enzyme that binds both substrates, performs activation and fusion of the mycolic acid and finally releases the product, β -oxo-mycolic acid.²⁴

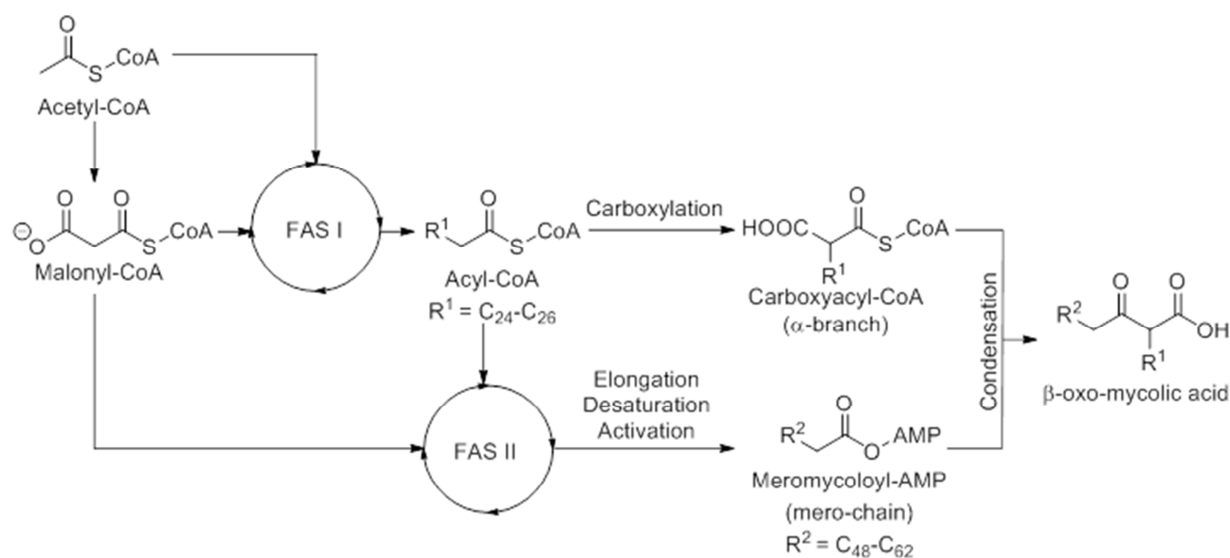


Fig. 1.1: Biosynthesis of immature mycolic acids. CoA: Coenzyme A. FAS: fatty acid synthase.

After trehalose is transferred onto the β -oxo-mycolic acid *via* esterification of one of its primary alcohol functions to form trehalose monomycolate (TMM), further reduction to the β -hydroxy acid is performed by the dehydrogenase CmrA²⁵ and the mature glycolipid is shuttled across the inner cell membrane by an ABC transporter MmpL3 (Fig. 1.2).²⁶ Trehalose has been shown to be essential for mycolic acid transfer regardless of its oxidation state, making it a substantial metabolite of mycobacterial persistence.²⁷ Once a TMM molecule has entered the periplasmic space it cannot be transported back into the cytosol. Instead it is either transferred onto AG and therefore covalently attached to the cell wall or the mycolic acid residue of one TMM molecule is transferred onto the free primary alcohol of a sugar, glucose or TMM to form glucose monomycolate (GMM) or trehalose dimycolate (TDM), respectively. All of these processes are catalyzed by a group of orthologous serine-

hydrolases, Antigen85 A/B/C (Ag85A/B/C).²⁸ TMM, GMM and TDM are incorporated into the outer cell membrane to form a bilayer with AG-linked lipids (Fig. 1.2). As they are attached by hydrophobic interactions it is possible to move within the membrane and to extract these lipids from the cell without disrupting its integrity.²⁹

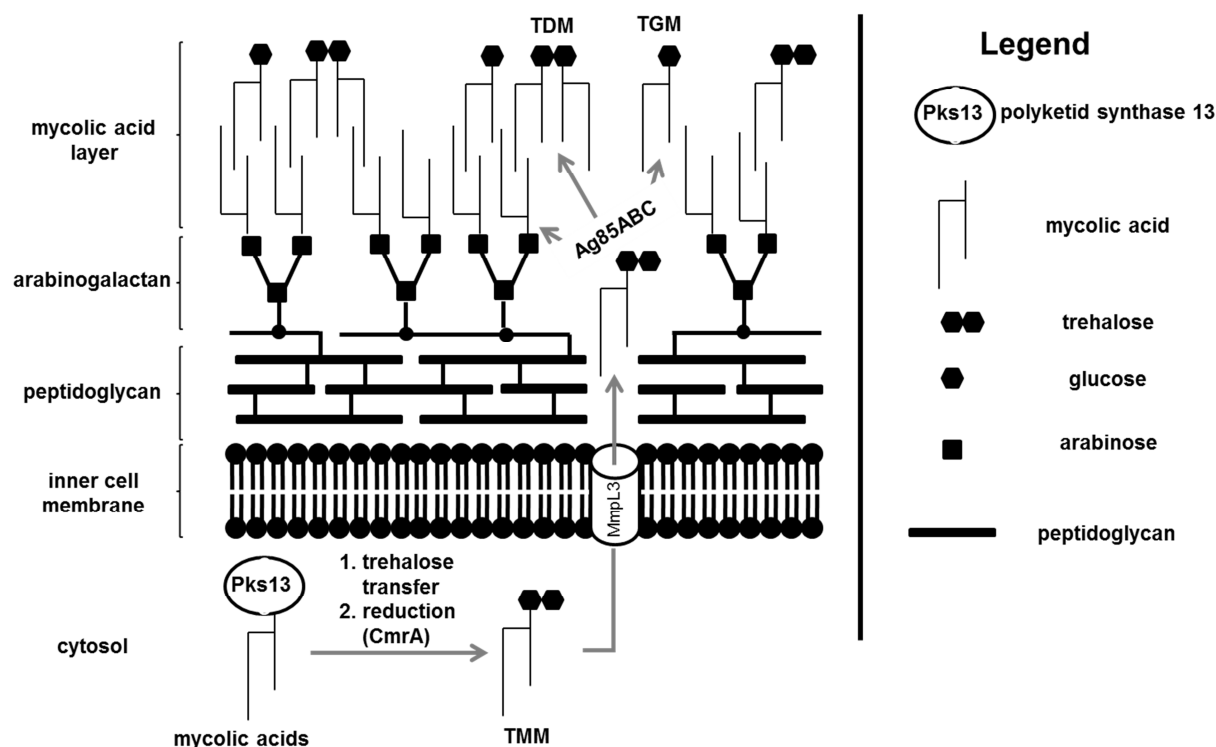


Fig. 1.2: Schematic representation of mycobacterial cell wall components. Mycolic acids are matured in the cytosol to TMM, transported in the periplasm to be transferred onto various acceptor substrates and incorporated in the mycomembrane.

1.3 Natural products as leads for drug design

Natural products present a major class of biologically active molecules. In general they are secondary metabolites of pro- and eukaryotes serving different purposes, like defense of enemies or attraction of mating partners as well as for establishment in their ecological niche. Due to their high activity and specificity they are widely used as starting points for the development of novel drugs.³⁰ The on-going research of newly identified and synthetically accessible molecules increases the structural diversity in this field and helps to fill the gap in chemical space to address new molecular targets.

Due to their co-evolution with cellular systems, natural products possess advantages in their physico-chemical properties distinguishing them from libraries of synthetic compounds.³¹ Addressing a variety of targets, natural products are valued inspirations for lead compounds in pharmaceutical research.³² The empirically found rule of five, stated by Lipinski and co-workers after analysis of thousands of drug structures, set a frame to physico-chemical properties of bioactive small molecules.³³ These rules specify a compound

to be of less than 500 Da molecular weight, its lipophilicity by the logarithmic partition coefficient between water and 1-octanol of less than five, the number of hydrogen donors of less than five and the number of hydrogen acceptors of less than ten, though one rule may be excluded.³³ This rule is further restricted to orally available molecules.

Bioactive natural products can be distinguished into two major groups by their way of binding to cellular interactors (mostly proteins). They can either bind non-covalently to an active- or allosteric site to inhibit or enhance its molecular function while the respective residence time in its binding pocket is defined by its affinity. Otherwise they bear an intrinsic reactivity and bind in a covalent manner forming a chemical bond between the small molecule and the binding partner. In case of the latter an electrophilic core of the natural product is required as proteins usually display (activated) amino acid nucleophiles in their structure. In fact about 30 % of marketed drugs interact covalently with their target molecules as part of their mode of action.^{34, 35}

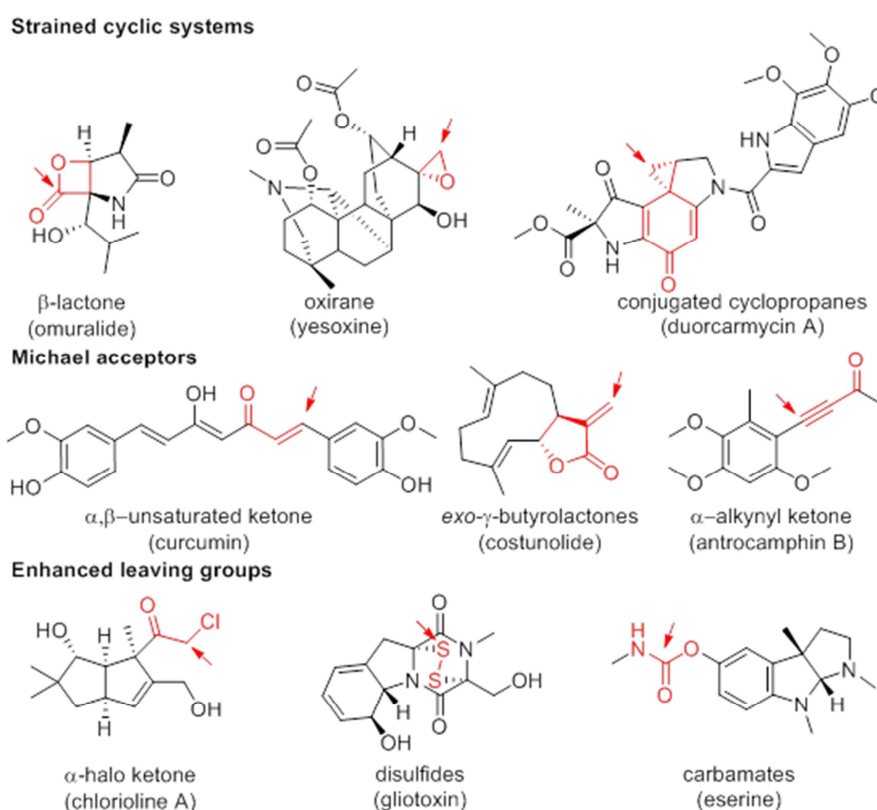


Fig. 1.3: Classes of electrophilic natural products. Electrophilic centers are highlighted in red. Arrows indicate site of nucleophilic attack.

Presented electrophiles in natural product scaffolds can be grouped by the following classes: strained cyclic systems, Michael-acceptors and enhanced leaving groups, (Fig 1.3); red arrows indicate the site of reactivity.³⁶ In case of strained cyclic systems three- and four-membered rings display a high reactivity towards nucleophiles as the free energy gain of ring opening is the major driving force enabling this irreversible reaction. An intermolecular

reaction can be further enhanced if the obtained product displays a more conjugated system. Michael-acceptors are found in various decorations of substituents primarily for steric interactions. The type of acceptor group regulates electronic features and promotes reactivity. In general Michael-acceptors present soft electrophiles often cross-reacting with thiol nucleophiles. Finally, enhanced leaving groups can be found in a broad class of intrinsically reactive natural products. Their activation can be due to various functionalities, i.e. α -halo ketones, intramolecular disulfide bonds or carbamate residues, which leads to a promiscuous biomolecule reactivity.

Not only natural products themselves but also their derivatives and precursors are of particular interest for pharmaceutical studies. In certain cases inverting the stereochemistry of a natural product by using its enantiomer can boost its potency or lead to a loss of function.³⁷ Utilizing total synthesis approaches gives access to individual building blocks of natural products and can therefore provide functional information for the parent molecule and its mode of action.³⁸ For example, the group of Romo and co-workers has shown how certain core structures of the natural products salinosporamide A and angelastatin A are essential for the overall activity of the compound and provide derivatives with enhanced biological activity.^{39, 40} However, accessing derivatives of natural products by total synthesis can be very time intensive and resource consuming. An alternative approach is suggested by so-called mutasynthesis.⁴¹⁻⁴³ Instead of isolation of a natural product by its original organism, specific genes essential for biosynthesis are knocked out and respectively derivatized precursors are fed to enable the synthesis of an altered product. This methodology can also be coupled to semisynthesis, i.e. incorporation of halogenated aromatic compounds can be followed by cross-coupling of various residues after isolation. A different strategy to access novel natural products or derivatives of known molecules is to activate, silence or selectively enhance gene expression of proteins involved in biosynthesis. This methodology named "Genome mining" has been shown to produce numerous unknown natural products including scaffolds with antibiotic activity.^{44, 45}

1.4 Activity-based protein profiling

Identifying cellular targets of a natural product is a field of interdisciplinary research. It requires the employment of techniques such as phenotypic screening, fluorescence microscopy, proteomics and more.^{46, 47} Recently established procedures use parent compound based small probes to isolate and identify biological interaction partners. A commonly used technique for selective target identification presents affinity chromatography.^{48, 49} It requires the initial covalent attachment of a molecule onto a solid support, while a mobile phase containing possible interactors is passed over it. In case of target recognition interaction partners are retained and other molecules are rapidly eluted enabling fast and broad screening, i.e. cell lysates. However, the use of cellular lysates

displays immediate drawbacks: the creation of an artificial environment might lead to false positive hits. Furthermore, the lack of a covalent bond between the interaction partners requires a tight binding with high affinity to isolate hits. Finally, the level of structural perturbation to the derivatized small molecular probe during attachment to the solid support is quite high; especially if it is unknown which part of the molecule is responsible for the biological interaction and molecular function.

Alternative methods aim to use a soluble molecular interacting probe in a less artificial manner. Activity-based protein profiling presents such an alternative as a mature technique to identify proteinogenic interactors.⁵⁰⁻⁵⁴ Especially the ability to utilize these probe molecules in living organisms and perform in-situ labeling experiments provides a huge advantage over other methods. Still, parent molecules must be derivatized to allow pull-down of interacting targets. Equipment of compounds with a small tag provides a handle for further derivatization of the probe-interactor complex. The general structure of such probes follows a strict pattern, consisting of three essential elements: active core, spacer and tag. The active core is the part of the parent molecule that interacts with biological targets either by intrinsic reactivity or affinity-based binding. It should stay unmodified and the spacer should be attached furthest away from that site. The spacer presents a molecular string connecting the functional core and its tag. It serves the purpose to access the bio-orthogonal tag after probe recognition by a much bigger biomolecule. Finally the tag is a functional group of discrete reactivity under a broad range of reaction conditions, i.e. solvent, temperature, pH or additives.

Pioneering work in the field of such reaction conditions, also referred to as bio-orthogonal, was the development of the Staudinger ligation by Saxon and Bertozzi.⁵⁵ Here, an aza-ylid is generated by modification of the *Staudinger* reaction of a phosphine and an azide, yielding a stable amid linkage.⁵⁶ Since this initial work, the number of new developed bio-orthogonal reactions has readily increased with various modifications to classical procedures.⁵⁷⁻⁵⁹ Most attractive is the cycloaddition of an azide and an alkyne, formerly described by Huisgen in the 1960s and revisited by Sharpless and Meldal in 2002.⁶⁰⁻⁶³ By addition of a ligand-bound copper(I) catalyst the reaction (CuAAC) is mediated to form the triazole at room temperature in water (Fig. 1.4). This type of reaction is also referred to as Click-chemistry and is widely used in the field of biological chemistry as both tags are amongst the smallest possible, the reaction proceeds fast (reaction time < 1h), both tags are rarely found in biological systems and even react in buffers with high salt content. While azides are more and more commercially found in functionalization reagents, a preference to place the alkyne tag onto the molecule of interest has emerged.⁶⁴

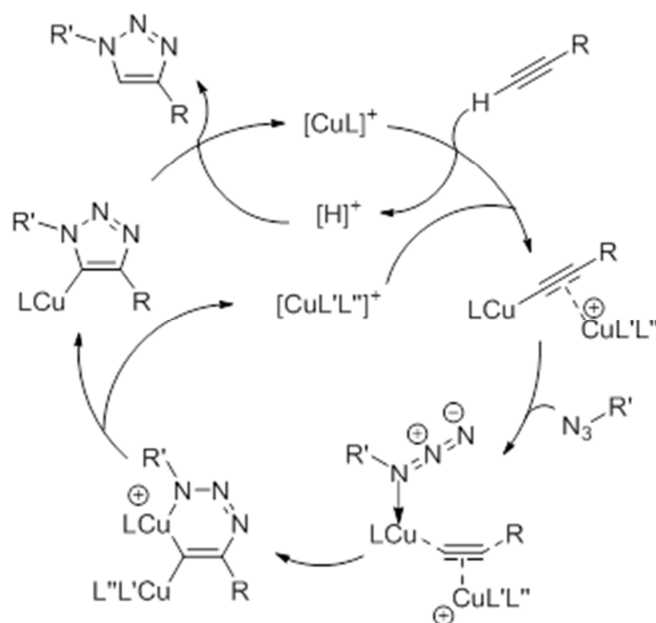


Fig. 1.4: Proposed molecular mechanism of copper(I) mediated cycloaddition of 1,2,3-triazoles from azides and terminal alkynes.

Unfortunately, incorporation of alkyne tags into natural products is not necessary trivial. Although terminal alkynes likely mimic residual methyl groups their incorporation and synthetic behavior is hindered by altered electronic features and reactivity. Desirably, the alkyne is positioned at the end of an alkyl-chain within the molecule, which usually requires a re-synthesis of the backbone structure as well as alkyne orthogonal chemistry or additional protection groups.⁶⁵⁻⁶⁸ Alternatively, one applies a masked alkyne synthesis strategy, i.e. utilizing/introducing a primary alcohol function, which is at a late stage of the synthesis oxidized to the respective aldehyde and further homologized into the alkyne.⁶⁹⁻⁷¹ Both models incorporate several synthetic steps with unknown outcome making the semisynthesis of an already existing natural product an attractive alternative, which is indeed applied in most cases. Therefore, functional groups of the natural product (i.e. alcohols, amines) are used to introduce alkyne tagged linkers.⁷²⁻⁷⁶

In doubt about the mode of action incorporation of so-called minimal UV-crosslinkers containing a diazirine group are common. Diazirines decay to highly reactive carbene species upon UV-irradiation that can react with amino acids in physical proximity; hence they are applied in case of non-covalent target interaction.⁷⁷

Probe molecules are added to live cells to cross their membrane and interact with their targets. In case of non-covalent target binding cells are UV irradiated in order to crosslink the probe with protein interactors. Afterwards cells are lysed and the small molecule – biomolecule complex is functionalized with an azide reagent (i.e. biotin-based) in the background of the remaining lysate. Proteins are enriched on solid support, washed and digested by a protease to give a complex mixture of peptides. These peptides are applied to

high performance liquid chromatography coupled mass-spectrometry fragmentation (HPLC-MS/MS) and further analysis to assign peptides to proteins. Possible mode of action of natural products are concluded from binding site identification experiments of respective proteins.⁷⁸

1.5 Objective

The purpose of this work is to find novel anti-mycobacterial compounds and to investigate their molecular mode of action. Therefore natural products, fragments of natural products and natural product-based derivatives are revised in this study:

The group of ramariolides presents a novel group of butenolides exhibiting an unusual spirocyclic core structure paired with a long aliphatic hydrocarbon chain.⁷⁹ The aim is to develop a total synthesis strategy to access this natural product, test these molecules for their activity against Mycobacteria and to synthesize alkyne analogs to find cellular protein targets by ABPP experiments.

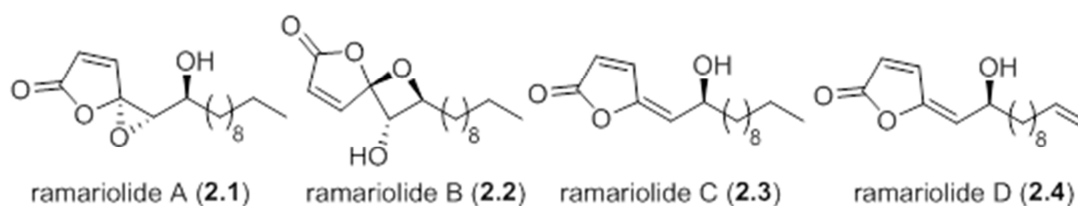


Fig. 1.5: Molecular structure of ramariolides A-D.

β -Lactones are commonly found in natural products as functional core structures and present excellent protein binders.⁸⁰⁻⁸² The goal is to screen a small library of these natural product fragments for their anti-mycobacterial activity and to elucidate its origin by utilizing genetic and biochemical methods.

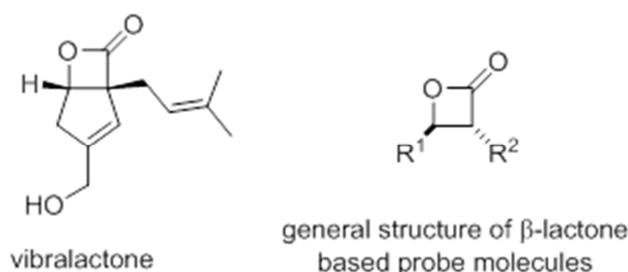


Fig. 1.6: β -lactones in natural products and derivatives.

Lalistat (**4.1**) is a known inhibitor of the human lysosomal acid lipase (hLAL), the same enzyme targeted by orlistat (THL), a marketed drug based on the natural product lipstatin.⁸³ THL has been shown to be a growth inhibitor in Mycobacteria mainly acting on hydrolase functions. Investigations on the anti-mycobacterial effect of lalistat are performed and target analysis is conducted by ABPP experiments.⁸⁴

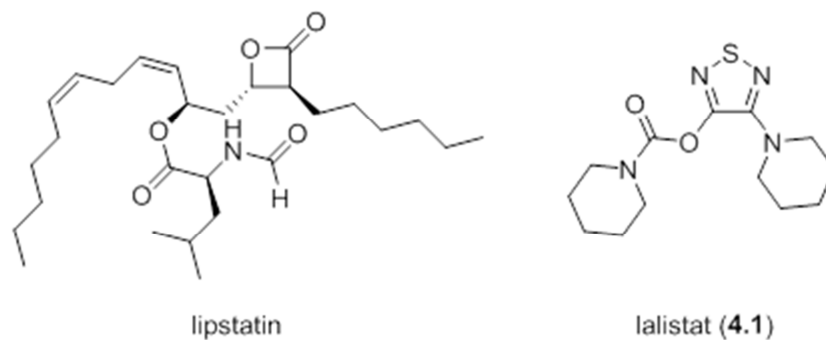


Fig. 1.7: Human lysosomal acid lipase inhibitors.

Chapter 2 Ramariolides

2.1 Background and synthetic analysis

The isolation of ramariolides A-D was first reported by Andersen and co-workers in 2012 (Fig. 1.4).⁷⁹ They described a group of four novel natural products from fruiting bodies of the coral mushroom *Ramaria cystidiphora*. Due to their shared 2-furanone functionality they are grouped within butenolides. In addition to this unsaturated γ -lactone, ramariolide A and B display a highly interesting spirocyclic acetal group. Although spirocyclic acetals are typical structural motives in nature, there has neither been a [3.5]- nor a [4.5]-membered system reported. These highly strained ring systems present a synthetic challenge and display an interesting electrophilic core. Furthermore the bivalent nature of ramariolides, including a polar head group combined with a long (C_{10}) aliphatic chain, makes these molecules interesting substrates for anti-mycobacterial research, as they appear to be able to cross the hydrophobic membrane and still be acting intracellular.

Applying the definition of a functional head and hydrocarbon tail, the molecule can be retrosynthetically divided. Olefination of the individual parts marks the synthetic key step leading to a common precursor that allows access to all members of this natural product family by interconversion (Fig. 2.1).

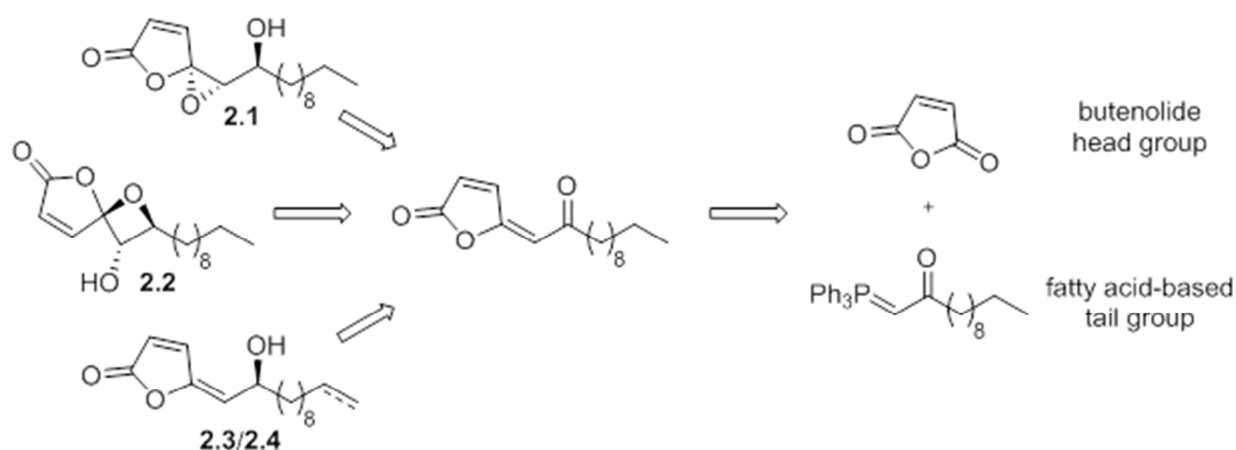
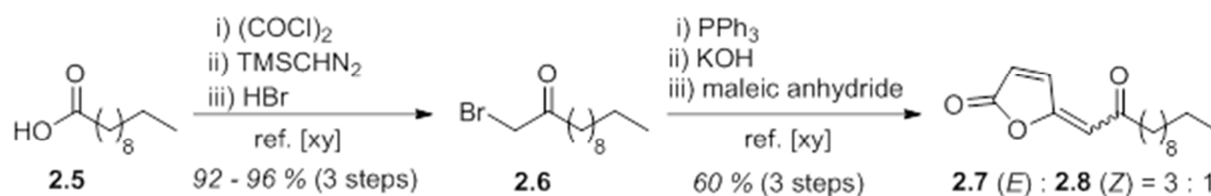


Fig. 2.1: Retrosynthetic analysis of ramariolide natural products.

2.2 Synthesis of ramariolides A-D

Long chain fatty acids were identified as a possible starting point for the total synthesis of the hydrocarbon tail. Corresponding building blocks are commercially available in large amounts. Following the initial steps of an *Arndt-Eistert* homologation the carboxylic acid is activated using oxalyl chloride in the presence of catalytic amounts of DMF. Transformation of these acid chlorides into a ketone functionality was accomplished using TMS-diazomethane as a mild reagent for elongation of the carbon chain.⁸⁵ TMS-

diazomethane acts as a nucleophile in this case replacing the chloride under loss of TMS. The obtained α -diazo-ketone can be isolated or used without further purification. As described by *Gangjee* et al. addition of concentrated hydrobromic acid under reflux to α -diazo-ketones led to release of molecular nitrogen forming α -bromo ketones.⁸⁶ The reactions can be carried out over three steps without further purification in excellent yields of **2.6** (Scheme 2.1).



Scheme 2.1: Assembly of the head and tail blocks to the central intermediate.

Introduction of the butenolide functionality was attempted as described by *Pattenden* et al. using maleic anhydride in a *Wittig* olefination.⁸⁷ Therefore, α -bromo ketones were treated with triphenyl phosphine in chloroform, precipitating the corresponding phosphonium salt. The so formed Wittig-salt was filtered off and deprotonation was performed in $\text{H}_2\text{O}/\text{MeOH} = 1/1$ (v/v) using KOH.⁸⁸ Once more the formed product crashed out and was readily available after drying. This recrystallization gave access to stable ylides in quantitative yield and high purity. Ylide and maleic anhydride were refluxed in toluene for 16 h to give a mixture of the corresponding (*E*)- and (*Z*)-configured olefins **2.7** and **2.8** in up to 60 % overall yield (Scheme 2.1). The decrease in yield can be explained by co-occurrence of partial homoolefination and polymerization of the acceptor substituted ylide. To prevent these side reactions, strong diluted conditions were applied but did not inhibit undesired product formation completely. Analysis of the products showed a 3:1 ratio in favor of the (*E*)-configured olefin over its (*Z*)-isomer, which were determined by the respective 4J - and 5J -coupling constants of olefinic protons by $^1\text{H-NMR}$ according to *Seltzer* et al. (Fig. 2.2).⁸⁹ Their drastic difference in polarity can be explained by the molecular dipole moment: Due to its inability to rotate around the formed carbon-carbon double bond the oxygen atoms in **2.8** create a significantly stronger dipole that results in a more polar molecule.

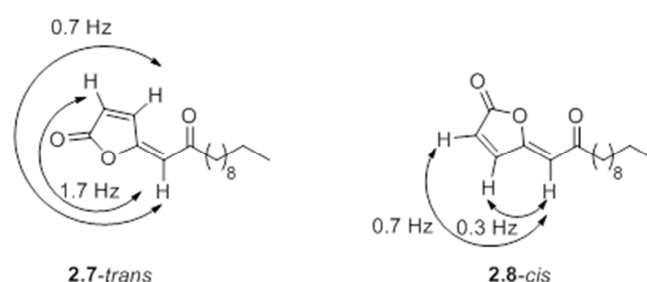
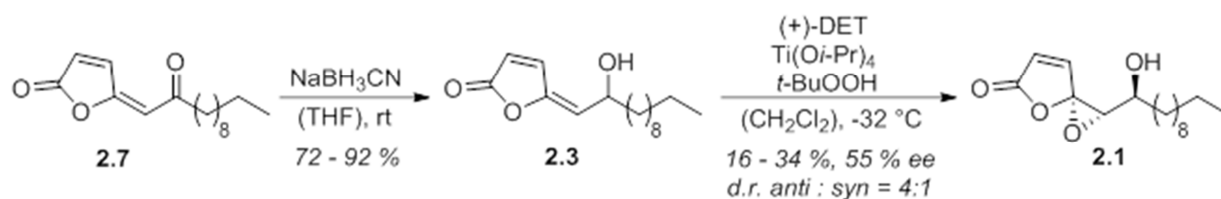


Fig. 2.2: Coupling constants of olefinic protons for structural determination.

Subsequent reduction of the (*E*)-configured ketone **2.7** was attempted using NaBH₄ as hydride donor. While conducting this reaction in MeOH mainly gave a methoxylated *Michael*-addition product, the solvent was changed to THF. Unfortunately, the solvent change only led to decomposition of the starting material, which required adjustment of the reduction agent. Utilizing NaBH₃CN in THF finally yielded the desired product **2.3** in up to 92 %.⁹⁰ These findings can be explained by the electron withdrawing effect of the cyanide substituent, which reduces the overall reactivity of the borohydrate to a moderate rate (Scheme 2.2). The obtained racemic product correlates to (±)-ramariolide C matching published data in MS and NMR spectra.⁷⁹



Scheme 2.2: Synthesis of ramariolide C and A.

Interconversion of ramariolide C (**2.3**) to A (**2.1**) required epoxidation of the exocyclic, conjugated double bond in *anti*-configuration to the newly formed hydroxyl group. Testing various reaction conditions including epoxidation agents like *m*-CPBA, H₂O₂, oxone and DMDO was resulted either in no conversion or decomposition. Finally, applying *Sharpless* conditions for epoxidation of allylic alcohols yielded ramariolide A (Scheme 2.2).^{91, 92} The reaction utilizes the alcohol functionality to coordinate a titanium-(IV) species, which is chelated by tartrate ester and *t*-butyl hydroperoxide, to perform the cycloaddition of oxygen onto the alkene. Furthermore the transition state enhances a *si*-sided attack leading to a 87:13 ratio of the desired stereoisomer. The overall moderate yield of this reaction can be explained by the formation of the spirocyclic core: After the transfer of the oxygen four heteroatoms are in close physical proximity coordinating to the titanium ions in the reaction, which hinders product separation during aqueous work up. Neither continuous extraction, nor acidification and alkalization led to increased product isolation. Analysis of optical rotation revealed (+)-tartrate to favor the formation of the desired enantiomer. Although the specific rotation of the synthetic product differed from reported values, enantiomeric access of 55 % could be determined by NMR titration using europium tris[3-(heptafluoropropylhydroxymethylene)-(+)-camphorate] (Fig 2.3).⁹³ Chiral Europium salts are reported to coordinate onto α-epoxy alcohols creating a diastereotopic environment, which enables differentiation of enantiomers by NMR.

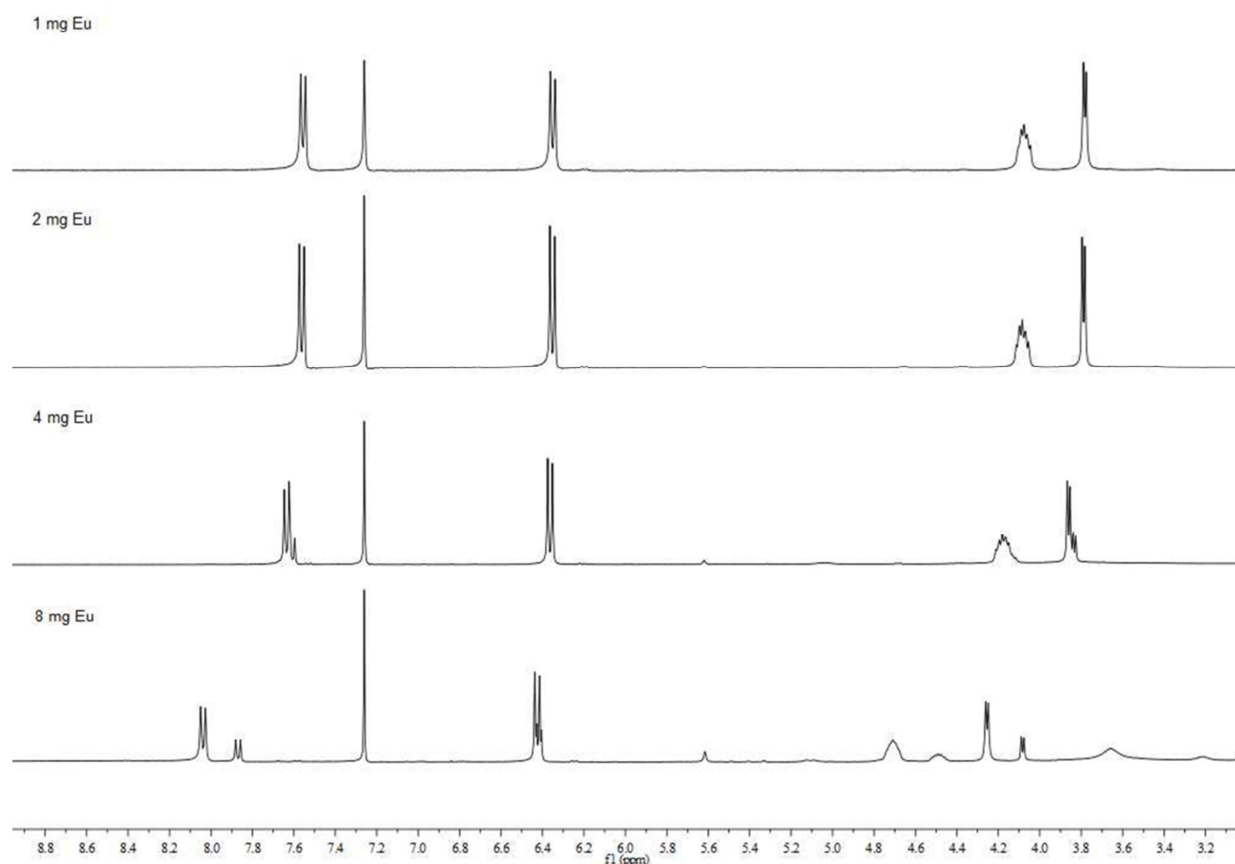
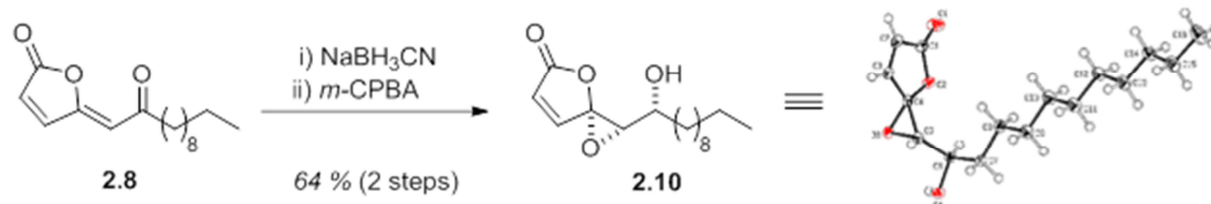


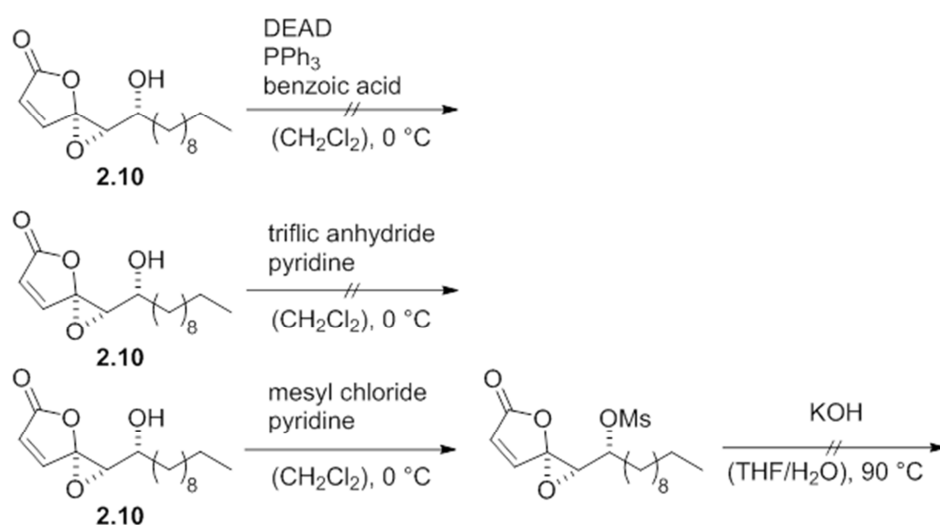
Fig. 2.3: NMR-titration of ramariolide A using europium tris[3-(heptafluoro-propylhydroxymethylene)-(+)-camphorate] in different amounts induced formation of a diastereomeric environment.

Ramariolide B (**2.2**) represents a structural isomer of ramariolide A, differing in the acetal forming hydroxyl group and the configuration of the spirocyclic rings. The interconversion of these natural products was attempted applying either alkaline or Brønsted/Lewis acidic conditions.⁹⁴ Although reacetalization could be observed, only the formation of the epimeric spirocycle (**2.9**) was achieved. It was therefore rationalized that the inverted stereochemistry of the (*Z*)-configured olefin **2.8** would provide a reasonable starting point for the desired isomer. While analogous reduction of the ketone with NaBH₃CN in THF led to the allylic alcohol, various epoxidation conditions (H₂O₂, dimethyldioxirane, vanadium-catalysis) resulted in exclusive formation the *syn*-configured α -hydroxy epoxide **2.10** (Scheme 2.3).



Scheme 2.3: Selective formation of a *syn*-configured α -epoxy alcohol and verification by X-ray analysis.

Possible explanations for this finding are the 1,3-allylic strain, which favors an attack from the less hindered side of the hydroxyl group, and a hydrogen-bond formation of peroxide donors by the lactone- and alcohol-oxygens leading to the *syn*-diastereomer. The structure of **2.10** was verified by 2D NMR analysis and X-ray crystallography (Scheme 2.3). As *syn*-configuration of the two functional groups would not give rise to the desired molecule, inversion of the alcohol functionality was anticipated. Although activated ester species of the alcohol were isolated, treatment of alkaline conditions or other nucleophiles resulted in decomposition (Scheme 2.4).



Scheme 2.4: Attempted inversion of the secondary α -epoxy alcohol.

Presumably the strained spirocyclic lactone is preferred over the attack of the enhanced leaving group. Alternatively, oxidation to the α -epoxy ketone provides a prochiral center for the reduction to the correctly configured substrate. Utilizing $\text{Zn}(\text{BH}_4)_2$ for the coordination to the epoxy- and keto-functionalities of the substrate a *re*-faced attack of the hydride is highly favored yielding the *anti*-configured diastereomer **2.11** in a 4:1 ratio (Fig. 2.4).⁹⁵

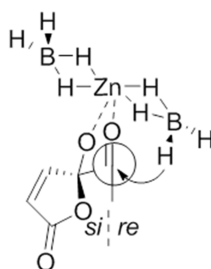
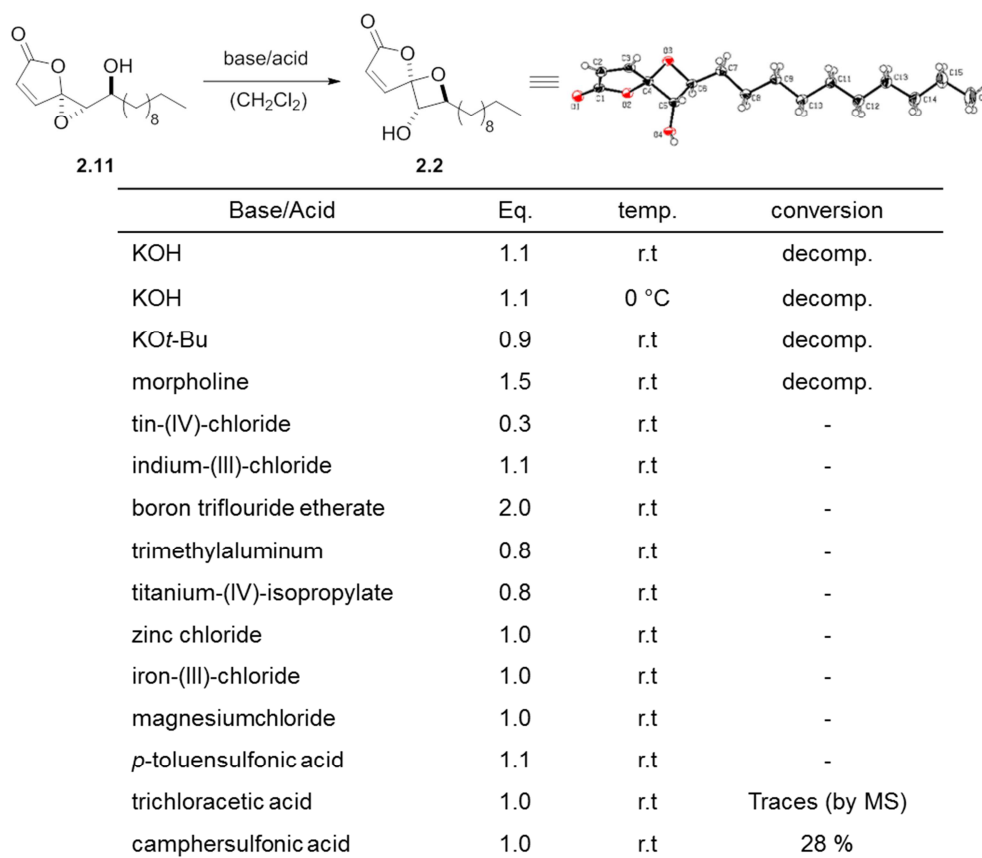


Fig. 2.4: Fischer-projection indicating the favored *re*-faced attack of hydride by oxygen coordination of zinc-ion.

With compound **2.11** in hand, a broad screen of conditions was conducted to form ramariolide B *via* homo-*Payne* rearrangement (Scheme 2.5).⁹⁴ Alkaline reagents repetitively led to decomposition of starting material, presumably due to attack of the spirocycle and opening of the lactone. The application of Lewis-acids in various equivalents did not show any conversion of starting material. Finally switching to Brønsted acidic conditions showed first promising results. The use of trichloroacetic acid formed a peak with differing retention time but identical molecular weight in LC-MS analysis. Although this product could not be isolated, a continuous screen of acids revealed camphersulfonic acid as viable reagent to catalyze the isomerization in quantitative amounts.⁹⁶ Spectral analysis showed high identity to published data in ¹H-, ¹³C- and 2D-NMR experiments.⁷⁹ Finally, structural conformation of **2.2** was validated by crystallization and X-ray analysis.



Scheme 2.5: Screening conditions for rearrangement to ramariolide B.

In addition to the desired molecule **2.2** a side product was isolated in minor amounts in this reaction. Analysis by 2D NOE NMR experiments revealed the spirocyclic epimer of ramariolide B (**2.9**). Due to the perpendicular nature of spirocycles substituents of the oxetan ring are in the same plane as atoms in the furanone ring to give strong signals (Fig 2.5).

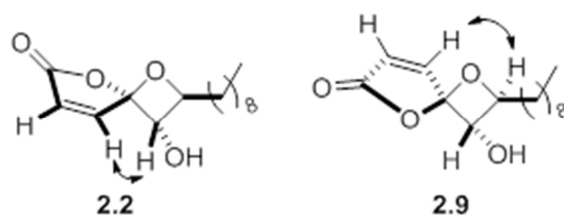
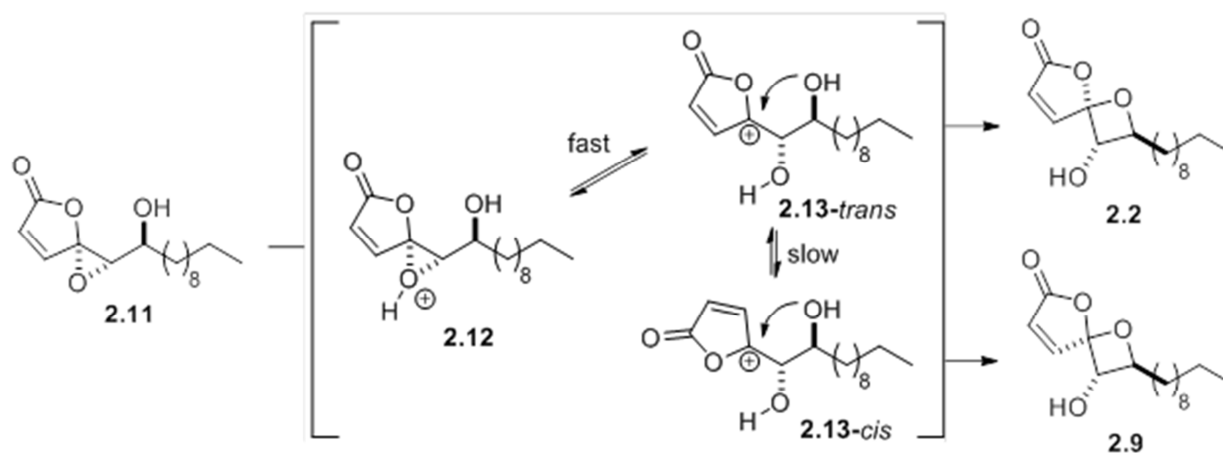


Figure 2.5: Isolated [4.5]-spirocyclic products. Arrows indicate observed NOE signals.

Furthermore, isolation of the spirocyclic epimer gave insight in the molecular reaction mechanism. Supposedly, the acid protonates the oxirane moiety (**2.12**) and subsequently forms an acyclic carbocation (**2.13-trans**), which is highly stabilized in conjugation to an electron donating oxygen and double bond. Attack of the free hydroxyl group leads to the kinetically favored ramariolide B formation. Rotation of the opened single bond (**2.13-cis**) and closing of the oxetan cycle is much slower and gives the observed side product in minor amounts (Scheme 2.6).



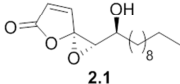
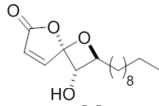
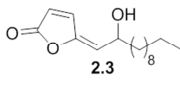
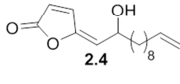
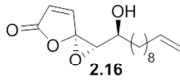
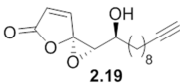
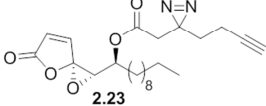
Scheme 2.6: Mechanistic rationale for acid-mediated rearrangement of the acetal.

Application of terminally unsaturated fatty acids to the established procedures resulted in structural alkene and alkyne derivatives (Appendix Fig. 6.2) and yielded amongst others ramariolide D. Inspired by the structural motive of a terminal olefin, alkyne analogues could be synthesized. Due to an alkyne orthogonal synthetic strategy derivatives were obtained without adjustment of protocols or use of protection groups. The hydrocarbon chain presents a natural linker spacing the functional core and the bio-orthogonal tag from each other.

2.3 Bioactive ramariolide ABPP probes for target identification

All natural products and their alkyne derivatives were tested against a series of pathogenic bacterial strains to determine their minimal inhibitory concentration of bacterial growth as summarized in Table 2.1.

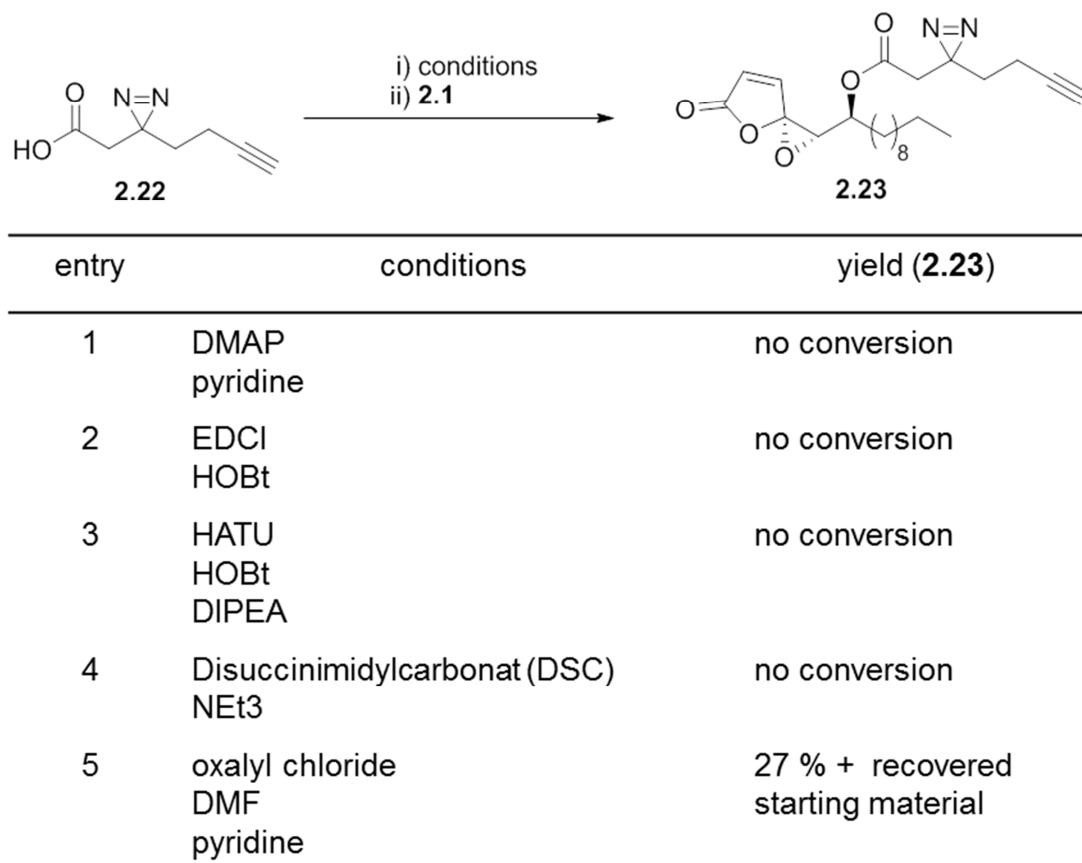
Table 2.1: Bioactivity screen of ramariolides A-D and analogues

compound	<i>S. aureus</i> USA 300	<i>L. monocytogenes</i> EGD-e	<i>M. smegmatis</i> mc(2) 155	<i>M. tuberculosis</i> H37Rv	<i>E. faecalis</i> V583	<i>P. aeruginosa</i> PAO1
 2.1	10 μ M	3 μ M	30 μ M	25 μ M	30 μ M	> 100 μ M
 2.2	30 μ M	-	30 μ M	-	-	> 100 μ M
 2.3	30 μ M	30 μ M	100 μ M	-	100 μ M	> 100 μ M
 2.4	30 μ M	-	100 μ M	-	-	> 100 μ M
 2.16	30 μ M	-	30 μ M	-	-	> 100 μ M
 2.19	> 100 μ M	-	> 100 μ M	-	-	> 100 μ M
 2.23	10 μ M	-	30 μ M	-	-	> 100 μ M

All ramariolides were active against diverse Gram-positive strains with ramariolide A exhibiting most pronounced potency against *Staphylococcus aureus* USA300 (30 μ M) as well as mycobacteria including *Mycobacterium tuberculosis* H37Rv (25 μ M). Unfortunately, the terminal alkynylated compound **2.19** did not maintain antimicrobial activity, which is essential for ABPP experiments, although the corresponding control substance **2.16** was bioactive. A possible explanation might be the altered geometry of the triple bond that negatively interferes with target binding.

Validation of the compound structure for alternative modification sites revealed the free secondary hydroxy group of ramariolide A as a synthetically accessible position for the introduction of an alkyne tag. Although ramariolide A contains possible protein reactive groups (i.e. oxirane, Michael acceptor) the mode of target binding could be also driven by reversible interactions. Therefore alteration by esterification was anticipated using a minimal photo-crosslinker.⁹⁷ This building block was designed as a general accessibility of

compounds for AfBPP experiments. It contains a terminal alkyne to allow functionalization *via* click chemistry, a diazirine moiety that can be activated to a highly reactive carbene species upon UV irradiation and a functional group (e.g. carboxylic acid) for covalent modification of the molecule of interest. Despite it is not known if the alcohol functionality of ramariolide A is actively involved in target interaction (i.e. hydrogen bond acceptor/donor) formation of an ester enables free interaction of the hydrocarbon chain with its binding pocket and the accessibility of the terminal alkyne. Initial attempts for esterification used a mild base, as pyridine, not to interfere with the reactive core of the natural product as well as catalytic amounts of DMAP. After no conversion was observed activation of the free acid function was attempted using classical coupling reagents as EDCI or HATU in the presence of HOBt to prevent racemization. Neither varying the solvent nor changing to less common disuccinimidylcarbonat (DSC) as coupling agent resulted in ester formation. Finally, conversion of the carboxylic group to an acid chloride gave the desired molecule in moderate yield. Although the natural product was used in small quantities in this reaction, starting material could be partially recovered but no minimal linker was reobtained, suggesting severe formation of side products upon activation with these harsh conditions. The newly synthesized probe **2.23** showed comparable bioactivity to the original natural product and was therefore used in all further experiments.



Scheme 2.7: Esterification of the secondary alcohol of ramariolide A.

2.4 Proteome analysis and target validation

Selective bioactivity of compounds is a commonly observed feature in chemical biology and also often found for natural products. The limitation of a substance to act only in Gram-positive bacteria can be explained by their ability to cross the cell wall. Nevertheless, an antimycobacterial effect is a rare feature and arose interest for cellular targets and the molecular mode of action. Initial analysis was started in the mycobacterial model strain Msmeg following established procedures.⁹⁸ Cells were grown and harvested in exponential growth phase to cover a wide spectrum of expressed proteins involved in cellular growth. For target evaluation cells were incubated with probe **2.23** and afterwards irradiated with UV-light (365 nm) to find all interacting protein partners. Furthermore cells were lysed and proteomic analysis was separated in a soluble and an insoluble fraction. Each partition was clicked to biotin azide and enriched on avidin beads before released by tryptic digestion (Fig 2.7). The obtained cleaved peptide fragments were further modified by dimethyl labeling using light, medium and heavy isotope reagents.⁹⁹ A label-switch was performed throughout biological replicates. Finally control and probe treated samples were pooled prior to LC-MS/MS analysis.

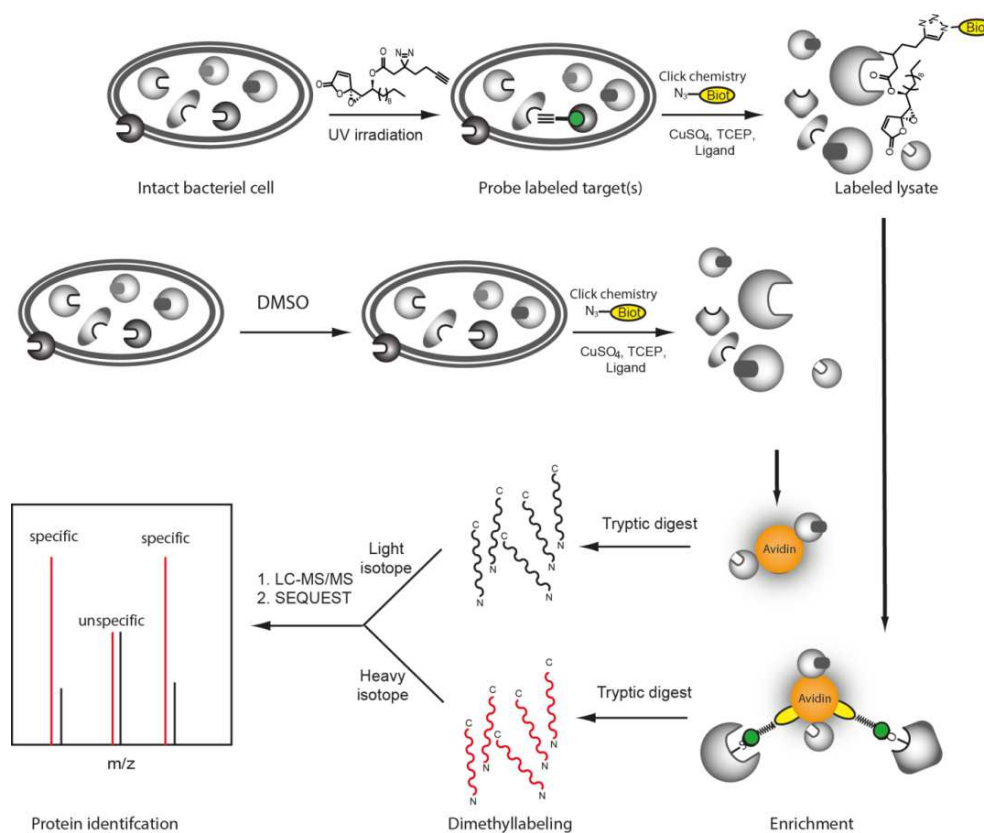


Fig. 2.7: Diagrammatic workflow of affinity based protein profiling utilizing dimethyl labeling for protein analysis.

Identified proteins were plotted as a (\log_2)-ratio of probe to DMSO treatment against statistical significance ($-\log_{10}$ p-value) (Fig. 2.8). Proteins enriched by a factor > 2 with a p-value of 0.05 or below were considered as hits (highlighted in green, cut-offs are marked by dashed lines). Evaluation of the soluble protein fraction revealed five hits as essential proteins (labeled in red) for mycobacterial growth (Fig. 2.9A)¹⁰⁰, while none were detected in the insoluble fraction (Fig. 2.9). These hits comprise the 30S ribosomal proteins S4 (RpsD) and S5 (RpsE), the caseinolytic protease subunit X (ClpX) and the metabolic enzymes aspartate kinase (Ask) and homoserine dehydrogenase (Hsd). RpsD and RpsE are small ribosome-associated proteins, which are highly abundant soluble proteins found in a prokaryotic cell. Previous proteomics experiments in *E. coli* also identified these proteins as possible contaminants during affinity enrichment.¹⁰¹ Therefore, these proteins were not considered in more detail. All non-essential hit proteins are summarized in Appendix Table 6.1.

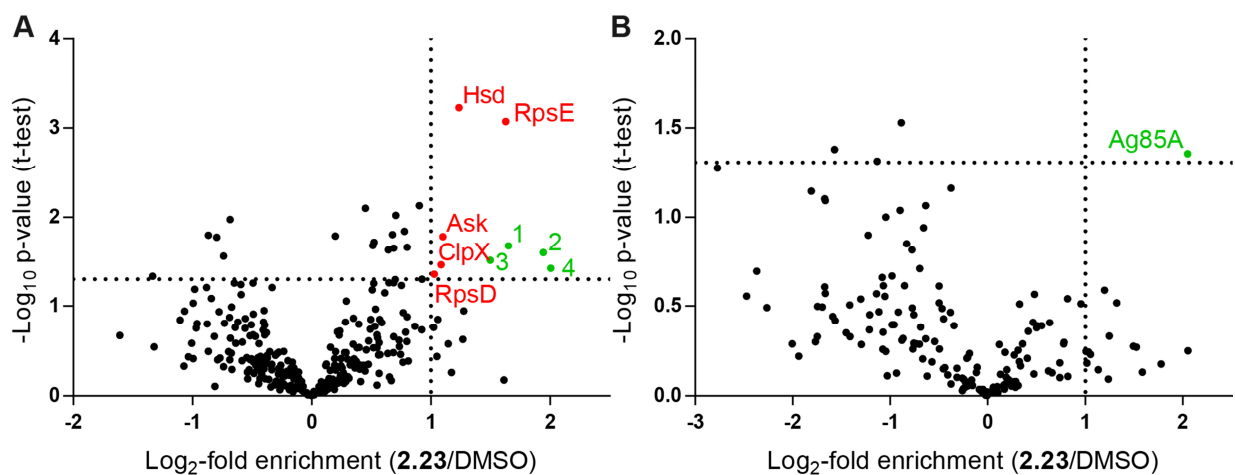


Fig. 2.9: Scatter plot of *M. smegmatis* mc(2) 155 proteome analysis after UV-irradiation of ABPP probe 2.23 versus DMSO **A.** soluble fraction **B.** insoluble fraction.

The molecular chaperon ClpX is well-studied and known to assist the ClpP subunit in protein degradation. Analysis of overexpressed mycobacterial protein did not reveal binding with probe **2.23** (Fig. 2.10).¹⁰²⁻¹⁰⁴

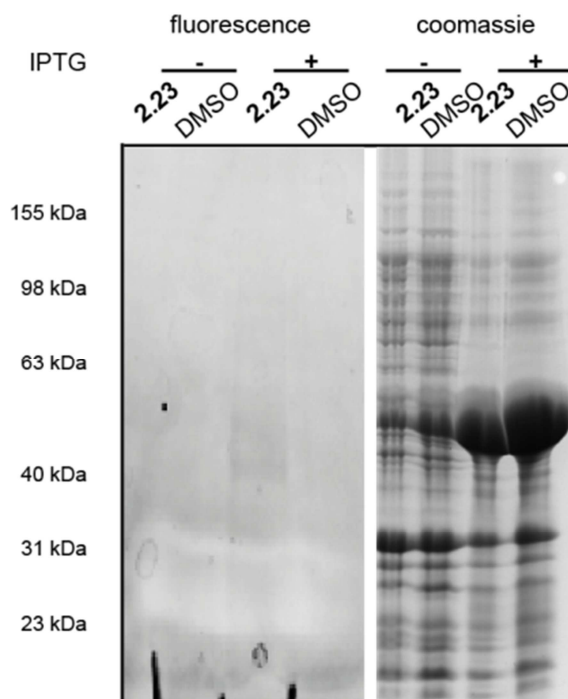


Fig. 2.10: Gel-based APBB of mycobacterial ClpX overexpressed in *E. coli* using 30 μ M **2.23** without UV-irradiation. Fluorescence scan after incubation in the dark and application of click-chemistry using rhodamine-azide. "+" indicates induction of protein expression by addition of IPTG; "-" represents absence of inducer.

Finally, Ask and Hsd catalyze subsequent steps in amino acid anabolism and have been shown to be essential for microbacterial growth.^{105, 106} It is thus intriguing to speculate that ramariolide A might compete with natural substrates for enzyme binding by blocking their active site pockets.

In order to validate this hypothesis mycobacterial ask was cloned in *E. coli* and gel-based ABPP experiments were conducted. Addition of **2.23** to Ask-overexpressing cells without UV-irradiation followed by rhodamine-azide click chemistry resulted in a strong fluorescent band of predicted molecular size upon induction of protein expression, indicating a covalent mode of binding (Fig. 2.11A). Furthermore gel-based labeling of purified protein was successful in contrast to heat disrupted control samples (Fig. 2.11B).

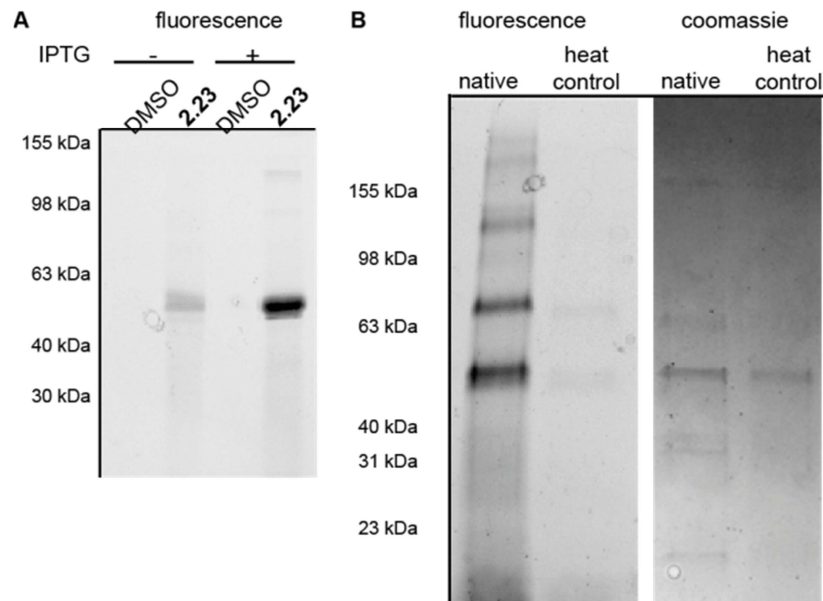


Fig. 2.11: Gel-based ABPP experiments on recombinant expressed Ask. **A.** Fluorescence scan of Ask labeled with **2.23** in *E. coli*. “+” indicates induction of protein expression by addition of IPTG; “-” represents absence of inducer. **B.** *In-vitro* labeling of purified Ask using 30 μM **2.23** without UV-irradiation under native and heat denatured conditions. Fluorescence scan after incubation in the dark and application of click-chemistry using rhodamine-azide.

These results suggest a specific interaction and the requirement of a native fold for ramariolide A binding. Based on the covalent binding mode gel-free ABPP experiments were repeated without UV crosslinking using **2.23** against DMSO (Fig. 2.12A) as well as competition with unmodified ramariolide A (Fig. 2.12B). Importantly, Ask was consistently among the most significantly enriched proteins in both experiments (remaining hits are listed in table 5.1). Although these findings highly imply interference of ramariolide natural products with amino acid anabolism in mycobacteria, binding to other target enzymes cannot be excluded and is under further evaluation.

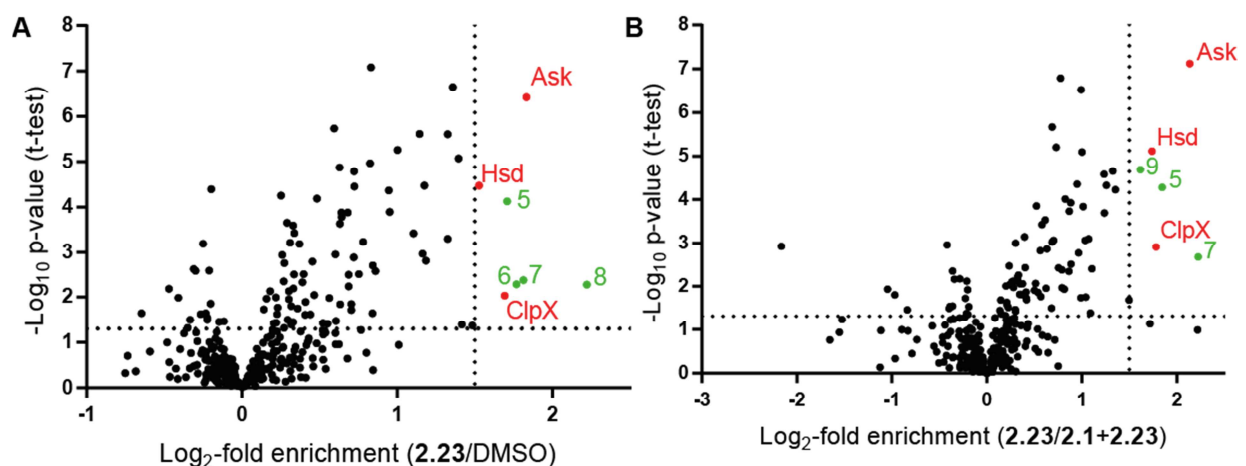


Fig. 2.12: Scatter plot of gel-free ABPP dimethyl labeling experiment in *M. smegmatis* mc(2) 155 soluble fraction without UV-irradiation **A.** 30 μM **2.23** vs. DMSO. **B.** 30 μM **2.23** vs. 100 μM **2.1**.

2.5 Conclusion

In summary the first total synthesis of ramariolides A-D was achieved. All compounds display anti-microbacterial activity in μM range in Gram-positive strains. Furthermore it was possible to introduce a terminal alkyne tag to the core-structure of the natural product. The corresponding AfBPP probe retained antibacterial activity and was therefore successfully applied for target identification in mycobacteria by ABPP experiments. Essential members of the bacterial amino acid metabolism were identified as interactors and validated by *in-situ* and *in-vitro* experiments providing strategies for future drug development.

Chapter 3 Mycobacterial targets of β -lactones

3.1 β -Lactones in natural products as enzyme inhibitors

β -Lactones are frequently found scaffolds in natural products that appear with various substitution patterns including polycyclic and spirocyclic systems (Fig. 3.1).

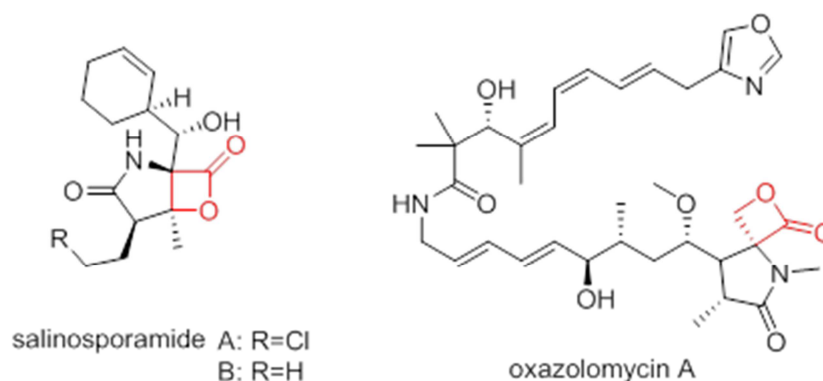


Fig. 3.1: β -Lactone containing poly- and spirocyclic natural products. Salinosporamide¹⁰⁷ and oxazolomycin¹⁰⁸ are depict as representative structures for this compound class. β -lactone core highlighted in red.

The electrophilic nature of β -lactones is fine tuned by electronic effects of immediate substituents that are able to enhance or restrict reactivity. The reason that these scaffolds are highly interesting for biological chemistry is their intrinsic reactivity towards nucleophilic active sites of enzymes.^{109, 110} In particular β -lactone containing natural products and their derivatives have been described to potently inhibit hydrolases such as the proteasome.¹¹¹⁻¹¹⁴ The key for this inhibition is the circular ring strain of these four-membered cyclic esters, which is released upon proteinogenic attack of Ser/Thr residues. The formation of a new, intermolecular ester bond leads to a covalent inhibition of the enzymes' active site restricting natural substrate binding (Fig. 3.2). Usually the opened β -lactone can be hydrolyzed over time restoring the original enzyme; however depending on the half-life of the newly formed bond cells might proteolyse dysfunctional enzymes.

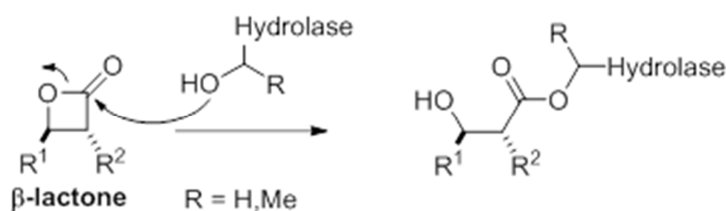
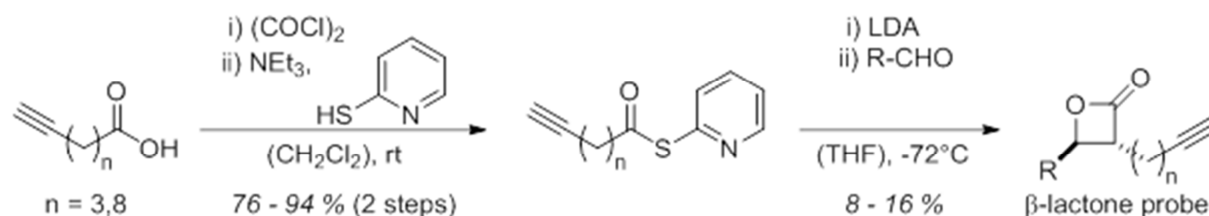


Fig. 3.2: Mechanism of β -lactone hydrolase inhibition by nucleophilic attack of Ser/Thr residue of hydrolases and subsequent ring opening.

For reasons stated above β -lactones have been subject of extensive studies to reveal cellular targets and off-targets in eukaryotic and prokaryotic cells.^{80, 84, 115} Simplified structures of natural products containing the reactive β -lactone core have been synthesized (Scheme 3.1) by one-pot cyclisation of a thioester and an aldehyde.¹¹⁶



Scheme 3.1: General procedure to access β -lactones.

Screening Gram-positive and Gram-negative pathogenic strains (*S. aureus*, *L. monocytogenes*, *E. coli*) for antibacterial activity only revealed antiviral effects.^{81, 82} In-depth analysis revealed the caseinolytic protease subunit P (ClpP) as the major target of these scaffolds.¹¹⁷ This enzyme is known as an ATP dependent serine protease responsible for degradation of cellular proteins and directly related to bacterial virulence.^{115, 118, 119} Application of β -lactone substances to mycobacteria indeed showed a cytotoxic effect. Mtb. Interestingly, some compounds showed a growth inhibitory effect at low μ M range (Table 3.1).

Table 3.1: MIC screening of β -lactones in bacterial strains.

β -lactone	<i>S. aureus</i> USA 300	<i>L. monocytogenes</i> EGD-e	<i>M. smegmatis</i> mc(2) 155	<i>M. tuberculosis</i> H37Rv	<i>E. coli</i> K12	% Inhibition of Mtb ClpP1/2 [50 μ M]
	> 100 μ M	> 100 μ M	> 100 μ M	>100 μ M	> 100 μ M	0
	> 100 μ M	> 100 μ M	100 μ M	> 100 μ M	> 100 μ M	65.7
	> 100 μ M	> 100 μ M	100 μ M	100 μ M	> 100 μ M	84.6
	> 100 μ M	> 100 μ M	50 μ M	12.5 μ M	> 100 μ M	0
	> 100 μ M	> 100 μ M	25 μ M	12.5 μ M	> 100 μ M	not determined
	> 100 μ M	> 100 μ M	50 μ M	1.6 μ M	> 100 μ M	28.3
	> 100 μ M	> 100 μ M	> 100 μ M	> 100 μ M	> 100 μ M	0

Application of these criteria reveals a variety of hydrolases (proteases, esterases, lipases) of typical α,β -fold as targets across mycobacterial strains in soluble and insoluble fractions. This is in large agreement to previous results.^{80, 120, 123} In order to detect protein targets responsible for cellular death, hit proteins were filtered again by essentiality on mycobacterial growth based on TnSeq-analysis.¹⁰⁰ Interestingly, ClpP(2) is the only protein matching these criteria for Msmeg, while Mtb shows polyketide synthase 13 (Pks13) as promising hit, which is also found in Msmeg with strong statistical significance but minor enrichment. Furthermore ClpP is only a minor target in Mtb, which provides a possible explanation for the discrepancy of **EZ120** MIC in Msmeg and Mtb.

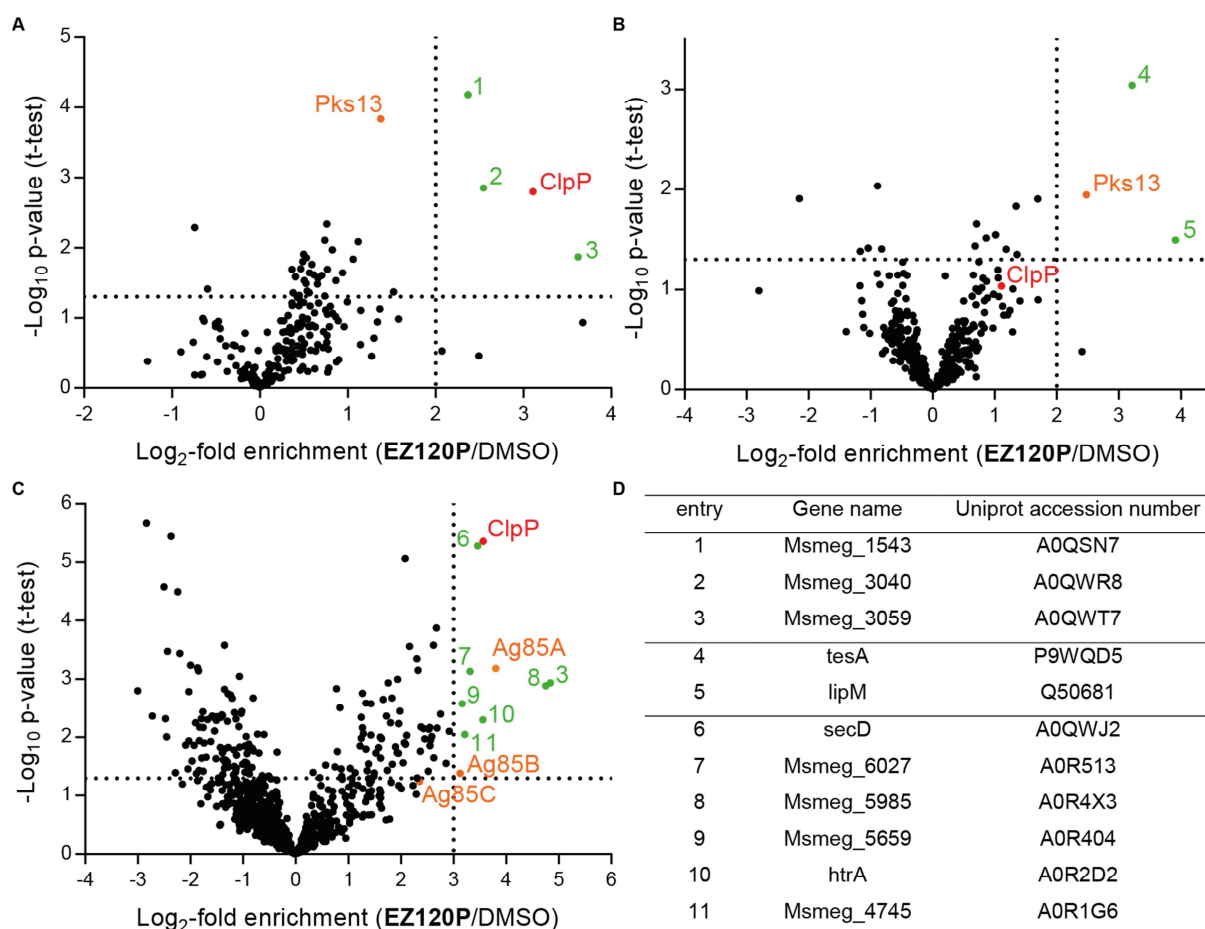


Fig. 3.4: Proteomic analysis of mycobacterial targets of **EZ120P** vs. DMSO **A.** Scatter plot of *M. smegmatis* mc(2)155 soluble fraction. **B.** Scatter plot of *M. tuberculosis* H37Rv soluble fraction. **C.** Scatter plot of *M. smegmatis* mc(2) 155 insoluble fraction. **D.** Overview of new essential protein hits. Dotted line: cut-off values (\log_2 -fold enrichment ≥ 2 for soluble and ≥ 3 for insoluble targets; p -value ≤ 0.05). Green: proteins not essential for growth. Red/orange: essential mycobacterial proteins.

Labeling analysis of the insoluble fraction of Msmeg showed a similar pattern of hydrolases, including proteins already found in the soluble fraction. As these proteins show a similar enrichment factor in both experiments they are considered as carry over between

fractions. Although searching for essential mycobacterial proteins did not deliver one direct hit, the fact that antigen 85 (Ag85) A and B are found within hit-criteria and Ag85C is also enriched, although to a lesser extent, indicates their involvement in this process. Despite the fact that each of these enzymes is not considered essential, targeting of all three of them is. They are described as homologs being able to compensate each other's physiological role.¹²⁴

As gel-free analysis is challenged by decreased fluidity and disruptiveness of mycobacterial membranes SDS-PAGE of the insoluble fraction in Msmeg was performed additionally (Appendix Fig. 6.3). Labeled proteome was clicked to a linker consisting of rhodamine and biotin moiety, samples were enriched before separation by SDS-PAGE. Fluorescent scanning showed a distinct set of protein bands, which were excised, digested and analyzed by LC-MS/MS. In line with gel-free data Ag85 enzymes A,B, and C were most prominently enriched compared to the DMSO control. These results highlight a preference of **EZ120P** for targeting Pks13 and Ag85 serine hydrolases in mycobacteria. With the exception of ClpP, no essential function could be assigned to any other protein hit suggesting that these proteins largely contribute to the observed antibiotic effect. We thus focused our target validation and functional analysis on Pks13 and Ag85.

3.3 Target validation of Pks13

Mtb Pks13 is a 186 kDa cytoplasmic polyketide synthase catalyzing the final step of fatty acid chain assembly in mycolic acid synthesis.^{24, 125} It consists of the following five domains: N-terminal acyl carrier protein, β -ketoacetyl synthase, acyltransferase, C-terminal acyl carrier protein and thioesterase.¹²⁶ The C-terminal thioesterase (TE) domain represents a serine hydrolase and is responsible for product release.^{24, 125} Being the strongest nucleophile within this multi-domain enzyme, the TE active site serine is a strong candidate for **EZ120** binding.

Therefore, the C-terminal part of Pks13 including the TE domain sequence was cloned in *E. coli* for recombinant expression and purification. In order to confirm putative binding an active site serine to alanine mutant (S1522A) was constructed and purified. With both constructs in hand gel-based ABPP experiments were conducted using **EZ120P** for labeling, followed by click chemistry utilizing rhodamine-azide for detection. Comparison of fluorescence (Fig. 3.5A) and coomassie (Fig. 3.5B) scanning clearly indicate the protein expression upon induction. Wild-type (wt) enzyme is specifically labeled upon treatment with probe meanwhile the mutant remains unaffected indicating modification of Ser 1533.

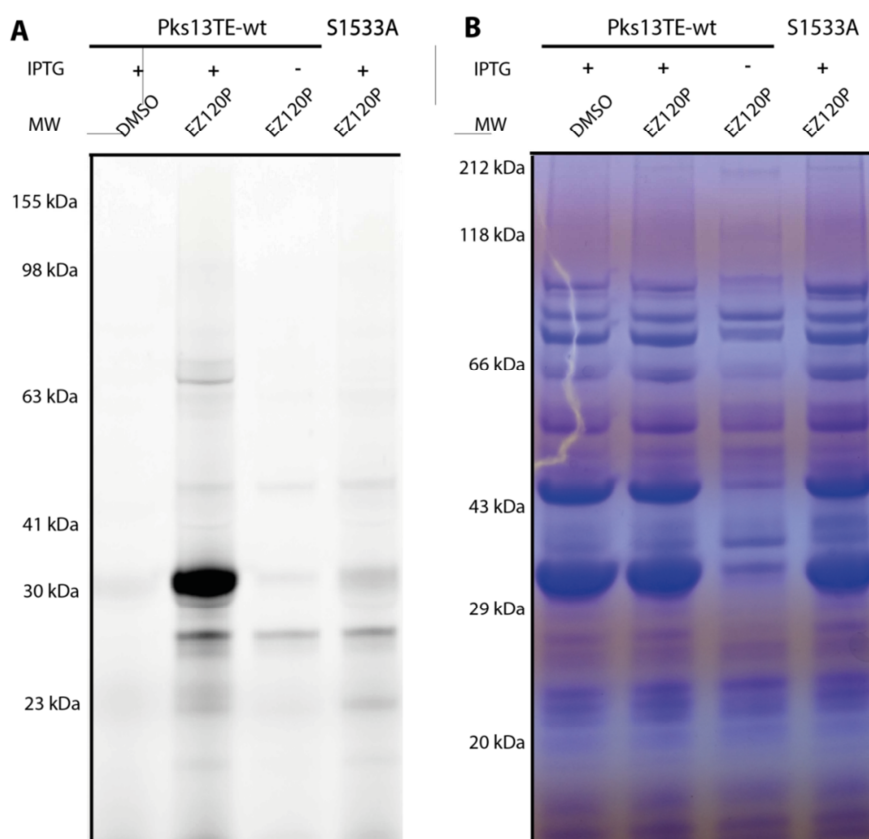


Fig. 3.5: Gel-based APBB of Mtb Pks13-TE domain and S1533A mutant overexpressed in *E. coli* using 30 μ M **EZ120P**. **A.** Fluorescence scan after incubation in the dark and application of click-chemistry using rhodamine-azide. **B.** Coomassie stain. “+” indicates induction of protein expression by addition of IPTG; “-” represents absence of inducer.

To validate previous results intact protein MS experiments were carried out with purified wt- and mutant enzyme. Addition of tenfold molar excess **EZ120** to wt-enzyme led to a mass increase corresponding to binding of one molecule (Fig. 3.6A) in contrast to the S1533A-mutant, which showed no adduct formation (Fig. 3.6B). These findings support the hypothesis of **EZ120** binding to the TE-domain of Pks13 and inhibition of the active site by modification of the serine nucleophile. For further elucidation of the specificity of the Pks13-TE domain a variety of specific and non-specific covalent binding hydrolase inhibitors was tested by intact protein MS. These comprised other initially tested β -lactones (**D3**, **P1**, **E2**) (Appendix Fig. 6.4A) as well as the commercially available lysosomal acid lipase inhibitors orlistat (β -lactone) and lalistat (thiadiazol carbamate) (Appendix Fig. 6.4).^{110, 127} Surprisingly, no other molecule showed mass-adduct formation indicating the selectivity and specificity of **EZ120** for Pks13-TE binding.

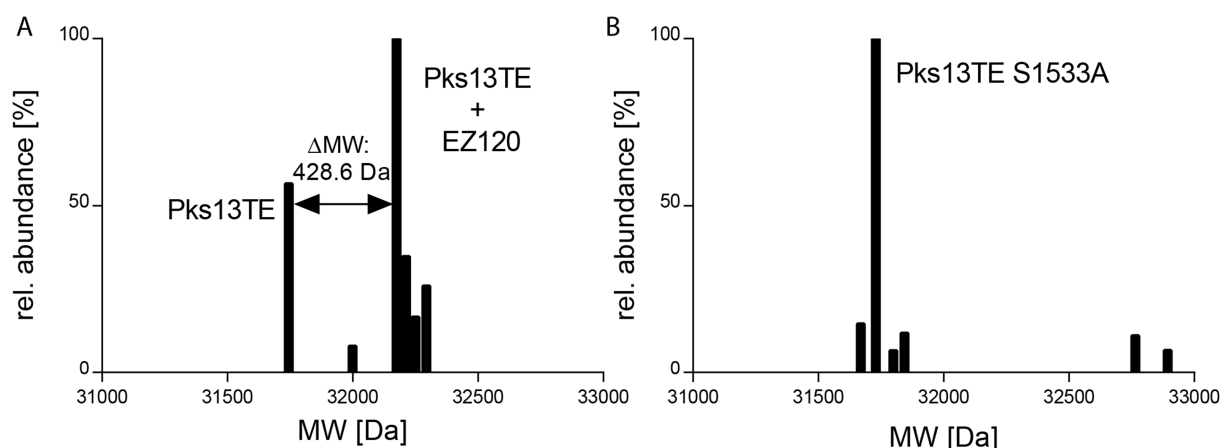


Fig. 3.6: Intact MS spectra of **A.** wt-TE domain and **B.** S1533A mutant with tenfold excess of EZ120.

In order to quantify the activity of Pks13-TE domain a screen on fluorescent hydrocarbon esters was performed revealing 4-methylumbelliferyl heptanoate as a suitable substrate to monitor turnover. The molecule presumably mimics natural fatty acid binding and is hydrolyzed releasing a fluorescent product. Initial studies showed discrete activity of wt-enzyme, while no activity could be observed for S1533A mutant. Application of **EZ120** reveals reduction of enzyme activity with increasing concentration of **EZ120** suggesting inhibition by active site acylation (Fig. 3.7).

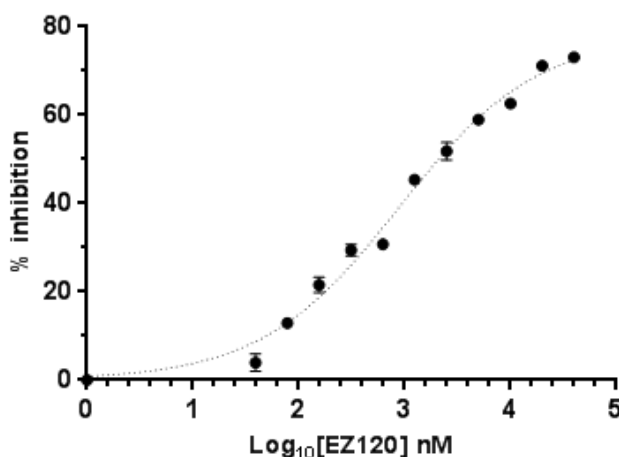


Fig. 3.7: Activity assay for Pks13-TE domain. Increasing concentrations of **EZ120** show significant inhibition of enzyme activity.

Considering the native action of the TE-domain includes binding of an extremely apolar molecule bearing two long hydrocarbon chains similar to the decoration of **EZ120**. Furthermore, opening of the β -lactone core leads to formation of a β -hydroxy ester adduct as with in mycolic acids. Unfortunately, this rationale does not explain the selectivity of **EZ120** over differently decorated β -lactones. Co-crystallization studies of active site bound inhibitor might provide a satisfying explanation.

3.4 Target validation of Ag85-family

ABPP experiments of the insoluble protein fraction of Msmeg suggested proteins of the Ag85 family as predominant targets. Their molecular function is described as mycolic acid transferases,^{28, 128} catalyzing the acylation reaction of a donor molecule (TMM) onto an acceptor substrate (TMM, AG, glucose) in mycobacterial periplasm.¹²⁹ The fact that they act downstream the mycolic acid metabolism makes them highly interesting protein targets. Furthermore the mode of β -lactone binding would be analogous to Pks13 miming β -hydroxy acids. The class of Ag85 enzymes presents homologous serine hydrolases with conserved catalytic triad suggesting functional interchangeability (Fig. 3.8).¹³⁰

A85A_MYCTU	1	---MQLVDRVRGAVTGM SRRLVVGAVGAALVSGLVGAVGGTATAGAF SRPGLPVEYLQVP	57
A85B_MYCTU	1	-----MTDVS RKIRAWGRRLMIGTAAAVVLPGLVGLAGGAATAGAF SRPGLPVEYLQVP	54
A85C_MYCTU	1	MTFFEQVRRLRSAATLPRRLAIAAMGAVLVVGLVGT FGGPATAGAF SRPGLPVEYLQVP	60
		: : ** ** *: *: *	
A85A_MYCTU	58	SPSMGRDIKQVQFQSGGANS PALYLLDGLRAQDDFGWDINTPAFEWYDQSGLSVVMVPGG	117
A85B_MYCTU	55	SPSMGRDIKQVQFQSGGNN SPAYLLDGLRAQDDYNGWDINTPAFEWYQSGLSIVMVPVGG	114
A85C_MYCTU	61	SASMGRDIKQVQFQGGGP--HAYVLLDGLRAQDDYNGWDINTPAFEEYYQSGLSVIMPVGG	118
		* *	
A85A_MYCTU	118	QSSFYSDWYQ PACGKAGCQTYKWETFLTSELP GWLQANRHVKPTGSAVVGL S MAASSALT	177
A85B_MYCTU	115	QSSFYSDWYSPACGKAGCQTYKWETFLTSELP QWLSANRAVKPTGSAAI GL S MAGSSAMI	174
A85C_MYCTU	119	QSSFYTDWYQPSQSNQNYTYKWETFLTREMPAWLQANKGV SPTGNAAVGL SMSGGSALI	178
		* *	
A85A_MYCTU	178	LAAYHPQQFVIYAGAMS LLDPSQAMGPTLIGLAMGDAGGYKASDMWGPKE DPAWQRNDPL	237
A85B_MYCTU	175	LAAYHPQQFIYAGSLS ALLDPSQGMG PSLIGLAMGDAGGYKAADMWGPSS DPAWERNDPT	234
A85C_MYCTU	179	LAAYYPQQFPPYAASLSGFLN PSEGWPTLIGLAMND SGGYNANS MWGPSS DPAWKRN DPM	238
		** * : *	
A85A_MYCTU	238	LNVGKLIANNTRVWVYCGNGKPSDLGGNNLPAKFL S GFVRTSNIK FQDAYNAGGGHNGVF	297
A85B_MYCTU	235	QQIPKLVANNTRLWVYCGNGT PNELGGANI PAEFL S NFVRSNLK FQDAYNAGGGHNAVF	294
A85C_MYCTU	239	VQIPRLVANNTRIWVYCGNGT PSDLGGDNI PAKFL S GLTLRTNQTFRDYAADGGRNGVF	298
		: : * : *	
A85A_MYCTU	298	DFPDSGT SWEYWG AQLNAMK PDLQRALGAT-PNTGPAPQGA	338
A85B_MYCTU	295	NFPNGT SWEYWG AQLNAMK GDLQSSLGAG-----	325
A85C_MYCTU	299	NFPNGT SWPYWNEQLVAMKADIQHVLNGATPPAAPAAPAA	340
		: *	

Fig. 3.8: Alignment of Mtb Ag85A, B and C by primary sequence. Amino acids of catalytic triad highlighted in red.

While none of the individual genes is essential double knock-out was reported to affect viability.¹³¹ In Msmeg six genes are annotated as members of the Ag85 group, hence only three of them have been reported to be expressed by q-PCR experiments with Ag85A being the most active enzyme. The same three proteins have been detected in the ABPP analysis. In Mtb only three genes (Ag85A, B and C) are known by genomic analysis, with the exception of a fourth one (Ag85D) with different function. All Mtb proteins have been previously expressed and functionally characterized stating Ag85C as the predominant enzyme.^{28, 132} The importance of this protein group as mycobacterial drug target was shown by the Ronning group that found ebselen as a small molecular covalent inhibitor.¹³³ Although binding to a near active site cysteine the mode of action is presumed to work for all three enzymes similarly and results in mycobacterial cell death upon treatment.¹³⁴

Binding of **EZ120P** to the class of Ag85 enzymes was already indicated by gel-based ABPP MS experiments. Nevertheless, further verification was expected by creation of a single gene knock out. For reasons of safety and time genetic implementation were performed in *Msmeg*. Successful construction of an Δ Ag85A strain and a complemented strain, carrying the knocked-out gene at the genomic L5 site (Δ Ag85A//Ag85A::L5), was shown by western blot. Using an Ag85A specific antibody caused loss of the corresponding protein band, while protein expression could be restored in case of the complement strain (Fig. 3.9A). Comparative gel-based ABPP experiments of wt- and knock-out strains revealed the disappearance of one characteristic band around 30 kDa as in Western analysis (Fig. 3.9C).

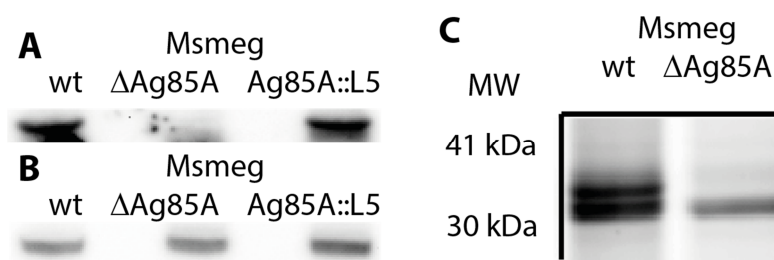


Fig. 3.9: Gel-based comparative analysis of wt-, Δ Ag85A and Δ Ag85A//Ag85A::L5 *Msmeg* strains. **A.** Western Blot of Ag85A. **B.** Western blot loading control. **C.** Fluorescence scan after **EZ120P** (10 μ M) incubation in the dark and application of click-chemistry using rhodamine-azide.

Access to the Ag85A knock-out strain enabled a number of phenotypical studies. The doubling time in liquid medium increased by 60 % and also bacterial growth on solid medium resulted in smaller colonies. Microscopic analysis revealed significant smaller individuals compared to wt-strain. Finally, MIC determination using standard drugs against mycobacteria showed a significant increase of cell susceptibility for rifampicin (16-fold), vancomycin (12-fold) and also for **EZ120** (fourfold). These findings presumably result from destabilized mycomembranes, which could be more permeable for drug application. In case of **EZ120** the lack of Ag85A leads to a faster inhibition of the mycolic acid transfer and results in cell death at lower concentrations. All observed phenotypes could be complemented to wt-level with reimplementation of Ag85A gene at L5-site.

Application of **EZ120** presumably blocks Ag85A/B/C activity in mycobacterial cells and has a similar effect on single gene knock-out strains, should result in similar MIC effects. As current treatment of tuberculosis requires the administration of several drugs in order to kill cells by synergistic effects β -lactone was tested in combination with the first-line drugs isoniazid (INH), rifampicin (Rif) and vancomycin (Vanc) in *Msmeg* by checkerboard resazurin assay (Fig. 3.10).^{135, 136} Synergistic effect were evaluated using fractional inhibitory concentration index (FICI). Application of INH and Rif did not show any increased or

decrease dose-response. In contrast combining Vanc and **EZ120** resulted in an MIC drop of four- and 125-fold, respectively and is strongly synergistic (Fig. 3.10). This drastic change of cell susceptibility might originate from a disrupted mycomembrane and increased influx as well as degenerated membrane synthesis.

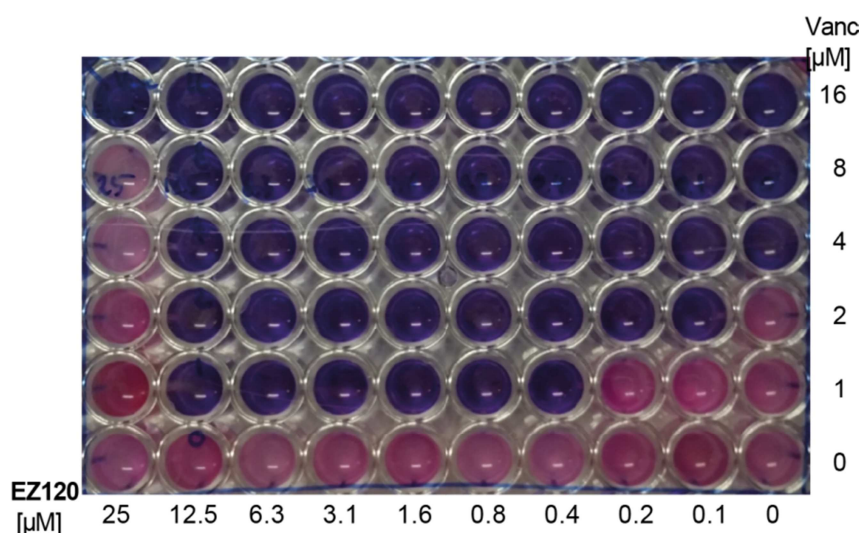


Fig. 3.10: Checkboard rasazurin assay applying Vancomycin vs. **EZ120** on Msmeg. Pink color indicates cellular growth. Blue color indicates no growth.

3.5 Effect of EZ120 on mycolic acid synthesis

Pks13 and the Ag85 proteins are not only shared members of the hydrolase family but also act on the same metabolic pathway catalyzing essential steps in mycobacterial cell membrane synthesis. It would therefore be intriguing to test the impact of β -lactone treatment on *de-novo* synthesis of mycolic acids. Classical methods utilize radiolabeling to track down and quantify metabolic pathways. As the application of radioactive material to a human pathogen increases handling and waste disposal exponentially, a method based on [^{13}C] MS detection had to be developed.¹³⁷ To establish the procedure initial experiments focused on mycolate levels of wt- and ΔAg85A Msmeg strains using INH as negative and a no-labeling replicate as positive control. In theory the mutant strain, lacking a mycolic acid transacylation enzyme, should incorporate less material in cell wall synthesis. Cells were grown in adjusted media to exponential phase and cell numbers were normalized. After short growth (~3h) in exponential phase [1,2- ^{13}C]acetate was added and bacteria were grown until stationary phase was entered. The cells were freeze-dried and normalized again by dry-weight. Free lipids were extracted and cell wall bound mycolates were saponified. Subsequent LC-MS analysis of isolated mycolates gave a complex pattern of peaks (Fig. 3.11A). Although no immediate interpretation could be made a significant change between applied conditions was observed and incorporation of [^{13}C -acetate] was successful. Comparison of trial runs with control clearly indicated that larger peaks represent mycolic acids without isotope

incorporation while “tailing” was created by far less abundant isotope labeled lipids. Problematically, a Gaussian-like distribution of incorporation interfered with variation of fatty acid chain length used for mycolic acid synthesis making the overall spectra unsuitable for analysis. Fortunately, ion-collision MS/MS experiments enabled directed fragmentation of mycolic acids into α - and mero-branch. As only charged particles of the α -branch were detectable, analysis of MS/MS spectra showed a significant difference of [^{13}C] incorporation and *de-novo* synthesis of cell wall associated mycolates (Fig. 3.11B).

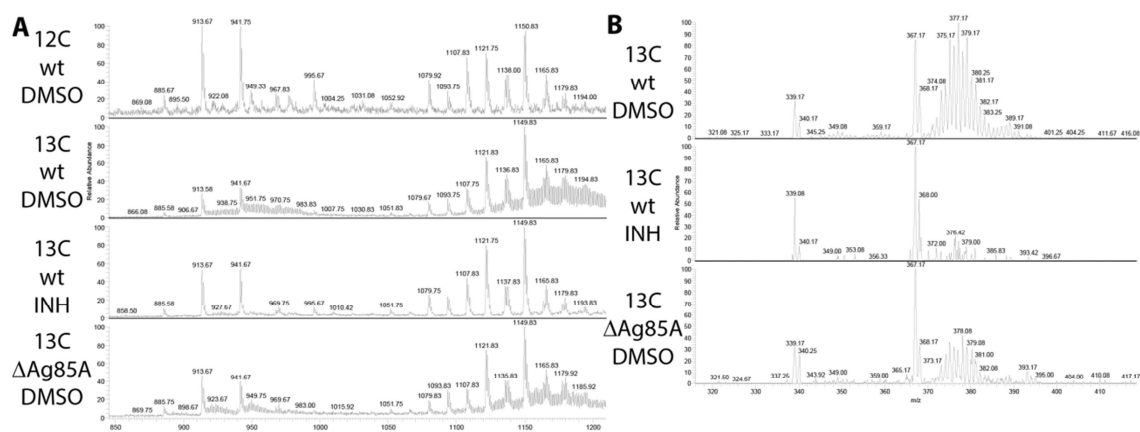


Fig. 3.11: Negative mode LC-MS analysis of cell wall bound MAs of Msmeg strains. A. Whole spectrum. B. Ion-induced fragmentation by MS/MS at 969 m/z.

With this functional novel methodology in hand following experiments aimed for dose response relations. As the MIC is more than 30-fold smaller in Mtb compared to Msmeg, switching from the model strain to the actual pathogen was necessary. Initial trials required control of bacterial growth under adjusted media conditions as well as pharmacokinetics of **EZ120** in Mtb. Furthermore working under biosafety level 3 conditions disables freeze-drying of cells and an adequate technique had to be established to reliably kill bacteria and extract lipids. Finally, Mtb was grown to exponential phase and normalized before **EZ120** was added in 1x, 5x and 10x MIC, as well as DMSO (positive control) and 5x INH MIC (negative control). Cells were grown for 3 h before [$1,2\text{-}^{13}\text{C}$]acetate was added and growth continued until stationary phase was entered. Bacteria were harvested, washed and suspended in $\text{CHCl}_3/\text{MeOH}=2/1$ over-night. Concentration of the supernatant to dryness gave extractable lipids, while dead cells could be saponified to yield cell wall bound mycolates. Subsequent LC-MS analysis applying multidimensional MS fragmentation of saponified samples resolved [^{13}C] incorporation levels as a direct measure of MA synthesis (Fig. 3.12A). Summing up all intensities of individual isotope labeled species shows *de-novo* incorporation of mycolates in cell wall structure (Fig. 3.12B). Increasing concentrations of **EZ120** showed a clear tendency to reduce cell wall bound MAs to about 30% of initial level. All experiments were performed in technical triplicates and at least biological duplicates.

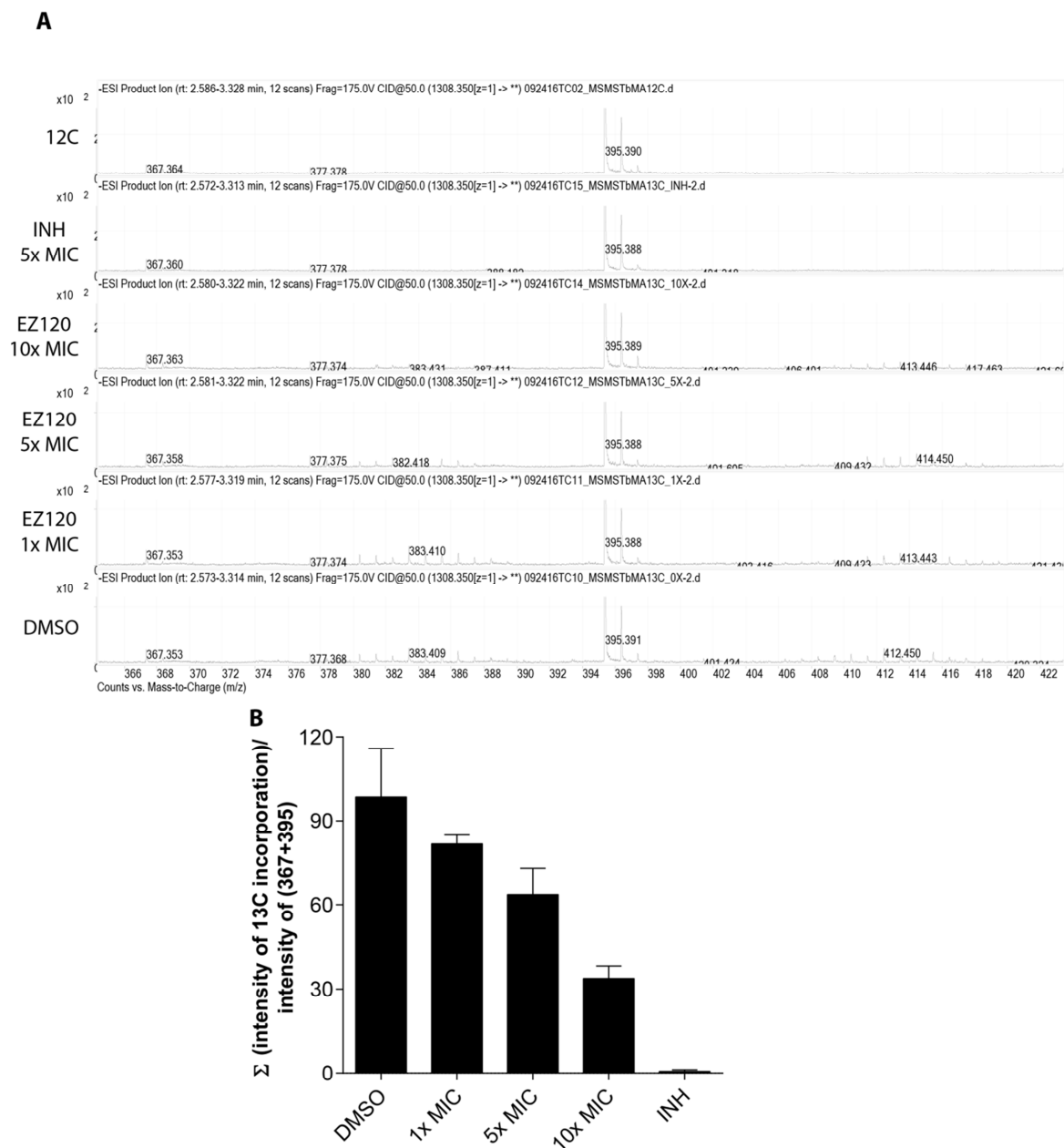


Fig. 3.12: Negative mode LC-MS analysis of cell wall bound MAs of Mtb with increasing concentration of EZ120. A. Full spectrum B. Sum of ¹³C incorporated fragment intensities of EZ120 treated cells. INH-negative control.

3.6 Conclusion

In summary β -lactones were tested for their anti-mycobacterial activity in *Msmeg* and *Mtb*. Target identification was conducted using probes based on parent compounds with retained activity utilizing state of the art methods of biological chemistry, genetics and proteomics. In-depth proteome analysis revealed two enzymes involved in mycobacterial lipid metabolism and cell wall assembly as prominent hits. *In-situ* and *in-vitro* studies of these enzymes provided sufficient data showing covalent binding and inhibition of the active site. Furthermore, extensive examinations of mycobacterial lipids led to the successful development of an isotope-based methodology to quantify mycolates from bacteria. This presents a major advantage to circumvent hazardous radiolabeling in pathogenic microorganisms. Application of this technique to initially found compounds underlined the assumption of involvement in essential lipid metabolism and provides a reasonable rationale for selective compound activity in mycobacteria.

Chapter 4 Lalistat

4.1 Lipid metabolism in mycobacteria

The integrity of mycobacterial cell membrane is essential for cellular survival and pathogenesis.¹ Serving as the primary defense line, bacteria require specialized membranes to protect the cell from environmental influences.¹⁹ In particular, prokaryotes able to endure inside eukaryotes, i.e. listeria or mycobacteria, are experts for membrane modification in order to adapt altered conditions, such as phagocytosis or immune response. Infection experiments with Mtb have shown that triacylglycerides (TAGs), one of the main membrane building blocks, accumulate within intracellular inclusion bodies.¹³⁸⁻¹⁴⁰ The metabolic turnover of TAGs to fatty acids is strictly regulated by hydrolases and lipases (Fig. 4.1).^{6, 141, 142} Homeostasis of lipids and fatty acids presents an important feature during bacterial infection of the host, providing a valuable energy source as well as a regulator for membrane fluidity and permeability.^{143, 144} Finally lipids are required for cell division to extend membranes building block for primary metabolic purposes. In addition fatty acids are crucial for mycobacterial survival in latent state.¹⁴⁵

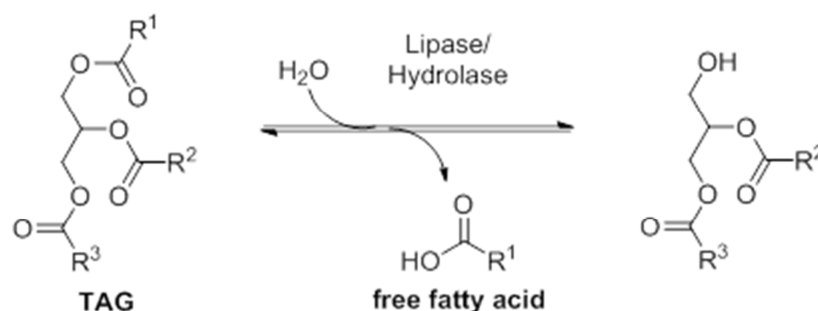
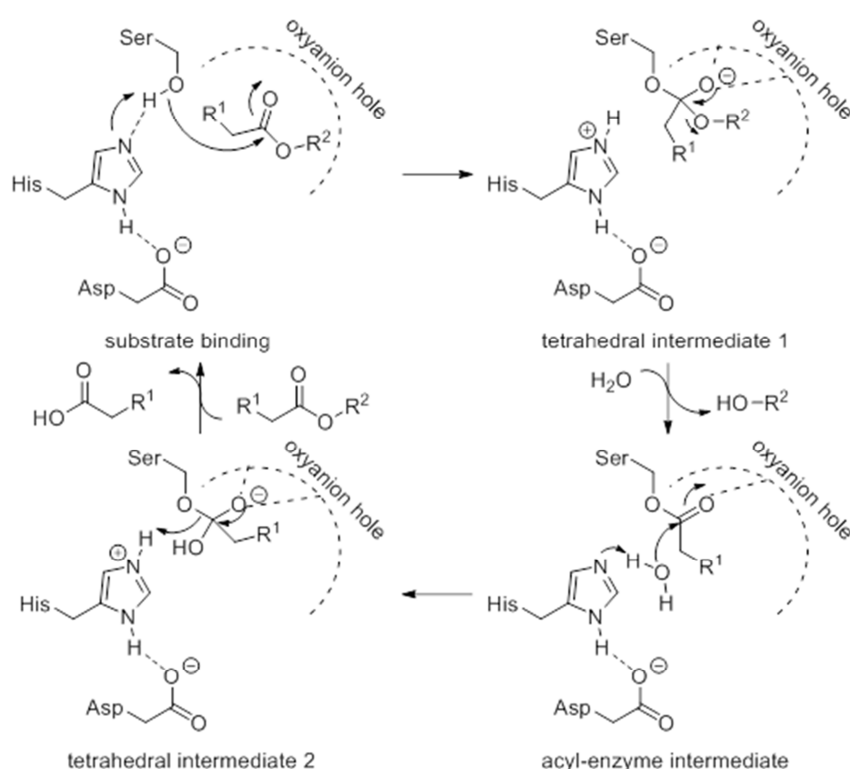


Fig. 4.1: Simplified mechanism of enzymatic TAG-hydrolysis. R₁-R₃ are usually long, unbranched hydrocarbon chains.

4.2 Mycobacterial hydrolases

Hydrolases make up an entire enzyme class ubiquitously found in nature. Lipases present a subclass specified to saponify hydrophobic esters, which are mostly fatty acid- or steroid based-molecules. The main common feature of this enzyme class is the conserved catalytic triad at the active site displaying a general mode of action (Scheme 4.1).¹⁴⁶ This triade consists of a nucleophile (serine, threonine or cysteine), a base (histidine, lysine or serine) and an acid (asparate or glutamate). In order to increase the strength of the nucleophile a hydrogen bond is formed by the base, which is itself activated by hydrogen bonding to the regularly charged acid. Additionally, active sites are usually equipped with an

oxyanion hole, which presents a pocket of positively charged residues (lysine, arginine and histidine) to stabilize a (partial) negative charge.



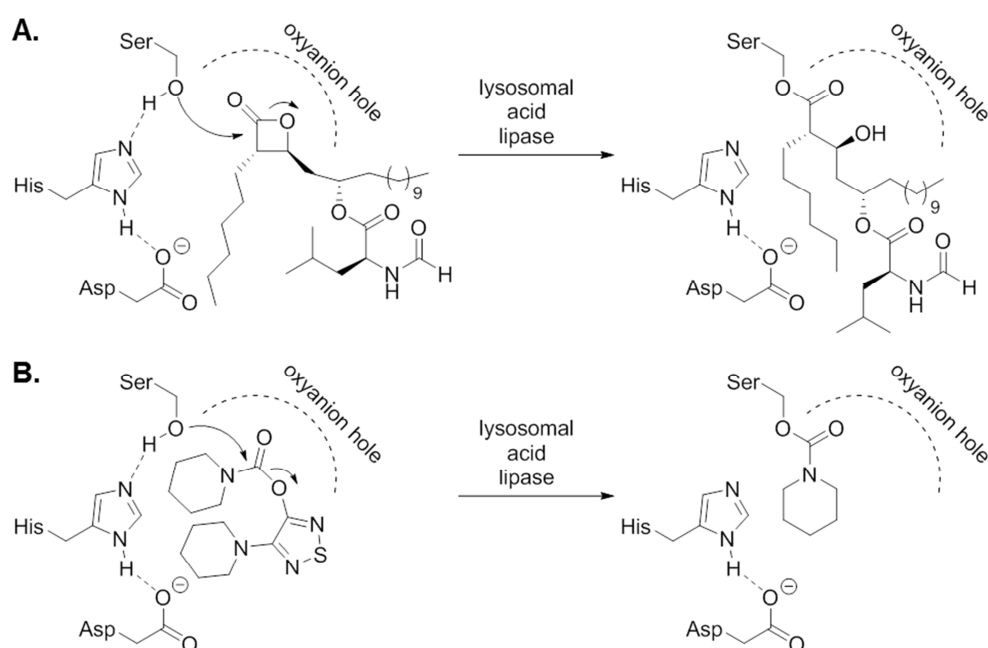
Scheme 4.1: General catalytic cycle of hydrolytic ester cleavage.

The ester substrate is recognized by the active site by affinity and steric demand of the binding pocket. In the initial step the nucleophile attacks the carbonyl functionality of the ester creating a primary tetrahedral intermediate with an oxyanion pointing into the corresponding pocket. During this process the base is protonated, forming an ionic bond to the previous hydrogen association. The formed anion stabilizes by reformation of a carbonyl group and thereby releases the alcoholate, which gets protonated by the charged base, and makes room for water. The previous substrate is now covalently bound to the enzyme by a newly formed ester bond. The associated water molecule is pre-activated by the base in a way that the oxygen serves as a nucleophile and attacks the carbonyl group again. Once more a tetrahedral intermediate with an oxyanion is formed and stabilized before the carbonyl functionality is retained under release of the free acid. The base donates a proton originating from water onto the nucleophile to restore the initial state in order to enable a new substrate turnover.

Functional restriction of certain enzymes can be anticipated to regulate cell specific processes externally. This can be to compensate a hyperfunction or to shut down a metabolic pathway completely. Molecular inhibitors are therefore commonly found and can be commercially available for certain enzymes.¹⁴⁷ Due to the conserved mode of action

reversible binding small molecules are more target selective but their efficacy highly depends on the affinity to its target protein. Reversible inhibitors mostly act on an allosteric site and induce conformational changes or block the active site. In contrast covalent binders modify parts of the catalytic triad to disrupt the catalytic mechanism. The enhanced nucleophilicity at the active site is frequently used to form a stable, hardly hydrolysable bond. Typically inhibitors mimic substrate properties to rest the catalytic cycle in the acyl-enzyme state.¹⁴⁸

An example for such covalent inhibition is orlistat, a marketed drug that primarily targets human lysosomal acid lipase (LAL) and is used to treat adiposity.^{38, 83, 149, 150} The molecule is based on the natural product lipstatin (Fig. 1.5) and characterized by a β -lactone ring, which provides an excellent electrophile to be attacked by the active site serine.¹⁵¹ Upon binding to the enzyme the lactone opens, additionally mediated by the cyclic ring strain, and the acylated enzyme cannot be hydrolyzed nor bind regular substrate (Scheme 4.2A).¹⁵² Based on this principle investigation on a second generation of inhibitors were made revealing the thiodiazole lalistat (**4.1**) as a more potent compound.¹²⁷ This molecule carries a piperidine carbamate as reactive group.¹²³ Similar to an ester the active site nucleophile attacks the carbonyl and the heterocyclic alcohol is released forming a new carbamate that disrupts the catalytic triade (Scheme 4.2B).



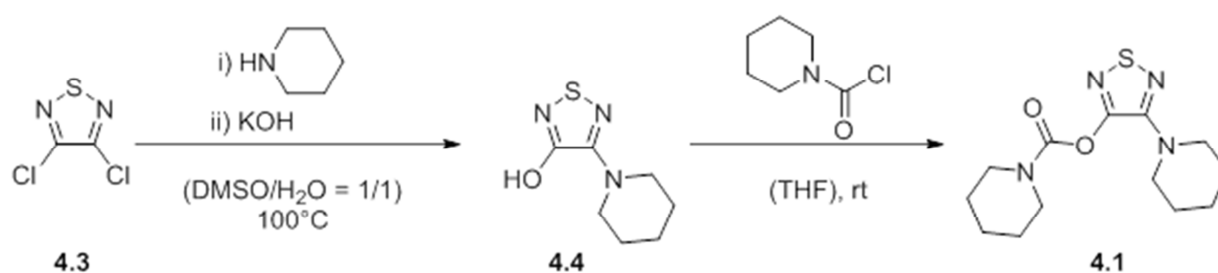
Scheme 4.2: Covalent inhibition of serine-hydrolases. **A.** Binding of orlistat under β -lactone opening. **B.** Binding of lalistat under carbamate reformation.

Since orlistat's mode of action and cellular targets had been elucidated in humans application to prokaryotic systems were analyzed.³⁸ Focusing on known mammalian lipase inhibitors could present a novel therapeutic strategy to treat bacterial infections. The mycobacterial genome encodes numerous hydrolytic enzymes involved in lipid

metabolism.¹⁵³ Among those, the lip gene family consisting of 24 lipid/ester hydrolases termed Lip C to Z, which share a conserved consensus sequence as well as alpha/beta hydrolase fold.¹⁵⁴ Previous studies already revealed an anti-mycobacterial effect of orlistat.¹⁵⁵ In-depth target analysis *via* ABPP with an alkynylated orlistat probe in *M. bovis* (BCG) revealed binding of multiple enzymes belonging to the Lip family. Inhibiting the TAG metabolism of mycobacteria could provide a new opportunity to shorten current treatment and encourages a detailed analysis of lalistat and its target spectrum.

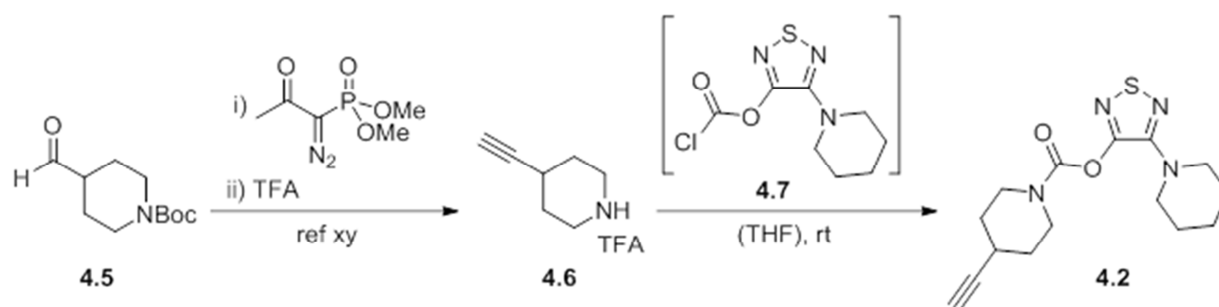
4.3 Synthesis of lalistat and ABPP probe

The synthesis of lalistat followed the published procedure of *Rosenbaum et al.* (Scheme 4.3).¹²⁷ Therefore, commercially available 3,4-dichloro-1,2,5-thiadiazole (**4.3**) was refluxed in piperidine replacing one chlorine substituent. Consecutively, a hydroxy functionality was generated by treatment of potassium hydroxide in a DMSO-water mixture at 100 °C. Finally, the obtained alcohol (**4.4**) was deprotonated using potassium *tert*-butanoate in THF and commercially available piperidine carbonylchloride was added to yield lalistat (**4.1**). Analysis of the final product by ¹H- and ¹³C-NMR as well as LC-HRMS was in agreement with published data.¹²⁷



Scheme 4.3: Synthetic route to lalistat.

In order to identify proteinogenic targets of lalistat a molecular ABPP probe (**4.2**) was required carrying an alkyne tag in a position that remains protein bound even after alteration of the active site. Therefore introduction of an acetylene moiety was anticipated onto the carbamate forming piperidine. This derivatization can be achieved by modification of the last step of the synthetic route. 4-Ethynylpiperidine (**4.6**) was obtained as a TFA-salt from commercially available *N*-Boc-piperidine-4-carboxaldehyde by subsequent Ohira-Bestmann homologation and deprotection.¹⁵⁶ Coupling of the two building blocks **4.7** and **4.6** was achieved by phosgene mediated activation of the alcohol **4.4** to the corresponding chloroformate **4.7**, which yielded the anticipated probe molecule **4.2** (Scheme 4.4).



Scheme 4.4: Synthetic design of a lalistat-based ABPP probe.

4.4 Bioactivity

Having lalistat (**4.1**) and its alkynylated derivative **4.2** in hand, enabled conduction of *in-situ* experiments in procaryotes. First, a broad screen of antibacterial activity was conducted to determine MICs against various bacterial stains. Lalistat showed no effect up to 200 μM concentration against Gram-negative strains and also no impact on viability on most Gram-positive bacteria was found (Table 4.1). Interestingly, the compound exhibited bioactivity against the human pathogenic strain Mtb H37Rv of about 25-30 μM whereas no growth deficit was observed for Msmeg mc(2) 155.

Table 4.1: MIC determination of lalistat and probe against various bacterial strains.

compound	<i>S. aureus</i> USA 300	<i>L. monocytogenes</i> EGD-e	<i>M. smegmatis</i> mc(2) 155	<i>M tuberculosis</i> H37Rv	<i>S. thyphimurium</i> It2	<i>P. aeruginosa</i> PAO1
 4.1	> 200 μM	> 200 μM	> 200 μM	25 μM	> 200 μM	> 200 μM
 4.2	> 200 μM	> 200 μM	> 200 μM	30 μM	> 200 μM	> 200 μM

For additional information of lalistat's anti-tuberculosis properties growth of green fluorescent protein (GFP) expressing Mtb H37Rv was monitored for 7 days in presence of either **4.1** or rifampicin and DMSO as controls.¹⁵⁷ A bacteriostatic effect was observed for lalistat down to a concentration of 4 μM (Fig. 4.2), which support the previous findings.

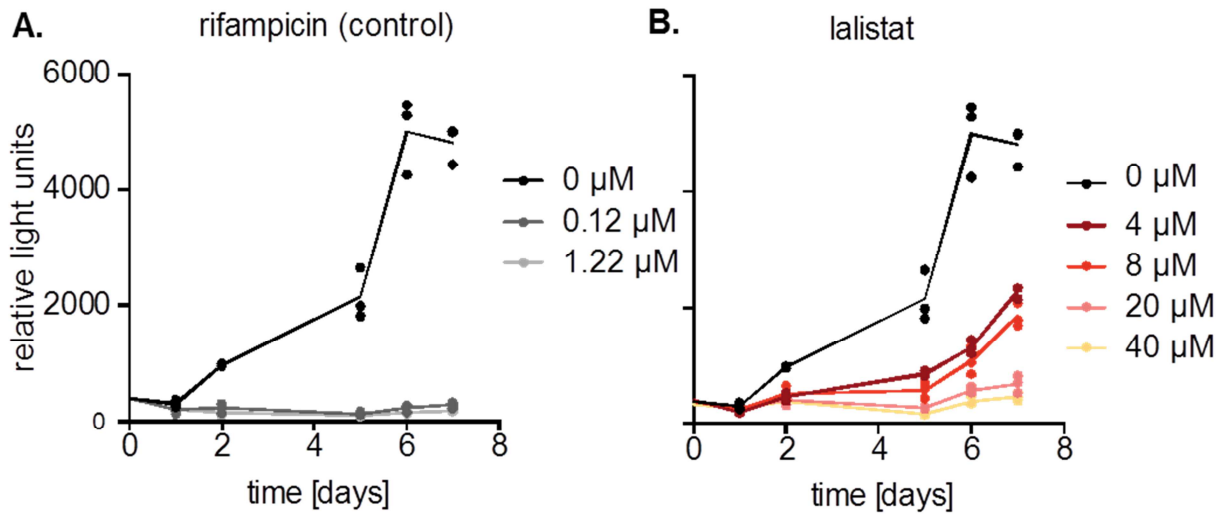


Fig. 4.2: Growth curves of GFP expressing Mtb strains in presence of varying concentrations of **A.** rifampicin or **B.** lalistat.

Finally, the effect of La-0 on intracellular growth of *M. tuberculosis* in human macrophage host cells was determined. Therefore human monocytes derived macrophages were treated with Mtb in a 1:1 ratio for 4 h. The cells were subsequently cultured for 7 days with various concentrations of 4.1 and DMSO as control. Afterwards cells were lysed and CFUs were determined.¹⁵⁸ Addition of lalistat during this process showed a sustainable reduction of the bacterial load by up to 55 % compared to the untreated control suggesting that the compound can even address intracellular bacteria (Fig. 4.3).

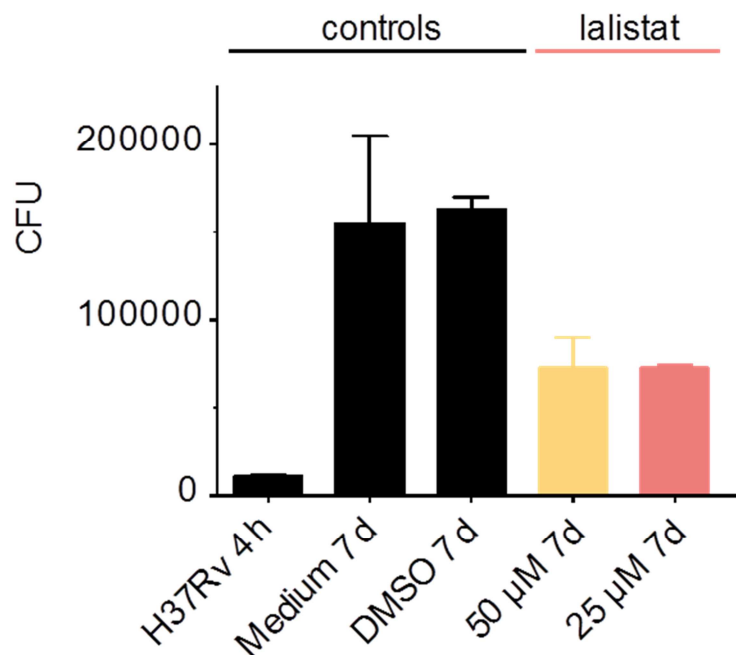


Fig. 4.3: CFU count of Mtb after macrophage infection and drug treatment.

Currently, Mtb infection is treated by a combination of up to four different drugs; therefore combinations of lalistat and various (myco-)bacterial drugs, namely INH, rif and Vanc, were tested by checkerboard assay. Remarkably, a strong effect was obtained for the combined application of lalistat and vancomycin resulting in a MIC drop of factor 4 for lalistat and 16 for vancomycin (Figure 4.4). Using the fractional inhibitory concentration index (FICI)^{135, 136} a cooperative effect could be concluded, which might originate from membrane disruption.

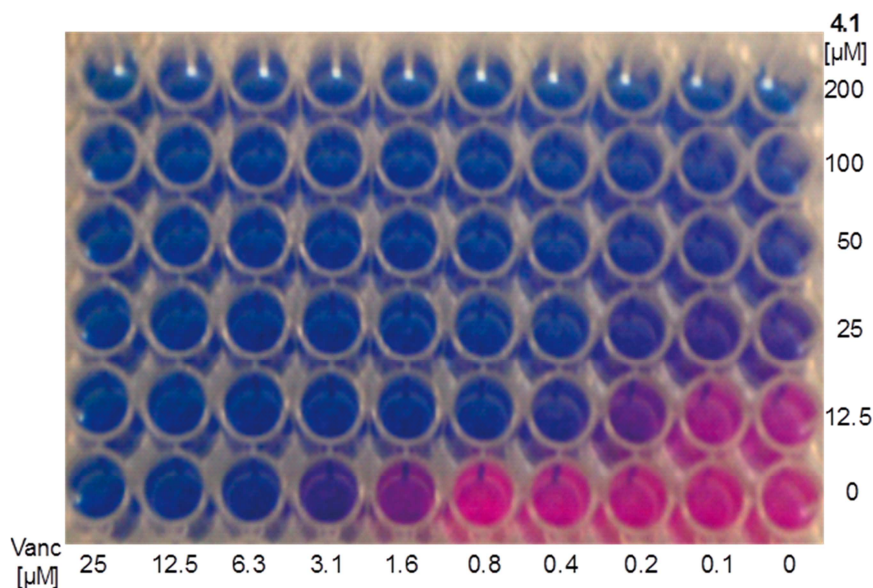


Fig. 4.4: Checkerboard resazurin assay for 4.1 and vancomycin against Mtb. Pink: growth. Purple: no growth.

4.5 Target identification

Probe compound **4.2**. retained the activity of the parent molecule making it suitable for further target identification studies (Table 4.1). First of all covalent protein labeling was examined by using analytical SDS-PAGE. Mtb cells were grown to exponential phase and treated with **4.2**. or DMSO as control for 1 h. After cell lysis a rhodamine tag was attached to the alkyne moiety via click-chemistry. Modified proteins were visualized by fluorescence scanning after gel separation (Fig. 4.5). Gel-based analysis of target specificity is obtained by competitive ABPP experiments. Bacteria are primarily treated with **4.1** before **4.2** is added to compete for specific binding sites. Interestingly, proteins around a molecular size of 30 kDa showed increased fluorescent signal response with raising probe concentration while others (~50 kDa) only marginally changed intensity. A concentration between 30 µM and 60 µM was sufficient to achieve saturated labelling, whereas excess of 3:1 of lalistat to probe enabled a strong decrease of signal intensity.

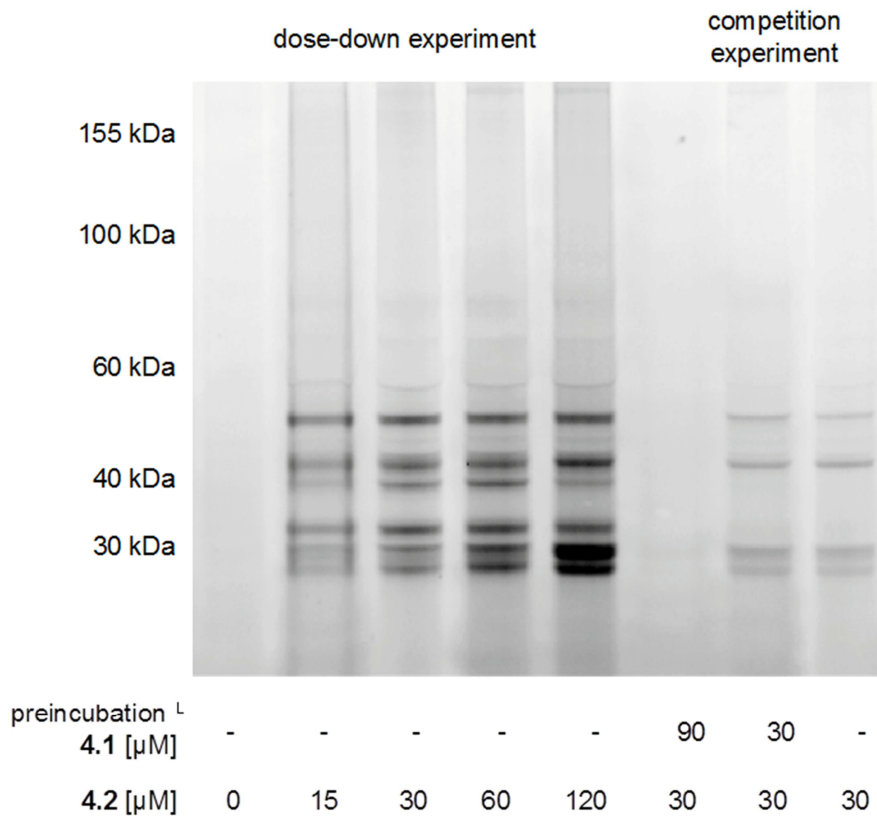


Fig. 4.5: Fluorescent signal of analytical SDS-PAGE of Mtb cytosolic fraction treated with lalistat.

For a detailed analysis of cellular targets gel-free proteomic experiments were conducted. As described previously (Chapter 2.4) modified proteins were clicked onto biotin azide after probe treatment and cell lysis.⁹⁸ This procedure enabled enrichment on avidin followed by a tryptic digest to obtain peptides, which were dimethyl labeled using light, medium and heavy isotope reagents including a label switch.⁹⁹ Pooling of differently labeled samples and LC-MS/MS analysis led to identification of enriched proteins, displayed in a volcano plot by the normalized and $\log_2(x)$ transformed labelling ratios of probe versus DMSO as a function of statistical significance ($-\log_{10} p$ -value) (Fig. 4.6A). To validate these enriched hits competitive experiments were performed using a 2:1 ratio of lalistat to probe concentration (Fig. 4.6B). Proteins enriched by a factor ≥ 4 with a p -value of 0.05 or below were considered as hits (cutoffs highlighted by dashed lines).

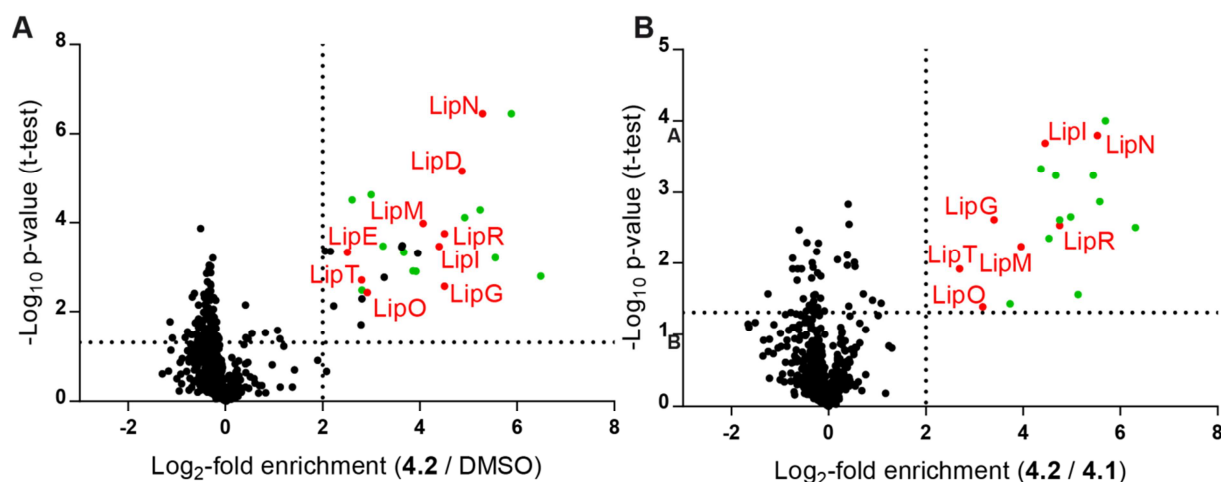


Fig. 4.6: Scatter plot of Mtb H37Rv cytosolic proteome analysis of **4.2** versus **A. DMSO** and **B. 4.1**. Red: Members of Lip protein family. Green: annotated hydrolases.

Using the set criteria for target identification revealed the majority of significantly enriched proteins as hydrolases (labeled in green). Even more striking is the fact that nine members of the Lip enzyme family were identified as promising hits (highlighted and annotated in red). Analyses of the competition experiments strongly support the initial findings as only hydrolases cross the set threshold. Furthermore seven Lip enzymes are shown to be selectively reacting with lalistat.

A comparison of lalistat hits with results of previous orlistat proteome labeling studies in *M. bovis* (BCG)⁸⁴ revealed Lip M, O, N, I and G as shared targets. Interestingly, the orlistat-based ABPP probe also revealed Lip H, V and W as targets, while Lip R and T were selectively captured by **4.2** (Table 4.2). This complementary lipase profile can be traced back to different physico-chemical properties and the mode of action of the two covalent inhibitors. It is thus intriguing to speculate that the shared preference for a common set of Lip enzymes may contribute to the growth inhibitory effects of both compounds.

Table 4.2: Comparative analysis of Lip-enzymes identified with hydrolase inhibitors.

Orlistat	shared	Lalistat
Lip H	Lip G	Lip R
Lip V	Lip I	Lip T
Lip W	Lip M	
	Lip N	
	Lip O	

4.6 Target validation

LipR is one of the most strongly enriched hits that was selectively found by proteomic analysis with **4.2**. Therefore it was exemplary confirmed as target by gel-based ABPP experiments. Heterologous overexpression of the Mtb enzyme in *E. coli* resulted in strong fluorescent in-situ labeling, whereas non-induced expression only showed a background signal indicating specific binding (Fig. 4.7). Coomassie stain reveals the protein selectivity of the overexpressed enzyme in presence of the *E. coli* proteome.

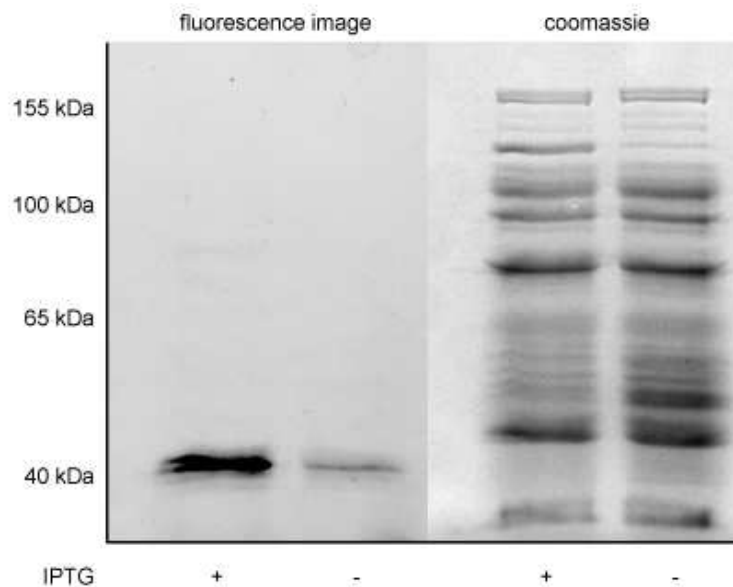


Fig. 4.7: Validation of LipR targeting by gel-based ABPP using **4.2**. “+”: addition of IPTG to induce protein expression.”-“: represents absence of inducer.

4.7 Conclusion

In summary lalistat has been shown to specifically inhibit growth of Mtb by independent experiments. Proteomic analysis revealed a selective set of lipases/hydrolases that are defunctionalized, which might result in disruption of membrane integrity. Especially reduced growth of lalistat treated Mtb in macrophages as well as combination with vancomycin lead to this conclusion. Given the importance of these enzymes for *M. tuberculosis* viability during infection they may represent promising drug targets. Future studies need to further dissect and characterize the exact function and mechanism of these enzymes in order to design customized inhibitors suited to interfere with essential metabolic processes specifically in the bacteria. With regard to the paucity of potent anti-mycobacterial inhibitors future tuberculosis treatment approaches could largely benefit from adding these compounds into treatment regimens. They could also pave the way for the development of more specific drugs targeting mycobacterial lipases. Their use in combination with known anti-mycobacterial agents may offer an urgently needed opportunity to improve and shorten tuberculosis therapy.

Chapter 5 Experimental Section

5.1 Organic chemistry

5.1.1 General Methods and Material

All reactions with air- or moisture-sensitive substances were carried out using standard SCHLENK techniques with Argon (Ar 4.6) as inert gas. Unless indicated otherwise, glass equipment was dried under high vacuum (10^{-3} mbar) at 500–600 °C using a heat gun. All chemical reagents and solvents were of reagent grade or of higher purity and used without further purification as obtained from commercial sources. Reactions at temperatures below 0 °C were carried out using Dewar-vessels for cooling. Reaction temperatures correlate to the following cooling substances: ice/CaCl₂ (-32 °C), acetone/dry-ice (-78 °C). Yields refer to purified, dried and spectroscopically pure substances if not reported otherwise.

Flash column chromatography was performed on Merck silica gel (Geduran Si 60, 0.040 – 0.063 mm) using a forced flow eluent at 0.3 – 0.5 bar pressure. Analytical thin layer chromatography (TLC) was performed on aluminum-backed TLC Silica gel 60 F254 plates by Merck and compounds were visualized by UV detection ($\lambda = 254$ nm) or staining via one of the listed stains followed by heating:

- Cerammonium molybdate [CAM]: 2.00 g cer-(IV)-sulfate, 50.0 g ammonium molybdate, 50.0 mL conc. sulfuric acid, 300 mL water
- Potassium permanganate [KMnO₄]: 3.00 g potassium permanganate, 20.0 g potassium carbonate, 5.00 mL 5 % sodium hydroxide solution, 300 mL water
- Ninhydrin solution: 300 mg ninhydrin, 3.00 mL glacial acetic acid, 100 mL *n*-butanol

Reverse-phase HPLC analysis was performed on a Waters 2695 separation module, equipped with a Waters PDA 2996 and a Waters XBridge C18 column (3.5 mm, 4.6 x 100 mm, flow = 1.2 mL/min). For preparative scale RP-HPLC separation a Waters 2545 quaternary gradient module in combination with a Waters PDA 2998 and a Waters XBridge C18 (5.0 μ m, 30 x 150 mm, flow = 50 mL/min) column or a YMC Triart C18 (3.5 μ m, 10 x 250 mm, flow = 10 mL/min) column was used. The mobile phase for elution consisted of a gradient mixture of 0.1 % (v/v) TFA in water (buffer A, HPLC grade) and 0.1 % (v/v) TFA in ACN (buffer B, HPLC grade) unless noted otherwise.

¹H NMR and ¹³C NMR spectra were recorded at RT on Bruker Avance 200, Avance 360, Avance 400, Avance 500 and Avance III 500cr spectrometers. Chemical shifts (δ -values) were referenced to the residual proton or carbon signal of the deuterated solvent in

Chapter 5

ppm. Coupling constants (J) are reported in Hertz (Hz) and multiplicity is reported as follows: s – singlet, d – doublet, t – triplet, q – quartet, m – multiplet, br – broad.

High resolution mass spectra were obtained on a Thermo Scientific LTQ-FT Ultra via electron ionization (ESI-MS) or atmospheric-pressure chemical ionization (APCI-MS).

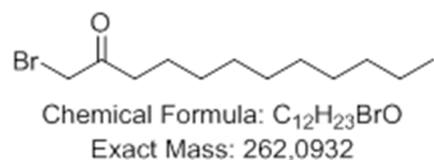
Specific optical rotation spectra were obtained on a Perkin-Elmer polarimeter 241 MC using a 1 dm cuvette at $\lambda = 589$ nm (Na-D-line) at RT. Substances were used in g/100 mL concentrated solutions. Optical rotations are annotated in $10^{-1} \text{ }^\circ \text{ cm}^2 \text{ g}^{-1}$.

5.1.2 Synthesis

5.1.2.1 General procedure for α -bromo ketones^{85, 86}

Carboxylic acid (1.00 eq) was dissolved in CH_2Cl_2 (0.5 M) and DMF (0.05 eq) was added dropwise at rt. Oxalyl chloride (1.20 eq) was added dropwise in portions while gas formation was observed. The reaction mixture was stirred for 3 h and concentrated under reduced pressure. The crude residue was dissolved in ACN (0.5 M) and cooled to 0 °C. TMS diazomethane (1.10 eq, 2 M in Et_2O) was slowly added dropwise. The reaction was stirred for 16 h and warmed to rt. Solvents were removed *in-vacuo* and the remaining residue was dissolved in Et_2O (0.4 M) at rt. Hydrogen bromine (10.0 eq, 37% in H_2O) was slowly added and gas formation could be observed. The reaction mixture was heated under reflux for 3 h and stopped by addition of saturated NaCO_3 solution. After separation of phases the aqueous layer was extracted with EtOAc (3 x 50 mL) and the combined organic layers were washed with brine, dried over MgSO_4 , filtered and concentrated to dryness under reduced pressure. The crude residue was applied to flash chromatography. The product was isolated as a white wax.

1-Bromododecan-2-one



Yield: 97%

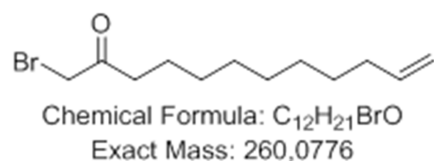
R_f = 0.32 (Pentane/ Et_2O = 98/2).

$^1\text{H-NMR}$ (400 MHz, CDCl_3): δ [ppm] = 3.88 (s, 2 H), 2.64 (t, J = 7.4 Hz, 2 H), 1.66-1.56 (m, 2 H), 1.35-1.18 (m, 14 H), 0.87 (t, J = 6.6 Hz, 3 H).

$^{13}\text{C-NMR}$ (91 MHz, CDCl_3): δ [ppm] = 202.5, 40.0, 34.4, 32.0, 29.6, 29.5, 29.5, 29.4, 29.2, 24.0, 22.8, 14.3.

HRMS (APCI): calc. for $\text{C}_{12}\text{H}_{24}\text{BrO}$ $[\text{M}+\text{H}]^+$: 263.1005; found: 263.1008.

1-Bromododec-11-en-2-one



Yield: 94%

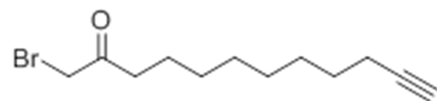
R_f = 0.34 (Pentane/ Et_2O = 98/2).

¹H-NMR (300 MHz, CDCl₃): δ [ppm] = 5.81 (ddt, *J* = 6.7, 10.1, 16.9 Hz, 1 H), 5.03- 4.89 (m, 2 H), 3.88 (s, 2H), 2.64 (t, *J* = 7.4 Hz, 2 H), 2.08-1.98 (m, 2 H), 1.63-1.55 (m, 2 H), 1.39-1.27 (m, 10 H).

¹³C-NMR (76 MHz, CDCl₃): δ [ppm] = 202.4, 139.3, 114.3, 40.0, 34.5, 33.9, 29.4, 29.3, 29.2, 29.0, 24.0, 23.7.

HRMS (APCI): calc. for C₁₂H₂₂BrO [M+H]⁺: 261.0849; found: 261.0841.

1-Bromododec-11-yn-2-one



Chemical Formula: C₁₂H₁₉BrO
Molecular Weight: 259.19

Yield: 96%

R_f = 0.35 (Pentane/Et₂O = 98/2).

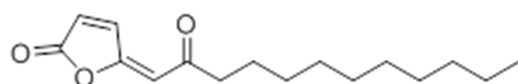
¹H-NMR (300 MHz, CDCl₃): δ [ppm] = 3.87 (s, 2 H), 2.64 (t, *J* = 7.4 Hz, 2 H), 2.17 (td, *J* = 2.6, 7.0 Hz, 2 H), 1.93 (t, *J* = 2.6 Hz, 1 H), 1.68-1.44 (m, 4 H), 1.45-1.20 (m, 8 H).

¹³C-NMR (63 MHz, CDCl₃): δ [ppm] = 202.3, 84.8, 68.2, 39.9, 34.4, 29.3, 29.1, 29.0, 28.8, 28.6, 24.0, 18.5.

HRMS (APCI): calc. for C₁₂H₂₀BrO [M+H]⁺: 259.0692; found: 259.0691.

5.1.2.2 General procedure for 5-(2-Oxododecylidene)furan-2(5H)-ones^{79, 87, 89}

α-Bromo ketone (1.00 eq) was dissolved in CHCl₃ (0.2 M) at rt and PPh₃ (1.10 eq) was added. The clear solution turned turbid within 30 min and was stirred for 16 h. Solvents were removed under reduced pressure and the residue was dissolved in MeOH/H₂O (v/v = 4/1, 0.4 M). KOH (10.0 eq, 5 M in H₂O) was added at rt. The reaction mixture immediately turned into an orange/yellow suspension, which was rigorously stirred for 3 h. After separation of layers the aqueous phase was extracted with CH₂Cl₂ (3 x 40 mL). The combined organic layers were combined, washed with brine, dried over MgSO₄, filtered and concentrated to dryness under reduced pressure. The waxy residue was dissolved in toluene (0.02 M) and maleic anhydride (1.20 eq) was added at rt. The reaction mixture was heated to 110 °C and refluxed for 16 h. The reaction was allowed to cool down to rt and solvents were removed *in-vacuo*. The residue was applied to flash chromatography to yield the corresponding (*E*)- and (*Z*)- constituted olefins as white solids.

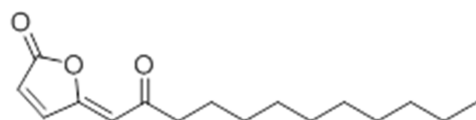
(E)-5-(2-Oxododecylidene)furan-2(5*H*)-one (**2.7**)Chemical Formula: C₁₆H₂₄O₃

Exact Mass: 264,17

Yield: 45% R_f = 0.22 (H/EtOAc = 92/8).

¹H-NMR (500 MHz, CDCl₃): δ [ppm] = 8.32 (dd, J = 0.7, 5.6 Hz, 1 H), 6.47 (dd, J = 1.7, 5.6 Hz, 1 H), 6.24 (dd, J = 0.7, 1.7 Hz, 1 H), 2.58 (t, J = 7.4 Hz, 2 H), 1.67-1.55 (m, 2 H), 1.34-1.20 (m, 14 H), 0.87 (t, J = 6.8 Hz, 3 H).

¹³C-NMR (126 MHz, CDCl₃): δ [ppm] = 200.1, 168.2, 158.7, 143.0, 125.2, 107.9, 45.3, 32.0, 29.7, 29.6, 29.5, 29.4, 29.2, 24.1, 22.8, 14.3.

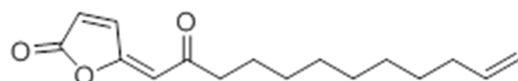
HRMS (ESI): calc. for C₁₆H₂₅O₃ [M+H]⁺: 267.1798; found: 267.1796.*(Z)*-5-(2-Oxododecylidene)furan-2(5*H*)-one (**2.8**)Chemical Formula: C₁₆H₂₄O₃

Exact Mass: 264,17

Yield: 15% R_f = 0.30 (H/EtOAc = 70/30).

¹H-NMR (500 MHz, CDCl₃): δ [ppm] = 7.48 (d, J = 5.6 Hz, 1 H), 6.42 (d, J = 5.6 Hz, 1 H), 5.56 (s, 1 H), 2.87 (t, J = 7.3 Hz, 2 H), 1.66-1.58 (m, 2 H), 1.34-1.20 (m, 14 H), 0.86 (t, J = 7.1 Hz, 3 H).

¹³C-NMR (75 MHz, CDCl₃): δ [ppm] = 199.2, 168.0, 154.4, 145.8, 123.4, 110.7, 43.6, 32.0, 29.7, 29.6, 29.6, 29.5, 29.3, 24.0, 22.8, 14.3.

HRMS (ESI): calc. for C₁₆H₂₅O₃ [M+H]⁺: 265.1798; found: 265.1796.*(E)*-5-(2-Oxododec-11-en-ylidene)furan-2(5*H*)-one (**2.15**)Chemical Formula: C₁₆H₂₂O₃

Exact Mass: 262,16

Yield: 42% R_f = 0.26 (H/EtOAc = 90/10).

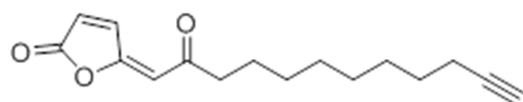
¹H-NMR (300 MHz, CDCl₃): δ [ppm] = 8.32 (dd, J = 0.7, 5.6 Hz, 1 H), 6.47 (dd, J = 1.7, 5.6 Hz, 1 H), 6.24 (dd, J = 0.7, 1.7 Hz, 1 H), 5.81 (ddt, J = 6.7, 10.1, 17.0 Hz, 2 H), 5.04-4.88

(m, 1 H), 2.60 (t, $J = 7.4$ Hz, 2 H), 2.09-1.98 (m, 2 H), 1.67-1.55 (m, 2 H), 1.34-1.20 (m, 12 H).

$^{13}\text{C-NMR}$ (126 MHz, CDCl_3): δ [ppm] = 200.0, 168.2, 158.8, 143.0, 139.3, 125.2, 114.3, 107.9, 45.3, 33.9, 29.5, 29.4, 29.2, 29.0, 24.1.

HRMS (ESI): calc. for $\text{C}_{16}\text{H}_{23}\text{O}_3$ $[\text{M}+\text{H}]^+$: 263.1642; found: 263.1644.

(*E*)-5-(2-Oxododec-11-yn-ylidene)furan-2(5*H*)-one (**2.17**)



Chemical Formula: $\text{C}_{16}\text{H}_{20}\text{O}_3$
Exact Mass: 260,14

Yield: 37%

$R_f = 0.29$ (H/EtOAc = 90/10).

$^1\text{H-NMR}$ (300 MHz, CDCl_3): δ [ppm] = 8.32 (dd, $J = 0.7, 5.6$ Hz, 1 H), 6.47 (dd, $J = 1.7, 5.6$ Hz, 1 H), 6.23 (dd, $J = 0.7, 1.7$ Hz, 1 H), 2.58 (t, $J = 7.4$ Hz, 2 H), 2.18 (dt, $J = 2.6$ Hz, 7.1, 2 H), 1.93 (t, $J = 2.6$ Hz, 1 H), 1.68-1.60 (m, 2 H), 1.55-1.49 (m, 4 H), 1.43-1.34 (m, 2 H), 1.34-1.20 (m, 6 H).

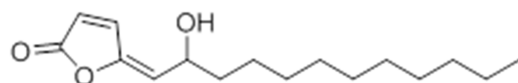
$^{13}\text{C-NMR}$ (90.6 MHz, CDCl_3): δ [ppm] = 199.9, 168.2, 158.8, 143.0, 125.2, 107.9, 83.7, 68.3, 45.3, 29.4, 29.2, 29.0, 28.8, 28.6, 24.1, 18.5.

HRMS (ESI): calc. for $\text{C}_{16}\text{H}_{21}\text{O}_3$ $[\text{M}+\text{H}]^+$: 261.1485; found: 261.1485.

5.1.2.3 General procedure for 5-(2-Hydroxydodecylidene)furan-2(5*H*)-ones⁹⁰

5-(2-Oxododecylidene)furan-2(5*H*)-one (1.00 eq) was dissolved in THF (1.0 M) at rt. NaBH_3CN (5.00 eq, 2 M in THF) was added at rt and the reaction mixture was stirred for 1 h. The reaction was stopped by addition of HCl (15 mL, 2 M) and stirred for 1 h. The solution was diluted with EtOAc and after separation of layers the aqueous phase was extracted with EtOAc (3 x 15 mL). The combined organic layers were washed with brine, dried over MgSO_4 , filtered and concentrated *in-vacuo*. The remaining residue was applied to flash chromatography to yield the desired alcohols as white waxes.

(±)-Ramariolide C (**2.3**)



Chemical Formula: $\text{C}_{16}\text{H}_{26}\text{O}_3$
Exact Mass: 266,19

Yield: 93%

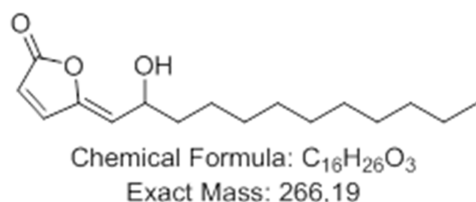
R_f = 0.24 (H/EtOAc = 70/30).

$^1\text{H-NMR}$ (500 MHz, CDCl_3): δ [ppm] = 7.80 (d, J = 5.6 Hz, 1 H), 6.24 (dd, J = 1.7, 5.6 Hz, 1 H), 5.75 (dd, J = 1.7, 8.1 Hz, 1 H), 4.52 (dt, J = 6.5, 8.1 Hz, 1 H), 1.80 (bs, 1 H), 1.76-1.66 (m, 1 H), 1.66-1.57 (m, 1 H), 1.36-1.20 (m, 14 H), 0.87 (t, J = 6.8 Hz, 3 H).

$^{13}\text{C-NMR}$ (126 MHz, CDCl_3): δ [ppm] = 169.5, 150.6, 140.8, 121.2, 117.6, 68.4, 38.1, 32.0, 29.7, 29.7, 29.6, 29.5, 29.4, 25.4, 22.8, 14.3.

HRMS (ESI): calc. for $\text{C}_{16}\text{H}_{27}\text{O}_3$ $[\text{M}+\text{H}]^+$: 267.1955; found: 267.1952.

(*Z*)-5-(2-Hydroxydodecylidene)furan-2(5*H*)-one (**2.20**)



Yield: 95%

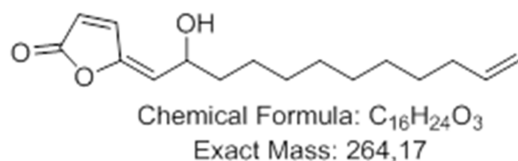
R_f = 0.22 (H/EtOAc = 70/30).

$^1\text{H-NMR}$ (500 MHz, CDCl_3): δ [ppm] = 7.37 (d, J = 5.4 Hz, 1 H), 6.22 (d, J = 5.4 Hz, 1 H), 5.32 (d, J = 8.4 Hz, 1 H), 4.82-4.76 (m, 1 H), 1.92 (bs, 1 H), 1.74-1.69 (m, 1 H), 1.63-1.54 (m, 1 H), 1.36-1.21 (m, 14 H), 0.87 (t, J = 6.8 Hz, 3 H).

$^{13}\text{C-NMR}$ (126 MHz, CDCl_3): δ [ppm] = 169.5, 149.0, 144.0, 120.5, 118.5, 67.2, 37.2, 32.0, 29.7, 29.7, 29.7, 29.6, 29.5, 25.3, 22.8, 14.3.

HRMS (ESI): calc. for $\text{C}_{16}\text{H}_{27}\text{O}_3$ $[\text{M}+\text{H}]^+$: 267.1955; found: 267.1961.

(\pm)-Ramariolide D (**2.4**)



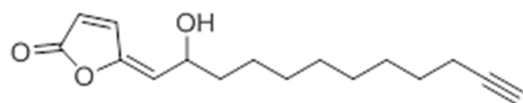
Yield: 82%

R_f = 0.29 (H/EtOAc = 65/45).

$^1\text{H-NMR}$ (500 MHz, C_6D_6): δ [ppm] = 6.98 (dd, J = 0.6, 5.6 Hz, 1 H), 5.81 (ddt, J = 6.7, 10.2, 17.0 Hz, 1 H), 5.57 (dd, J = 1.8, 5.6 Hz, 1 H), 5.36 (dd, J = 1.8, 7.9 Hz, 1 H), 5.06 (dq, J = 1.7, 17.0 Hz, 1 H), 5.01 (dt, J = 1.6, 10.2 Hz, 1 H), 3.94-3.88 (m, 1 H), 2.07-1.97 (m, 2 H), 1.38-1.31 (m, 4 H), 1.31-1.08 (m, 10 H).

$^{13}\text{C-NMR}$ (126 MHz, C_6D_6): δ [ppm] = 167.9, 149.8, 139.3, 138.4, 120.2, 115.7, 113.7, 67.2, 37.4, 33.3, 29.2, 29.1, 29.1, 28.8, 28.6, 24.8.

HRMS (ESI): calc. for $\text{C}_{16}\text{H}_{25}\text{O}_3$ $[\text{M}+\text{H}]^+$: 265.1798; found: 265.1798.

(E)-5-(2-Hydroxydodec-11-yn-ylidene)furan-2(5*H*)-one (**2.18**)Chemical Formula: C₁₆H₂₂O₃

Exact Mass: 262,16

Yield: 72%**R_f** = 0.27 (H/EtOAc = 65/45).

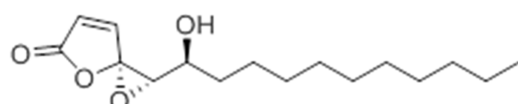
¹H-NMR (250 MHz, CDCl₃): δ [ppm] = 7.80 (dd, *J* = 0.7, 5.6 Hz, 1 H), 6.25 (dd, *J* = 1.8, 5.6 Hz, 1 H), 5.75 (ddd, *J* = 0.7, 1.8, 8.2 Hz, 1 H), 4.52 (dt, *J* = 6.5, 8.2 Hz, 1 H), 2.18 (td, *J* = 2.6, 6.9 Hz, 2 H), 1.94 (t, *J* = 2.6 Hz, 1 H), 1.78-1.43 (m, 4 H), 1.43-1.18 (m, 10 H).

¹³C-NMR (91 MHz, CDCl₃): δ [ppm] = 169.4, 150.7, 140.8, 121.3, 117.5, 84.9, 68.4, 68.3, 38.1, 29.5, 29.1, 28.8, 28.6, 25.4, 18.5.

HRMS (ESI): calc. for C₁₆H₂₃O₃ [M+H]⁺: 263.1642; found: 263.1642.

5.1.2.4 General procedure for 1-Hydroxyundecyl)-1,4-dioxaspiro[2.4]hept-6-en-5-ones^{91, 92}

(E)-5-(2-Hydroxydodecylidene)furan-2(5*H*)-one (1.00 eq) was dissolved in CH₂Cl₂ (0.5 M) at -32 °C. Titanium-(IV)-isopropoxide (1.20 eq) and (+)-DIPT (1.40 eq) were added and the reaction mixture was stirred for 30 min before *t*BuO₂H (4.50 eq, 5.5 M in H) was added. The reaction was allowed to warm to rt under constant stirring for 16 h. The reaction was stopped by addition of one volume of saturated potassium tartrate solution, freezing and rethawing. After separation of layers the aqueous phase was extracted with CH₂Cl₂ (3 x 10 mL) and the organic layers were combined, washed with brine, dried over MgSO₄, filtered and concentrated to dryness under reduced pressure. The remaining residue was applied to flash chromatography followed by RP-HPLC to yield the desired product as a white wax. Ee-values were determined by NMR-titration using Europium tris[3-(heptafluoropropylhydroxymethylene)-(+)-camphorate].

(-)-Ramariolide A (**2.1**)Chemical Formula: C₁₆H₂₆O₄

Exact Mass: 282,18

Yield: 35% (d.r. anti/syn = 87/13, ee = 55 %)**R_f** = 0.31 (H/EtOAc = 70/30).

RP-HPLC (analytical setup, method: gradient 2% B → 98% B over 10 min): $t_R = 9.53$ min.

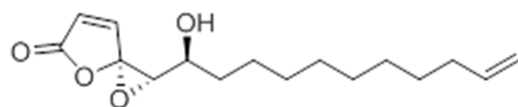
$^1\text{H-NMR}$ (400 MHz, CDCl_3): δ [ppm] = 7.55 (d, $J = 5.7$ Hz, 1 H), 6.35 (d, $J = 5.7$ Hz, 1 H), 4.08 (ddd, $J = 3.2, 4.4, 7.7$ Hz, 1 H), 3.78 (d, $J = 3.2$ Hz, 1 H), 1.93 (bs, 1 H), 1.70-1.56 (m, 2 H), 1.56-1.43 (m, 2 H), 1.35-1.20 (m, 14 H), 0.87 (t, $J = 6.8$ Hz, 3 H).

$^{13}\text{C-NMR}$ (101 MHz, CDCl_3): δ [ppm] = 168.5, 149.2, 126.4, 89.9, 67.6, 64.9, 33.7, 32.0, 29.7, 29.7, 29.6, 29.6, 29.4, 25.3, 22.8, 14.3.

HRMS (ESI): calc. for $\text{C}_{16}\text{H}_{25}\text{O}_4$ $[\text{M-H}]^-$: 281.1758; found: 281.1763.

$[\alpha]_D^{25}$ -78 (c 5.4, MeOH).

(2*S*,3*S*)-2-((*S*)-1-Hydroxyundec-10-en-1-yl)-1,4-dioxaspiro[2.4]hept-6-en-5-one (**2.16**)



Chemical Formula: $\text{C}_{16}\text{H}_{24}\text{O}_4$
Exact Mass: 280,17

Yield: 27%

$R_f = 0.30$ (H/EtOAc = 70/30).

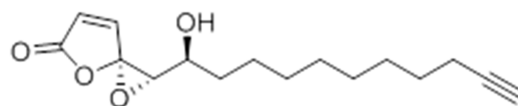
RP-HPLC (analytical setup, method: gradient 2% B → 98% B over 10 min): $t_R = 9.48$ min.

$^1\text{H-NMR}$ (500 MHz, CDCl_3): δ [ppm] = 7.44 (d, $J = 5.7$ Hz, 1 H), 6.39 (d, $J = 5.7$ Hz, 1 H), 5.81 (ddt, $J = 6.7, 10.2, 17.0$ Hz, 1 H), 4.99 (dt, $J = 1.8, 17.0$ Hz, 1 H), 4.95-4.88 (m, 1 H), 3.89-3.82 (m, 1 H), 3.78 (d, $J = 4.0$ Hz, 1 H), 2.04 (q, $J = 7.0, 7.2$ Hz, 2 H), 1.74-1.58 (m, 4 H), 1.37-1.23 (m, 10 H).

$^{13}\text{C-NMR}$ (126 MHz, CDCl_3): δ [ppm] = 162.2, 148.5, 139.3, 126.9, 114.3, 110.1, 90.4, 68.4, 65.5, 34.9, 33.9, 29.5, 29.5, 29.2, 29.0, 25.1.

HRMS (ESI): calc. for $\text{C}_{16}\text{H}_{25}\text{O}_4$ $[\text{M+H}]^+$: 281.1747; found: 281.1748.

(2*S*,3*S*)-2-((*S*)-1-Hydroxyundec-10-yn-1-yl)-1,4-dioxaspiro[2.4]hept-6-en-5-one (**2.19**)



Chemical Formula: $\text{C}_{16}\text{H}_{22}\text{O}_4$
Exact Mass: 278,15

Yield: 13%

$R_f = 0.30$ (H/EtOAc = 70/30).

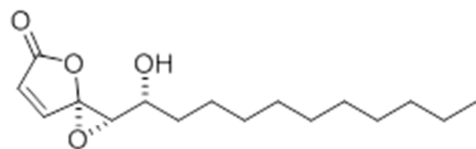
RP-HPLC (analytical setup, method: gradient 2% B → 98% B over 10 min): $t_R = 9.59$ min.

$^1\text{H-NMR}$ (500 MHz, CDCl_3): δ [ppm] = 7.56 (d, $J = 5.7$ Hz, 1 H), 6.36 (d, $J = 5.7$ Hz, 1 H), 4.09 (ddd, $J = 3.1, 4.3, 7.7$ Hz, 1 H), 3.79 (d, $J = 3.1$ Hz, 1 H), 2.18 (td, $J = 2.6, 7.1$ Hz, 2 H), 1.94 (t, $J = 2.6$ Hz, 1 H), 1.67-1.58 (m, 2 H), 1.53-1.44 (m, 4 H), 1.42-1.21 (m, 8 H).

$^{13}\text{C-NMR}$ (126 MHz, CDCl_3): δ [ppm] = 168.6, 149.2, 126.4, 110.1, 89.9, 84.9, 68.3, 67.5, 64.9, 33.6, 29.5, 29.1, 28.8, 28.5, 25.3, 18.5.

HRMS (ESI): calc. for $\text{C}_{16}\text{H}_{23}\text{O}_4$ $[\text{M}+\text{H}]^+$: 279.1591; found: 279.1591.

5.1.2.5 (2*S**,3*R**)-2-((*R**)-1-Hydroxyundecyl)-1,4-dioxaspiro[2.4]hept-6-en-5-one (**2.9**)



Chemical Formula: $\text{C}_{16}\text{H}_{26}\text{O}_4$

Exact Mass: 282,18

(*Z*)-5-(2-Hydroxydodecylidene)furan-2(5*H*)-one (563 mg, 2.1 mmol) was dissolved in CH_2Cl_2 (21 mL) and 3-Chloroperoxybenzoic acid (466 mg, 2.7 mmol) was added at rt. The reaction was monitored by TLC. After 3 h complete conversion of starting material was observed. The reaction was stopped by addition of saturated NaHCO_3 solution (5 mL) and layers were separated. The aqueous phase was extracted with EtOAc (3 x 10 mL) and organic phases were combined, washed with brine, dried over MgSO_4 and filtered. The filtrate was evaporated to dryness under reduced pressure and the remaining residue was applied to flash chromatography (H/EtOAc = 80/20 \rightarrow 70/30). The desired product (464 mg, 1.6 mmol, 78%) was obtained as a white wax.

R_f = 0.38 (H/EtOAc = 70/30).

$^1\text{H-NMR}$ (500 MHz, CDCl_3): δ [ppm] = 7.56 (d, J = 5.7 Hz, 1 H), 6.36 (d, J = 5.7 Hz, 1 H), 4.09 (ddd, J = 3.2, 4.4, 7.7 Hz, 1 H), 3.79 (d, J = 3.2 Hz, 1 H), 1.94 (bs, 1 H), 1.69-1.43 (m, 4 H), 1.43-1.21 (m, 14 H), 0.88 (t, J = 6.8 Hz, 3 H).

$^{13}\text{C-NMR}$ (126 MHz, CDCl_3): δ [ppm] = 168.6, 149.2, 126.4, 89.9, 67.5, 64.9, 33.6, 32.0, 29.7, 29.7, 29.6, 29.6, 29.5, 25.3, 22.8, 14.3.

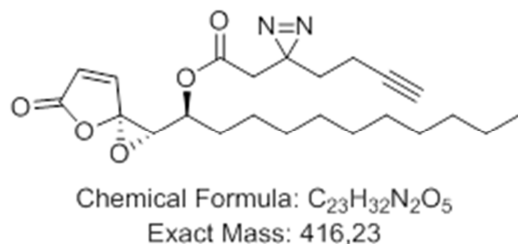
HRMS (ESI): calc. for $\text{C}_{16}\text{H}_{27}\text{O}_4$ $[\text{M}+\text{H}]^+$: 283.1904; found: 283.1911.

5.1.2.6 General procedure for (*S*)-1-((2*S*,3*S*)-5-Oxo-1,4-dioxaspiro[2.4]hept-6-en-2-yl)undecylnoates⁷⁹

Carboxylic acid (1.10 eq) was dissolved in CH_2Cl_2 (1.0 M) at rt. DMF (0.05 eq) and oxalyl chloride (1.20 eq) were added dropwise and the reaction mixture was stirred for 2 h at rt. Solvents were removed under reduced pressure and the remaining residue was dissolved in CH_2Cl_2 (1.0 M). Ramariolide A (1.00 eq) was dissolved in CH_2Cl_2 (1.0 M) and pyridine (3.00 eq) was added and cooled to 0 °C. The solution of activated acid was added dropwise to the reaction mixture and a deep orange color change was observed. The reaction was allowed to warm to rt and monitored by TLC. After 2 h no further consumption of starting

material could be observed and the reaction was stopped by addition of saturated NH_4Cl solution. After separation of phases the aqueous layer was extracted with CH_2Cl_2 (3 x 10 mL). Combined organic phases were washed with brine, dried over MgSO_4 , filtered and concentrated to dryness under reduced pressure. The remaining residue was applied to flash chromatography to give the desired product as a yellow oil.

(*S*)-1-((2*S*,3*S*)-5-Oxo-1,4-dioxaspiro[2.4.]hept-6-en-2-yl)undecyl 2-(3-(but-3-yn-1-yl)-3*H*-diazirin-3-yl)acetate (**2.23**)



Yield: 24%

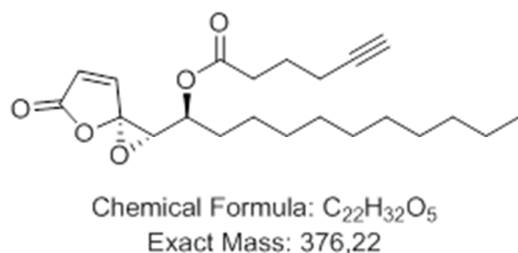
R_f = 0.28 (H/EtOAc = 90/10).

$^1\text{H-NMR}$ (300 MHz, CDCl_3): δ [ppm] = 7.37 (d, J = 5.7 Hz, 1 H), 6.38 (d, J = 5.7 Hz, 1 H), 4.80 (ddd, J = 4.6, 7.1, 8.3 Hz, 1 H), 3.72 (d, J = 7.1 Hz, 1 H), 2.48 (td, J = 1.9, 7.3 Hz, 2 H), 2.25 (td, J = 2.6, 6.9 Hz, 2 H), 1.97 (t, J = 2.6 Hz, 1 H), 1.87-1.76 (m, 4 H), 1.34-1.21 (m, 14 H), 0.88 (t, J = 6.9 Hz, 3 H).

$^{13}\text{C-NMR}$ (76 MHz, CDCl_3): δ [ppm] = 172.4, 152.4, 148.2, 126.6, 90.1, 82.8, 69.9, 69.9, 69.6, 62.1, 41.3, 32.7, 32.5, 32.0, 31.6, 29.7, 29.6, 29.4, 24.8, 23.5, 22.8, 17.8, 14.3.

HRMS (ESI): calc. for $\text{C}_{23}\text{H}_{31}\text{N}_2\text{O}_5$ $[\text{M}+\text{H}]^+$: 417.2384; found: 417.2388.

(*S*)-1-((2*S*,3*S*)-5-Oxo-1,4-dioxaspiro[2.4.]hept-6-en-2-yl)undecyl hex-5-ynolate



Yield: 37%

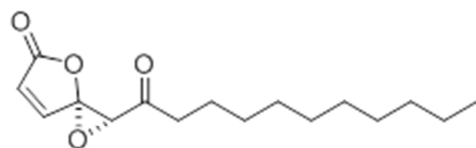
R_f = 0.25 (H/EtOAc = 85/15).

$^1\text{H-NMR}$ (300 MHz, CDCl_3): δ [ppm] = 7.37 (d, J = 5.7 Hz, 1 H), 6.38 (d, J = 5.7 Hz, 1 H), 4.80 (ddd, J = 4.5, 7.0, 8.2 Hz, 1 H), 3.73 (d, J = 7.0 Hz, 1 H), 2.48 (td, J = 1.9, 7.4 Hz, 2 H), 2.25 (td, J = 2.7, 6.9 Hz, 2 H), 1.97 (t, J = 2.7 Hz, 1 H), 1.88-1.80 (m, 2 H), 1.79-1.68 (m, 2 H), 1.36-1.21 (m, 16 H), 0.87 (t, J = 6.9 Hz, 3 H).

$^{13}\text{C-NMR}$ (76 MHz, CDCl_3): δ [ppm] = 172.4, 168.4, 148.2, 126.6, 123.6, 90.1, 82.9, 70.0, 69.6, 62.2, 32.8, 32.0, 31.7, 29.7, 29.6, 29.5, 29.4, 24.9, 23.5, 22.8, 17.8, 14.3.

HRMS (ESI): calc. for $C_{22}H_{33}O_5$ $[M+H]^+$: 377.2323; found: 377.2326.

5.1.2.7 (2*S**,3*R**)-2-Undecanoyl-1,4-dioxaspiro[2.4]hept-6-en-5-one (2.21)



Chemical Formula: $C_{16}H_{24}O_4$

Exact Mass: 280,17

(2*S**,3*R**)-2-((*R**)-1-Hydroxyundecyl)-1,4-dioxaspiro[2.4]hept-6-en-5-one (464 mg, 1.65 mmol) was dissolved in CH_2Cl_2 (15 mL) at rt. DMP (773 mg, 1.82 mmol) are added to the reaction mixture. The reaction was monitored by TLC and after 2 h complete conversion was observed. The solvents were removed under reduced pressure and the remaining residue was applied to flash chromatography (H/EtOAc = 80/20) to yield 68% of the desired product (313 mg, 1.12 mmol) as a white powder.

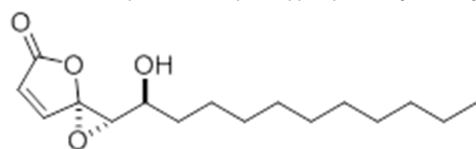
R_f = 0.27 (H/EtOAc = 80/20).

1H -NMR (300 MHz, $CDCl_3$): δ [ppm] = 7.11 (d, J = 5.6 Hz, 1 H), 6.48 (d, J = 5.6 Hz, 1 H), 3.84 (s, 1 H), 2.67 (td, J = 3.0, 7.2 Hz, 2 H), 1.68-1.53 (m, 2 H), 1.36-1.22 (m, 14 H), 0.87 (t, J = 6.7 Hz, 3 H).

^{13}C -NMR (126 MHz, $CDCl_3$): δ [ppm] = 203.3, 167.4, 148.3, 127.6, 89.2, 62.7, 39.2, 32.0, 29.7, 29.6, 29.5, 29.4, 29.1, 22.8, 22.7, 14.3.

HRMS (ESI): calc. for $C_{16}H_{25}O_4$ $[M+H]^+$: 281.1747; found: 281.1754.

5.1.2.8 (2*S**,3*R**)-2-((*S**)-1-Hydroxyundecyl)-1,4-dioxaspiro[2.4]hept-6-en-5-one (2.11)⁹⁵



Chemical Formula: $C_{16}H_{26}O_4$

Exact Mass: 282,1831

(2*S**,3*R**)-2-Undecanoyl-1,4-dioxaspiro[2.4]hept-6-en-5-one (313 mg, 1.12 mmol) was dissolved in THF (20 mL) at rt. $Zn(BH_4)_2$ (1.12 mL, 5 M in THF) was added dropwise via syringe at 0 °C. The cloudy mixture was allowed to warm to rt and monitored by TLC. After 2 h complete conversion was observed and the reaction was stopped by addition of HCl (5 mL, 2 M). The mixture was diluted with EtOAc and after separation of layers the aqueous phase was extracted with EtOAc (3 x 15 mL). The combined organic layers were washed with brine, dried over $MgSO_4$, filtered and concentrated to dryness *in-vacuo*. The remaining residue was applied to flash chromatography (H/EtOAc = 75/25 → 70/30). The desired product (170 mg, 605 μ mol) could be isolated in 54% yield as a white wax.

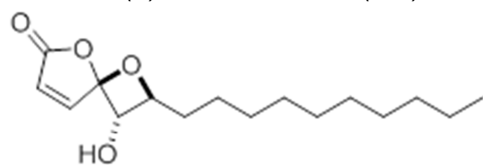
$R_f = 0.34$ (H/EtOAc = 70/30).

$^1\text{H-NMR}$ (500 MHz, CDCl_3): δ [ppm] = 7.14 (d, $J = 5.6$ Hz, 1 H), 6.4 (d, $J = 5.6$, 1 H), 3.90 (td, $J = 4.5, 8.0$ Hz, 1 H), 3.36 (d, $J = 7.7$ Hz, 1 H), 1.92 (bs, 1 H), 1.83-1.73 (m, 1 H), 1.73-1.64 (m, 1 H), 1.63-1.49 (m, 1 H), 1.48-1.39 (m, 1 H), 1.38-1.20 (m, 14 H), 0.88 (t, $J = 6.9$ Hz, 3 H).

$^{13}\text{C-NMR}$ (126 MHz, CDCl_3): δ [ppm] = 168.6, 149.8, 126.4, 90.3, 69.6, 64.2, 34.9, 32.1, 29.7, 29.7, 29.6, 29.5, 24.9, 22.8, 14.3.

HRMS (ESI): calc. for $\text{C}_{16}\text{H}_{27}\text{O}_4$ $[\text{M}+\text{H}]^+$: 283.1904; found: 283.1901.

5.1.2.9 (\pm)-Ramariolide B (**2.2**)⁹⁴



Chemical Formula: $\text{C}_{16}\text{H}_{26}\text{O}_4$

Exact Mass: 282,1831

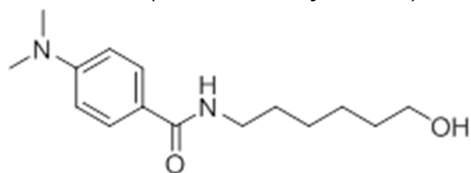
($2S^*,3R^*$)-2-((S^*)-1-Hydroxyundecyl)-1,4-dioxaspiro[2.4]hept-6-en-5-one (50 mg, 177 μmol) was dissolved in CH_2Cl_2 (10 mL) at rt. (\pm)-CSA (41 mg, 177 μmol) was added at rt and the reaction was monitored by TLC. Over a period of 3 h a color change from light yellow, orange to deep red could be observed until complete conversion of starting material. The reaction was stopped by addition of saturated NaHCO_3 solution. After separation of layers the aqueous phase was extracted with CH_2Cl_2 (3 x 10 mL). The combined organic phases were washed with brine, dried over MgSO_4 , filtered and concentrated under reduced pressure. The remaining residue was applied to flash chromatography (H/EtOAc = 75/25 \rightarrow 70/30). Ramariolide B could be obtained as a white wax (12 mg, 42 μmol , 24%).

$R_f = 0.33$ (H/EtOAc = 70/30).

$^1\text{H-NMR}$ (500 MHz, C_6H_6): δ [ppm] = 6.08 (d, $J = 5.6$ Hz, 1 H), 5.38 (d, $J = 5.6$ Hz, 1 H), 4.37 (q, $J = 6.7$ Hz, 1 H), 3.84 (dd, $J = 6.1, 12.2$ Hz, 1 H), 2.29 (d, $J = 12.2$ Hz, 1 H), 1.54-1.45 (m, 1 H), 1.43-1.38 (m, 1 H), 1.38-1.21 (m, 14 H), 0.93 (t, $J = 6.8$ Hz, 1 H).

$^{13}\text{C-NMR}$ (126 MHz, C_6H_6): δ [ppm] = 168.2, 148.8, 124.4, 112.8, 90.4, 74.1, 34.4, 32.2, 29.9, 29.8, 29.7, 29.6, 29.5, 24.5, 23.0, 14.2.

HRMS (ESI): calc. for $\text{C}_{16}\text{H}_{25}\text{O}_4$ $[\text{M}+\text{H}]^+$: 283.1904; found: 283.1904.

5.1.2.10 4-(*N,N*-Dimethylamino)-*N'*-(6-hydroxyhexyl)benzamide

Chemical Formula: $C_{15}H_{24}N_2O_2$
Molecular Weight: 264,3690

4-(*N,N*-Dimethylamino)benzoic acid (332 mg, 2.00 mmol) was dissolved in DMF (20 mL) and EDCI (402 mg, 2.10 mmol) as well as HOBt (321 mg, 2.10 mmol) were added at rt. The resulting suspension was stirred for 20 min to become a clear solution. NEt_3 (1.39 mL, 10.0 mmol) and 6-amino-1-hexanol (246 mg, 2.10 mmol) were added at rt. The reaction was monitored by TLC and indicated complete conversion after 2 additional hours. The reaction was stopped by addition of brine. After separation of phases the organic phase was extracted with saturated NH_4Cl solution (3 x 100 mL). The combined aqueous layers were extracted with EtOAc (2 x 40 mL). The combined organic layers were dried over $MgSO_4$ and concentrated to dryness under reduced pressure. The crude mixture was applied to flash chromatography (H/EtOAc = 30/70 \rightarrow 20/80) to yield 239 mg (0.91 mmol, 45%) of product as a white solid.

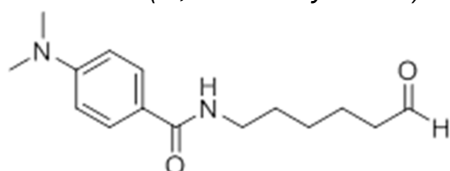
R_f = 0.37 (H/EtOAc = 20/80).

1H -NMR (360 MHz, $CDCl_3$): δ [ppm] = 7.69 (d, J = 8.8 Hz, 2 H), 6.66 (d, J = 8.8 Hz, 2 H), 6.25 (bs, 1 H), 3.62 (t, J = 6.3 Hz, 2 H), 3.44-3.42 (m, 2 H), 3.00 (s, 6 H), 2.23 (bs, 1 H), 1.67-1.51 (m, 4 H), 1.48-1.33 (m, 4 H).

^{13}C -NMR (91 MHz, $CDCl_3$): δ [ppm] = 167.6, 152.4, 128.3, 121.5, 111.1, 62.6, 45.8, 40.1, 39.6, 26.5, 8.6.

HRMS (ESI): calc. for $C_{15}H_{25}N_2O_2$ $[M+H]^+$: 265.1916; found: 265.1907.

Mp: 101 °C.

5.1.2.11 4-(*N,N*-Dimethylamino)-*N'*-(6-oxohexyl)benzamide

Chemical Formula: $C_{15}H_{22}N_2O_2$
Molecular Weight: 262,3530

Sulfur trioxide pyridine complex (174 mg, 1.09 mmol) was dissolved in DMSO (50 mL) at -72 °C. After 10 min 4-(*N,N*-dimethylamino)-*N'*-(6-hydroxyhexyl)benzamide (239 mg, 0.91 mmol) was added and after 30 min NEt_3 (747 μ L, 5.46 mmol) was added. The reaction mixture was stirred at -78 °C until TLC indicated consumption of starting material and then

allowed to warm to rt. The reaction was stopped by addition of saturated NH_4Cl solution and phases were separated. The aqueous layer was extracted with EtOAc (3 x 30 mL) and organic layers were combined, washed with brine, dried over MgSO_4 and concentrated to dryness under reduced pressure. The crude mixture was applied to flash chromatography (H/EtOAc = 30/70) to yield 172 mg (0.66 mmol, 72%) of product as a white solid.

R_f = 0.30 (H/EtOAc = 30/70).

$^1\text{H-NMR}$ (300 MHz, CDCl_3): δ [ppm] = 9.77 (t, J = 1.7 Hz, 1 H), 8.02-7.43 (m, 2 H), 6.71-6.65 (m, 2 H), 6.15 (bs, 1 H), 3.45 (td, J = 0.6, 7.2 Hz, 2 H), 3.02 (s, 6 H), 2.46 (td, J = 1.7, 7.2 Hz, 2 H), 1.75-1.57 (m, 4 H), 1.49-1.35 (m, 2 H).

$^{13}\text{C-NMR}$ (75 MHz, CDCl_3): δ [ppm] = 202.6, 167.5, 152.4, 128.3, 121.5, 111.1, 43.7, 40.2, 39.5, 29.6, 26.5, 21.7.

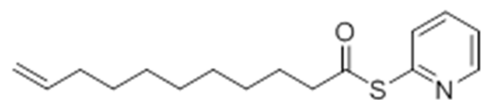
HRMS (ESI): calc. for $\text{C}_{15}\text{H}_{23}\text{N}_2\text{O}_2$ $[\text{M}+\text{H}]^+$: 263.1760; found: 263.1755.

Mp: 66 °C.

5.1.2.12 General procedure for *S*-(Pyridin-2-yl) thiolates

Carboxylic acid (1.00 eq) was dissolved in CH_2Cl_2 (0.5 M) at rt and DMF (0.05 eq) was added. Oxalyl chloride (1.20 eq) was added dropwise under strong gas formation. The reaction mixture was stirred for 3 h and the solvents were removed under reduced pressure. The remaining residue was dissolved in CH_2Cl_2 (1.0 M) and 2-pyridylmercaptane (1.20 eq) and NEt_3 (2.16 eq) were added at 0°C. The reaction mixture was allowed to warm to rt and stirred for 2 h. The reaction was stopped by addition of 1 M HCl and phases were separated. The aqueous layer was extracted with EtOAc (3 x 30 mL) and organic layers were combined and washed with saturated NaHCO_3 solution, brine and dried over MgSO_4 . The crude product was concentrated to dryness under reduced pressure and applied to flash chromatographie. The product was isolated as a light yellow solid.

S-(Pyridin-2-yl)-10-undecene thiolate



Chemical Formula: $\text{C}_{16}\text{H}_{23}\text{NOS}$

Molecular Weight: 277,4260

Yield: 92%

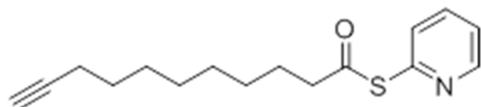
R_f = 0.35 (H/EtOAc = 96/4).

$^1\text{H-NMR}$ (360 MHz, CDCl_3): δ [ppm] = 8.65-8.62 (m, 1 H), 7.78-7.72 (m, 1 H), 7.65-7.61 (m, 1 H), 7.2 (ddd, J = 1.0, 5.0, 7.0 Hz, 1 H), 5.89-5.76 (m, 1 H), 5.05-4.92 (m, 2 H), 2.71 (t, J = 7.0 Hz, 2 H), 2.09-2.00 (m, 2 H), 1.79-1.68 (m, 2 H), 1.45-1.25 (m, 10 H).

$^{13}\text{C-NMR}$ (91 MHz, CDCl_3): δ [ppm] = 196.6, 151.7, 150.4, 139.2, 137.0, 130.1, 123.4, 114.2, 44.2, 33.8, 29.2, 29.1, 29.0, 28.9, 28.9, 25.4.

HRMS (ESI): calc. for $\text{C}_{16}\text{H}_{24}\text{NOS}$ $[\text{M}+\text{H}]^+$: 278.1579; found: 278.1564.

S-(Pyridin-2-yl)-10-undecyne thiolate



Chemical Formula: $\text{C}_{16}\text{H}_{21}\text{NOS}$
Molecular Weight: 275,4100

Yield: 76%

R_f = 0.36 (H/EtOAc = 96/4).

$^1\text{H-NMR}$ (360 MHz, CDCl_3): δ [ppm] = 8.66-8.63 (m, 1 H), 7.77-7.72 (m, 1 H), 7.65-7.61 (m, 1 H), 7.28-7.19 (m, 1 H), 2.67 (t, J = 7.5 Hz, 1 H), 2.21 (td, J = 2.6, 7.5 Hz, 1 H), 1.96 (t, J = 2.6 Hz, 1 H), 1.73-1.68 (m, 2 H), 1.62-1.28 (m, 7 H).

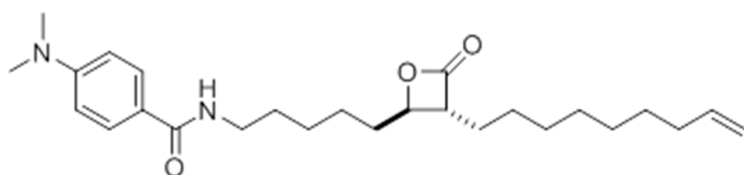
$^{13}\text{C-NMR}$ (91 MHz, CDCl_3): δ [ppm] = 197.5, 134.5, 129.3, 129.1, 84.7, 68.1, 43.7, 29.1, 28.9, 28.8, 28.7, 28.4, 25.6, 18.4.

HRMS (ESI): calc. for $\text{C}_{16}\text{H}_{22}\text{NOS}$ $[\text{M}+\text{H}]^+$: 276.1417; found: 276.1421.

5.1.2.13 General procedure for (3*R**,4*R**) oxetan-2-ones¹¹⁶

Diethylamine (1.05 eq) was dissolved in THF (2.0 M) and cooled to -72°C . *n*BuLi (1.10 eq) was added dropwise and the solution was stirred for 10 min. S-(Pyridin-2-yl) thiolate (1.00 eq) was dissolved in THF, added to the reaction mixture and stirred for 1.5 h. 4-(*N,N*-Dimethylamino)-*N'*-(6-oxohexyl)benzamide was dissolved in THF and added dropwise to the reaction over a period of 45 min via a syringe externally cooled by a dry ice filled aluminum funnel. The reaction mixture was stirred for 2 h while being gradually warmed up to 0°C . The reaction was stopped by addition of saturated NH_4Cl solution. After separation of phases the aqueous layer was extracted with ethyl acetate (3 x 30 mL). The combined organic layers were washed with brine, dried over MgSO_4 and filtered. The solvent was removed under reduced pressure and the crude product was applied to flash chromatography. The product was isolated as a pale yellow oil.

(3*R**,4*R**)-4-(4-(*N,N*-Dimethylamino)benzamino-5-pentyl)-3-(non-8-enyl)oxetan-2-one



Chemical Formula: $C_{26}H_{40}N_2O_3$
Molecular Weight: 428,6170

Yield: 12%

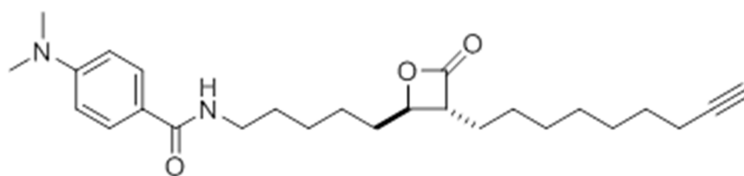
R_f = 0.18 (H/EtOAc = 70/30).

$^1\text{H-NMR}$ (500 MHz, CDCl_3): δ [ppm] = 7.73-7.68 (m, 2 H), 6.74 (d, J = 7.2 Hz, 2 H), 6.10 (bs, 1 H), 5.82 (ddt, J = 6.7, 10.1, 16.9 Hz, 1 H), 5.04-4.98 (m, 1 H), 4.95 (ddt, J = 1.2, 2.3, 10.3 Hz, 1 H), 4.23 (ddd, J = 4.0, 6.7, 8.7 Hz, 1 H), 3.46 (dd, J = 6.1, 13.4 Hz, 2 H) 3.18 (ddd, J = 4.0, 6.7, 8.7 Hz, 1 H), 3.04 (s, 6 H), 2.06 (dd, J = 6.7, 14.5 Hz, 2 H), 1.91-1.69 (m, 4H), 1.68-1.60 (m, 2 H), 1.55-1.27 (m, 16 H).

$^{13}\text{C-NMR}$ (91 MHz, CDCl_3): δ [ppm] = 171.5, 167.3, 151.9, 139.0, 128.3, 114.2, 111.6, 78.0, 77.2, 56.2, 40.5, 39.6, 34.3, 33.7, 29.7, 29.2, 29.1, 28.9, 28.8, 27.8, 26.9, 26.6, 24.8.

HRMS (ESI): calc. for $C_{26}H_{40}N_2O_3$ $[M]^+$: 428.3039; found: 428.3035.

(3*R**,4*R**)-4-(4-(*N,N*-Dimethylamino)benzamino-5-pentyl)-3-(non-8-ynyl)oxetan-2-one



Chemical Formula: $C_{26}H_{38}N_2O_3$
Molecular Weight: 426,6010

Yield: 14%

R_f = 0.15 (H/EtOAc = 70/30).

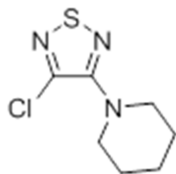
$^1\text{H-NMR}$ (500 MHz, CDCl_3): δ [ppm] = 7.69 (d, J = 9.0 Hz, 2 H), 6.70 (d, J = 9.0 Hz, 2 H), 6.01 (t, J = 6.0 Hz, 1 H), 4.24 (ddd, J = 4.0, 5.7, 7.60 Hz, 1 H), 3.47 (qd, J = 1.2, 7.0 Hz, 2 H), 3.19 (ddd, J = 4.0, 6.7, 8.6 Hz, 1 H), 3.04 (s, 6 H), 2.21 (td, J = 2.6, 7.1 Hz, 2 H), 2.02-1.92 (m, 1 H), 1.92-1.71 (m, 4 H), 1.71-1.30 (m, 16 H)..

$^{13}\text{C-NMR}$ (91 MHz, CDCl_3): δ [ppm] = 171.5, 167.4, 152.4, 128.3, 121.4, 111.1, 84.6, 78.0, 68.2, 56.2, 40.1, 39.6, 34.4, 29.7, 29.1, 28.8, 28.6, 28.4, 27.8, 26.9, 24.9, 18.35.

HRMS (ESI): calc. for $C_{26}H_{38}N_2O_3$ $[M+H]^+$: 427.2956; found: 427.2952.

Chapter 5

5.1.2.14 3-Piperidinyl-4-chloro-1,2,5-thiadiazol



Chemical Formula: $C_7H_{10}ClN_3S$
Molecular Weight: 203,69

3,4-Dichloro-1,2,5-thiadiazole (0.91 mL, 9.7 mmol) was dissolved in piperidine (3.8 mL, 38.7 mmol) at rt. The reaction mixture was heated to 100°C and continuously stirred for 2 h. After cooling to rt the mixture was poured in ice water (10 mL). Concentrated HCl was added until the pH of the aqueous solution was 2. The remaining solution was extracted with CH_2Cl_2 (3 x 10 mL). The organic layer was washed with brine, dried over $MgSO_4$ and filtered. The mixture was concentrated under reduced pressure to dryness and the residue was applied to flash chromatography (pure CH_2Cl_2). The desired product was isolated as a solid (1.86 g, 9.05 mmol, 93%).

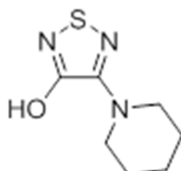
R_f = 0.42 (CH_2Cl_2).

1H -NMR (500 MHz, $CDCl_3$): δ [ppm] = 3.42-3.40 (m, 4 H), 1.73-1.70 (m, 4 H), 1.65-1.61 (m, 2 H).

^{13}C -NMR (91 MHz, $CDCl_3$): δ [ppm] = 160.2, 135.9, 50.3, 25.7, 24.3.

HRMS (ESI): calc. for $C_7H_{10}ClN_3S$ [M]⁺: 203.0284; found: 203.0302.

5.1.2.15 3-Hydroxy-4-piperidinyl-1,2,5-thiadiazole (**4.4**)¹²⁷



Chemical Formula: $C_7H_{11}N_3OS$
Molecular Weight: 185,24

3-Piperidinyl-4-chloro-1,2,5-thiadiazol (1.00 g, 4.91 mmol) was dissolved in a $H_2O/DMSO$ (4:1, 10 mL) mixture. To this solution KOH (1.13 g, 20.1 mmol) was added and refluxed for 4 h. The reaction was monitored by TLC and cooled to 0 °C after consumption of starting material. The reaction was stopped by addition of water (10 mL) and adjusted to pH 2 by addition of concentrated HCl. The white precipitate was filtered off, dried under reduced pressure and applied to flash chromatography ($CH_2Cl_2/MeOH$ = 98/2). The desired product was isolated as a white solid (580 mg, 3.1 mmol, 64%).

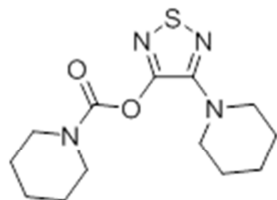
R_f = 0.28 ($CH_2Cl_2/MeOH$ = 98/2).

1H -NMR (500 MHz, $DMSO-d_6$): δ [ppm] = 12.68 (bs, 1 H), 3.46-3.41 (m, 4 H), 1.60-1.52 (m, 6 H).

$^{13}\text{C-NMR}$ (91 MHz, $\text{DMSO-}d_6$): δ [ppm] = 153.7, 150.7, 47.9, 24.9, 23.8.

HRMS (ESI): calc. for $\text{C}_7\text{H}_{11}\text{N}_3\text{OS}$ $[\text{M}]^+$: 185.0623; found: 185.0618.

5.1.2.16 Lalistat (La-0)(4.1)¹²⁷



Chemical Formula: $\text{C}_{13}\text{H}_{20}\text{N}_4\text{O}_2\text{S}$

Molecular Weight: 296,39

3-Hydroxy-4-piperidinyl-1,2,5-thiadiazole (150 mg, 0.81 mmol) was suspended in THF (3 mL) at rt. KO^tBu (405 μL , 0.81 mmol, 2 M in THF) was added via syringe and the reaction mixture was stirred for 10 min. Piperidinecarbonyl chloride (85 μL , 0.67 mmol) was added and the reaction was stirred for 16 h at rt. The reaction was stopped by addition of H_2O (10 mL) and extracted with CH_2Cl_2 (3 x 10 mL). The organic layers were combined, washed with brine, dried over MgSO_4 and filtered. The crude product was concentrated to dryness under reduced pressure and applied to RP-HPLC to yield 106 mg (0.43 mmol, 53%) of desired product as a white solid.

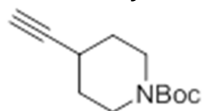
RP-HPLC (analytical setup, method: gradient 2% B \rightarrow 98% B over 10 min): t_{R} = 8.84 min.

$^1\text{H-NMR}$ (500 MHz, CDCl_3): δ [ppm] = 3.61-3.59 (m, 2 H), 3.54-3.51 (m, 2 H), 3.4-3.38 (m, 4 H), 1.69-1.60 (m, 12 H).

$^{13}\text{C-NMR}$ (91 MHz, CDCl_3): δ [ppm] = 154.0, 151.0, 146.9, 49.2, 46.1, 45.7, 26.2, 25.6, 24.4, 24.3.

HRMS (ESI): calc. for $\text{C}_{13}\text{H}_{21}\text{N}_4\text{O}_2\text{S}$ $[\text{M}+\text{H}]^+$: 297.1380; found: 297.1384.

5.1.2.17 *tert*-Butyl 4-ethynylpiperidine-1-carboxylate¹⁵⁶



Chemical Formula: $\text{C}_{12}\text{H}_{19}\text{NO}_2$

Molecular Weight: 209,29

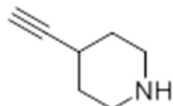
tert-Butyl 4-formylpiperidine-1-carboxylate (2.4 g, 12 mmol) was dissolved in MeOH (50 mL) at rt. Potassium carbonate (3.1 g, 24 mmol) and dimethyl-1-diazo-2-oxopropylphosphonate (2.2 g, 12 mmol) were slowly added to form a turbid suspension and stirred for 3 h at rt. The reaction was stopped by addition of saturated NaHCO_3 (50 mL) solution and diluted with Et_2O (50 mL). After separation of phases the aqueous layer was extracted with Et_2O (3x 30 mL) and the organic layers were combined and washed with

brine, dried over MgSO_4 , filtered and dried under reduced pressure. The obtained residue was a white solid, which proved to be the desired product (2.1 g, 11.2 mmol, 93%).

$^1\text{H-NMR}$ (200 MHz, CDCl_3): δ [ppm] = 3.68-3.66 (m, 2 H), 3.20-3.15 (m, 2 H), 2.58 (m, 1 H), 2.09 (s, 1 H), 1.77-1.75 (m, 2 H), 1.60-1.57 (m, 2 H), 1.45 (s, 9 H).

HRMS (ESI): calc. for $\text{C}_{12}\text{H}_{20}\text{NO}_2$ $[\text{M}+\text{H}]^+$: 210.1489; found: 210.1490.

5.1.2.18 4-Ethynylpiperidine (**4.6**)¹⁵⁶



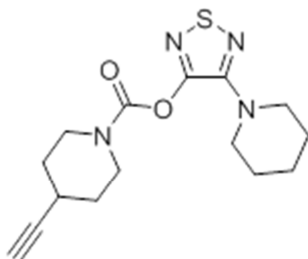
Chemical Formula: $\text{C}_7\text{H}_{11}\text{N}$

Molecular Weight: 109,17

tert-Butyl 4-ethynylpiperidine-1-carboxylate (1.5 g, 7.2 mmol) was dissolved in CH_2Cl_2 (20 mL) at rt and TFA (2 mL) was added. The reaction was monitored by LCMS, stirred for 90 min and solvents were removed *in-vacuo* to yield the desired product (780 mg, 7.2 mmol, 100%) without any further purification.

HRMS (ESI): calc. for $\text{C}_7\text{H}_{11}\text{N}$ $[\text{M}]^+$: 109.0891; found: 109.0891.

5.1.2.19 4-(Piperidin-1-yl)-1,2,5-thiadiazol-3-yl 4-ethynylpiperidine-1-carboxylate (**4.2**)



Chemical Formula: $\text{C}_{15}\text{H}_{20}\text{N}_4\text{O}_2\text{S}$

Molecular Weight: 320,41

4-(Piperidin-1-yl)-1,2,5-thiadiazol-3-ol (76.7 mg, 0.41 mmol) was dissolved in THF (10 mL). NaH (16.4 mg, 60% in mineral oil, 0.41 mmol) was added and the resulting suspension was stirred until recovery of a solution indicating complete deprotonation. A phosgene solution (234 μL , 20% in toluene, 1.75 M, 0.41 mmol) was added and the resulting solution was stirred at rt for 10 min. 4-Ethynylpiperidine-TFA salt (144 mg, 0.70 mmol) and DIPEA (120 μL , 0.70 mmol) were combined in THF (2 mL) and stirred for 5 min. This solution was added to the *in-situ* formed chloroformate solution and stirred at rt for 20 min. The reaction was stopped by addition of 1 M HCl (10 mL) and diluted with EtOAc (25 mL). After separation of phases the organic layer was washed three times with saturated NaHCO_3 solution, dried over MgSO_4 and concentrated *in-vacuo*. The product was purified by RP-HPLC as the HCl salt to yield as a clear oil.

RP-HPLC (analytical setup, method: gradient 2% B → 98% B over 10 min): $t_R = 8.73$ min.

$^1\text{H-NMR}$ (360 MHz, CDCl_3): δ [ppm] = 3.89-3.73 (m, 2 H), 3.59-3.43 (m, 2 H), 3.42-3.35 (m, 4 H), 2.73 (tq, $J = 3.7, 7.0$ Hz, 1 H), 2.15 (d, $J = 2.4$ Hz, 1 H), 1.95-1.83 (m, 2 H), 1.78-1.68 (m, 2 H), 1.67-1.57 (m, 6 H).

$^{13}\text{C-NMR}$ (91 MHz, CDCl_3): δ [ppm] = 153.8, 150.9, 146.6, 85.5, 70.5, 49.1, 43.2, 42.8, 31.4, 20.9, 26.4, 25.5, 24.3.

HRMS (ESI): calc. for $\text{C}_{15}\text{H}_{21}\text{N}_2\text{O}_2$ $[\text{M}+\text{H}]^+$: 321.1380; found: 321.1372.

5.2 Biochemistry

5.2.1 Microbiology

5.2.1.1 Material

5.2.1.1.1 Bacteria

- *Escherichia coli*: K12
- *Escherichia coli*: BL21
- *Enterococcus faecalis* V583
- *Pseudomonas aeruginosa* PAO1
- *Salmonella typhimurium* LT2
- *Staphylococcus aureus*: NCTC8325
- *Staphylococcus aureus*: Mu50
- *Staphylococcus aureus*: USA300
- *Listeria monocytogenes*: EGD-e
- *Mycobacterium smegmatis*: mc(2)155
- *Mycobacterium bovis*: Bacillus Calmette-Guérin (BCG) Pasteur
- *Mycobacterium tuberculosis*: H37Rv

5.2.1.1.2 Media

Media	Composition
Luria Broth (LB-Medium)	10.0 g/L casein digested 5.0 g/L yeast extract 5.0 g/L NaCl adjust to pH = 7.5, autoclave
B-Medium	10.0 g/L peptone extract 5.0 g/L NaCl 2.0 g/L dextrose 5.0 g/L yeast extract 1.0 g/L K ₂ HPO ₄ adjust to pH = 7.5, autoclave
BHB-Medium	17.5 g/L brain-heart-broth 2.5 g/L Na ₂ HPO ₄ 2.0 g/L dextrose 10.0 g/L peptone extract 5.0 g/L NaCl adjust to pH = 7.4, autoclave

7H9-Medium	4.7 g/L 7H9 powder 2 mL/L glycerol 2.5 mL/L 20% Tween 80 5 g/L BSA (fraction V) 2 g/L dextrose 850 mg/L NaCl 3 mg/L catalase filter sterile
Sauton's Medium	20 mL/L glycerol 1.33 g/L L-asparagine 833 mg/L Tween 80 660 mg/L citric acid 177 mg/L K ₂ PO ₄ 166 mg/L MgSO ₄ 56 mg/L NaH ₂ PO ₄ 35 mg/L NaCl 16.7 mg/L ferric ammonium citrate adjust to pH = 7.2, filter sterile
SOC	20.0 g/L yeast extract 5.0 g/L tryptone 0.50 g/L NaCl 0.2 g/L KCl 1.00 g/L MgCl ₂ 1.20 g/L MgSO ₄ 3.60 g/l dextrose adjust to pH = 7.3, autoclave

5.2.1.2 Methods

5.2.1.2.1 Over-night cultures

5 mL of the strain specific media for cultivation were inoculated with 5 µL of the desired bacterial cryostock (1:1,000) with a sterile tip in a culture tube. The culture was incubated for 16 h at 200 rpm in an Innova incubator shaker. Cultures were always prepared freshly to avoid genetic variations and sterile controls (medium not containing bacteria) were added each time.

5.2.1.2.2 Cryostocks

2 mL of a dense grown overnight culture were harvested by centrifugation for 5 min at 6000 g and 4 °C. The supernatant was discarded and the remaining pellet was resuspended

in 500 μL of fresh corresponding medium including antibiotics if required. To this suspension 500 μL of sterile glycerol was added and the mixture was transferred into a cryo-tube, mixed by inversion and frozen in liquid nitrogen to be stored at $-80\text{ }^{\circ}\text{C}$.

5.2.1.2.3 Competent cells

5.2.1.2.3.1 Chemically competent (*E. coli* K12, TOP10/BL21(+)/XL1 Blue)

An overnight culture of bacteria of the desired strain was started. 300 mL medium were inoculated 1:100 with the overnight culture. As soon as the culture reached an OD_{600} of 0.5 - 0.7 the cells were split in 50 mL aliquots and stored on ice for 15 min. All further working steps were performed on ice or using solutions pre-cooled to $4\text{ }^{\circ}\text{C}$. The cells were harvested by centrifugation for 2 min at 6000 g and $4\text{ }^{\circ}\text{C}$. The supernatant was discarded and the pellet was resuspended in 25 mL of sterile 50 mM CaCl_2 solution. The suspension was incubated on ice for 30 min and centrifuged for 2 min at 6000 g and $4\text{ }^{\circ}\text{C}$. The supernatant was discarded and the cells were resuspended in 1.25 mL of 50 mM CaCl_2 solution and incubated for 30 min on ice. 125 μL of glycerol was added and gently mixed. Aliquots of 50 μL were taken in sterile tubes, frozen in liquid nitrogen and stored at $-80\text{ }^{\circ}\text{C}$.

5.2.1.2.3.2 Electro competent (*E.coli* Artic Express, *M. smegmatis* mc(2) 155)

An overnight culture of bacteria of the desired strain was started. Cells were incubated at $37\text{ }^{\circ}\text{C}$ until OD_{600} of 0.5 – 0.7 was reached. Cells were harvested by centrifuging for 10 min at 6000 g and $4\text{ }^{\circ}\text{C}$. The supernatant was discarded and cells were resuspended in $\frac{1}{2}$ initial Volume of 10 % (v/v) glycerol. Cells were spun for 10 min at 6000 g and $4\text{ }^{\circ}\text{C}$. The supernatant was discarded and cells were resuspended in $\frac{1}{4}$ initial volume of 10 % (v/v) glycerol. After centrifugation for 10 min at 6000 g and $4\text{ }^{\circ}\text{C}$ the supernatant was discarded and cells were resuspended in $\frac{1}{20}$ initial Volume of 10 % (v/v) glycerol. 50 μL Aliquots were prepared in tubes and frozen in liquid nitrogen to be stored at $-80\text{ }^{\circ}\text{C}$.

5.2.1.2.4 Minimal Inhibitory Concentration (MIC) Assay

Probe-mediated growth inhibition was carried out using 96-well plates. A culture of stationary phase growing bacteria was diluted to a final $\text{OD}_{600} = 0.001$ in fresh media. 99 μL of the diluted bacteria was added to 1 μL of various concentrations (100 fold) of prepared compound stocks in DMSO and incubated at $37\text{ }^{\circ}\text{C}$ under a water impermeable membrane. Plates were checked daily for bacterial growth by eye (turbidity) and MIC was determined for the lowest concentration of compound inhibiting growth. Experiments were carried out in triplicates. To determine the growth of mycobacteria 100 μL of a 0.02 % resazurin solution was added after 2 days and 7 days for *M.smegmatis* and *M. tuberculosis*, respectively. A color change from purple to pink within 2 to 4 days indicated viable cells while purple colored wells suggested no bacterial growth.

5.2.1.2.5 FICI determination

Determination synergistic drug effects were calculated using fractional inhibitory concentration index (FICI):

$$FICI = \frac{MIC\ A + B}{MIC\ A} + \frac{MIC\ B + A}{MIC\ B}$$

MIC A+B – MIC of drug A when combined with drug B

MIC B+A – MIC of drug B when combined with drug A

Results were evaluated as follows: synergism: ≤ 0.5 , indifference: $> 0.5 - 4$, antagonism > 4 .

5.2.1.2.6 Analysis of mycobacterial lipids

Mycobacterial strains are inoculated in adjusted Sauton's medium for MS-analysis. Bacteria are grown at 37 °C under continuous rolling to mid-exponential phase ($OD_{600} = 0.5$) and cell numbers are normalized. Test substance as well as DMSO (positive control) and isoniazid (negative control) are added to separate flasks and grown for 3 h until [1,2-¹³C] sodium acetate is added (3 mg/ml). Cells are grown for 21 h and centrifuged at 6000 rpm for 10 min. at 4 °C. The supernatant is discarded and the pellet is washed with PBS. Repetition of the washing process resulted in a pellet of bacteria, which was resuspended in a 2:1 mixture of chloroform/methanol (20 mL). Bacteria are stored at room temperature of 24 h. Concentration of the supernatant to dryness yielded extractable lipids, which were used for TLC analysis. The remaining delipidated cell pelled was transferred into a glass vial, a 15 % KOH solution was added and the system was capped and heated to 120 °C for 2 h. The supernatant was extracted with chloroform/methanol = 1/1 and neutralized using diluted HCl. Concentration of the organic phase to dryness gave cell wall bound lipids, which were redissolved in chloroform/methanol = 1/1 to a 1 mg/mL solution, which was applied to MS measurements.

5.2.1.2.7 Mycobacterium tuberculosis Growth Analysis

GFP-expressing *Mycobacterium tuberculosis* H37Rv was generated using the plasmid 32362:pMN437 (Addgene), kindly provided by M. Niederweis (University of Alabama, Birmingham, AL). 1×10^6 bacteria were cultured in 7H9 medium supplemented with oleic acid-albumin-dextrose-catalase (OADC) (10%), Tween 80 (0.05%), and glycerol (0.2%) in a total volume of 100 ml in a black 96 well plate with clear bottom (Corning Inc, Corning, NY) sealed with an air-permeable membrane (Porvair Sciences, Dunn Labortechnik, Asbach, Germany). Growth was as measured as RLU at 528 nm after excitation at 485 nm in a fluorescence microplate reader (Synergy 2, Biotek, Winooski, VT) at indicated time points.

5.2.1.2.8 Analysis of M. tuberculosis growth in human macrophages

Mononuclear cells were isolated from peripheral blood (PBMC) of healthy volunteers by density gradient centrifugation. Monocytes were separated (purity consistently $>95\%$) by

counterflow elutriation. Human monocyte-derived Macrophages (hMDM) were generated in the presence of 10 ng/ml recombinant human M-CSF from highly purified monocytes as described.¹⁵⁹ *M. tuberculosis* growth in human macrophages was analyzed as described.¹⁵⁸ In brief 2×10^5 hMDMs were cultured in 500ml RPMI 1640 with 10% FCS and 4mM L-glutamine in 48-well flat-bottom microtiter plates (Nunc) at 37°C in a humidified atmosphere containing 5% CO₂. Macrophages were infected with *M. tuberculosis* strain H37Rv with an MOI of 1:1. Four hours post infection, non-phagocytosed bacteria were removed by washing three times with 0.5ml Hanks' balanced salt solution (HBSS; Invitrogen) at 37°C. After washing and after 3 days of cultivation, 0.5 ml media was added to the macrophage culture. At day 7 supernatants were completely removed and macrophage cultures were lysed at 4 hours and 7 days post infection by adding 10 ml 10% Saponin solution (Sigma) in HBSS at 37°C for 15 min. Lysates were serially diluted in sterile water containing 0.05% Tween 80 (Merck, Darmstadt, Germany) and plated twice on 7H10 agar containing 0.5% glycerol (Serva) and 10% heat-inactivated bovine calf serum (BioWest, France). After 3 weeks at 37°C the CFUs were counted.

5.2.2 Genomics

5.2.2.1 Materials

5.2.2.1.1 Buffers

Name	Composition
TAE-buffer stock (pH = 7.0)	2.0 M Tris-HCl 1.0 M HOAc 0.1 M EDTA
TAE-gel buffer	20 mL TAE-buffer stock 980 mL ddH ₂ O
TAE-running buffer	10 mL TAE-buffer stock 990 mL ddH ₂ O
TE buffer	10 mM Tris base 1 mM EDTA pH = 8.0
DNA loading buffer	250 mg bromphenol blue 250 mg xylen cyanol 33 mL Tris-HCl (150 mM) 60 mL glycerol 7 mL ddH ₂ O
Ethidium bromide stock	dissolve 1 tablet in 1 mL ddH ₂ O dilute 1:10 with ddH ₂ O

5.2.2.1.2 Plasmids

Name	Source	Resistance	Tags	Induction
pDONR 201	Invitrogen	Kanamycin	-	-
pET 300	Invitrogen	Ampicillin	N-His ₆	IPTG
pET 28	Invitrogen	Kanamycin	N-His ₆	IPTG

5.2.2.1.3 Primers

Construct: N-His₆-attB1-ask-Stop-attB2

Primer1: ggggacaagttgtacaaaaagcaggctttGCGCTCGTCGTACAGAAATAC

Primer2: ggggaccactttgtacaagaaagctgggtgTCAGCGCCCGTTCCCG

Construct: N-His₆-attB1-TEV-ClpX-Stop-attB2

Primer1: ggggacaagttgtacaaaaagcaggctttgagaatctttatttcagggcGCGCGCATTGGAGACG

Prim2: ggggaccactttgtacaagaaagctgggtgTTACGCGCTCTTGTCGC

Construct: N-His₆-attB1-TEV-LipR-Stop-attB2

Primer1: ggggacaagttgtacaaaaagcaggctttgagaatctttatttcagggcAACCTGCGCAAAAACG

Chapter 5

Primer2: ggggaccactttgtacaagaaagctgggtgTCATTTGACTACTCCCCGTGG

5.2.2.2 Methods

5.2.2.2.1 Extraction of DNA

5.2.2.2.1.1 Genomic DNA

Genomic DNA was prepared from overnight cultures of the respective Bacteria using the DNeasy Kit (Quiagen, Hilden, Germany). For mycobacteria the protocol was adjusted on lysing conditions as suggested within the Kit.

5.2.2.2.1.2 Plasmid DNA

Plasmid isolation of small scale cultures (≤ 5 mL) was performed using Promega PureYield™ Plasmid Prep System. DNA was eluted in ddH₂O or TE-buffer.

5.2.2.2.2 Polymerase Chain Reaction (PCR)

Polymerase chain reactions are carried out to amplify DNA fragments, create targeted mutations and many more purposes. Depending on the DNA polymerase reaction mixtures may vary. In this work either of the following conditions were applied. Unsuccessful reactions were modified with different additives as DMSO, MgCl₂ or template concentration:

KOD reaction

25 μ L KOD reaction buffer (2x)
10 μ L dNTPs (2 mM)
2.5 μ L DMSO
1.5 μ L primer (each)
1 μ L template DNA
1 μ L KOD polymerase
7.5 μ L ddH₂O

Q5 reaction

10 μ L Q5 reaction buffer (5x)
10 μ L GC enhancer (5x)
1 μ L dNTPs (10 mM)
2.5 μ L primer (each)
1 μ L template DNA
0.5 μ L Q5 polymerase
23.5 μ L ddH₂O

Genetic modifications on organisms were usually verified using colony PCRs.

Thereby intact cells served as DNA template using the following conditions:

Taq reaction

2 μ L Taq reaction buffer (5x)
1 μ L dNTPs (10 mM)
1 μ L primer (each)
0.5 μ L DMSO
0.5 μ L Taq polymerase
4 μ L ddH₂O
dip pipette tip of targeted colony into mixture

The following programs were used to amplify DNA fragments:

Tab. 5.1: Knock-down PCR.

step	temp. [°C]	time [sec]
1) hotstart	98	30
2) melting	98	15
3) annealing	68/72 (KOD/Q5)	30
4) elongation	68/72 (KOD/Q5)	30 per 500 bp
5) repeat step 2 – 4 20 times		
6) melting	98	15
7) annealing	55	30
8) elongation	68/72 (KOD/Q5)	30 per 500 bp
9) repeat step 6 – 8 20 times		
10) finish	68/72 (KOD/Q5)	180
11) hold	4	-

Tab. 5.2: Temperature gradient PCR.

step	temp. [°C]	time [sec]
1) hotstart	98	30
2) melting	98	15
3) annealing	temp. gradient: 55 - 68	30
4) elongation	68/72 (KOD/Q5)	30 per 500 bp
5) repeat step 2 – 4 35 times		
6) finish	68/72 (KOD/Q5)	180
7) hold	4	-

Tab. 5.3: Colony PCR.

step	temp. [°C]	time [sec]
1) hotstart	95	30
2) melting	95	15
3) annealing	59	30
4) elongation	72	30 per 500 bp
5) repeat step 2 – 4 30 times		
6) finish	72	180
7) hold	4	-

5.2.2.2.3 Agarose gel electrophoresis

PCR fragments and plasmids can be analyzed and purified using agarose gel electrophoresis. Agarose gel (1%): 500 mg of agarose were suspended in 50 mL TAE buffer and heated in a microwave until the agarose was completely dissolved. The solution was allowed to cool down to approximately 60 °C and poured into a fixed sled in a station. A comb with appropriate number of lanes was placed in the gel, which solidified upon further cooling. Samples were premixed with loading buffer and applied to the gel, which was run at 115 V for 15-20 min. The gel was stained in a diluted ethidium bromide bath for 15 min before bands were visualized by UV-irradiation. DNA-bands of interest were cut and extracted using a E.Z.N.A. Gel Extraction Kit (Omega Biotek, Germany).

5.2.2.2.4 Gateway Cloning

5.2.2.2.4.1 BP cloning reaction

To transfer the *attB*-PCR product into the destination vector pDONRTM207, containing an *attP* recombination site, a BP reaction with BP ClonaseTMII Enzyme Mix was performed. Therefore 1.0 µL of the vector (150 ng/µL) was added to 1.5 µL of the purified *attB*-PCR product (total amount of 150 ng) and 5.5 µL TE buffer at room temperature in a 1.5 mL Eppendorf cup and mixed. 2.0 µL of BP ClonaseTMII Enzyme Mix, thawed on ice, were added and the solution was incubated for 12 h at room temperature. 7 µL of the BP solution were then added to 200 µL of super competent *E. coli*/XL1-Blue cells, which were thawed on ice and incubated for 30 min on ice. The transformation was initiated by heat shock at 42 °C in a water bath for 30 sec and the eppi was placed back on ice for 2 min. The cells were grown for 2 h in 500 µL preheated (37 °C) SOC medium (see table 13) at 37 °C, plated on gentamycin LB agar plates for clone selection (50 - 100 µL per plate) and incubated for 12-24 h at 37 °C. Single clones were picked and grown in 10 mL LB medium containing gentamycin (15 µg/mL) for 16 h at 37 °C. Cryostocks of the overnight culture were prepared according to chapter 2.2 and additionally 5 mL of the cells were harvested (6000 rpm, 4 °C, 5 min) and the plasmid DNA was isolated using E.Z.N.A. Plasmid Mini Kit I (OMEGA Bio-Tek) according to the manufacturer's protocol. The DNA concentration was measured using Infinite® M200 Pro NanoQuant multiplate reader (Tecan) and the validity of the expression vector was proved by DNA sequencing by GATC Biotech AG.

5.2.2.2.4.2 LR cloning reaction

The gene of interest was then cloned into two different expression vector systems (pDest007 and pET300) enabled by the LR reaction. Therefore, 150 ng of the entry clone and 150 ng of the corresponding destination vector were added to 8 µL of TE buffer at room temperature in a 1.5 mL Eppendorf cup and mixed. LR ClonaseTMII Enzyme Mix was added and the reaction mixture was incubated overnight at room temperature. 10 µL of the resulting

attB-expression clone were transformed into 200 μ L of chemically competent *E. coli*/BL21(DE3) cells as described in the BP reaction and selected on ampicillin LB agar plates (100 μ g/mL). The plasmid DNA was isolated using E.Z.N.A. Plasmid Mini Kit I (OMEGA Bio-Tek) according to the manufacturer's protocol, the concentration was measured using Infinite® M200 Pro NanoQuant multiplate reader (Tecan) and the validity of the destination vector was proved via DNA sequencing by GATC Biotech AG.

5.2.2.2.5 Transformation

5.2.2.2.5.1 chemical

One aliquot of chemical competent cells was thawed on ice and respective DNA was added (1 μ L of previously assembled vector or 10 μ L of ligation reaction). The combined solution was incubated at 4 °C for 20 min. before heat shocked at 42 °C for 45 sec. The reaction was cooled on ice for 2 min. and 900 μ L of fresh media was added. Cells recovered for 1 h at 37 °C under continuous shaking and were split into $\frac{1}{4}$ and $\frac{3}{4}$ and plated on 2 plates with corresponding selection marker for the used vector.

5.2.2.2.5.2 electroporation

One aliquot of electrocompetent cells was thawed on ice and DNA of interest was added on ice. The mixture was transferred into an electroshock cuvette and electroporated at 2500 volts with a resistance of 125 ohms. An excess of 10-fold fresh media is added to the solution and gently mixed by inversion. The mixture is transferred into a clean tube and incubated for 1 h at 37 °C under continuous shaking. After recovery cells are spun down for 30 sec. at 6000 rpm, the supernatant was discarded and the remaining pellet was plated on solid medium with corresponding selection marker.

5.2.2.2.5.3 recombination

One aliquot of electrocompetent cells was thawed on ice and 100 – 300 μ g of DNA of interest was added on ice. The mixture was transferred into an electroshock cuvette and electroporated at 2500 volts with a resistance of 1000 ohms. An excess of 10-fold fresh media is added to the solution and gently mixed by inversion. The mixture is transferred into a clean tube and incubated for 1 h at 37 °C under continuous shaking. After recovery cells are spun down for 30 sec. at 6000 rpm, the supernatant was discarded and the remaining pellet was plated on solid medium with corresponding selection marker.

5.2.3 Proteomics5.2.3.1 *Material*5.2.3.1.1 *Buffers*

Name	Composition
PBS	8 g/L NaCl 0.2 g/L KCl 1.44 g/L Na ₂ HPO ₄ 0.24 g/L KH ₂ PO ₄ adjust to pH = 7.4
SDS-stacking gel buffer (10x)	0.5 M Tris Base in H ₂ O adjust to pH = 6.8
SDS resolving buffer (10x)	3.0 M Tris Base in H ₂ O adjust to pH = 8.8
Tris/Glycine buffer	25 mM Tris Base 192 mM Glycine adjust to pH = 8.3
SDS-buffer	0.1 % w/v SDS in Tris/Glycine buffer
Coomassie-stain	0.25 % (w/v) Coomassie Brilliant Blue 10 % (v/v) AcOH 50 % (v/v) MeOH
Destain solution	7.5 % (v/v) AcOH 5 % (v/v) MeOH
TBS buffer	10 mM Tris HCl 150 mM NaCl adjust to pH = 7.5
WTB buffer	15 % (v/v) MeOH in Tris/Glycine buffer
TTBS	200 µL/L Tween 20 in TBS buffer
Rhodamine azide (RhN ₃) stock (300x)	9.9 mg RhN ₃ in 100 µL MeOH
RhN ₃ working stock (1x)	1 µL RhN ₃ -stock in 295 µL DMSO
TBTA ligand-stock (50x)	8.85 mg in 200 µL DMSO
TBTA ligand (1x)	20 µL 50x stock solution 180 µL DMSO 800 µL <i>tert</i> -BuOH
CuSO ₄ (50 mM)	12.5 mg/mL in H ₂ O
DTT (10 mM)	1.54 mg/mL in H ₂ O
IAA (55 mM)	10.2 mg/mL in H ₂ O

5.2.3.2 Methods

5.2.3.2.1 Activity based protein profiling (ABPP)

5.2.3.2.1.1 Gel-based protein profiling

Analytical *in-situ* labeling and click reaction

For analytical *in situ* labeling, 50 mL of the respective cultivation media were inoculated with 5 mL of an overnight culture of the desired bacterial strain (1:10 v/v) in a 250 mL flask and incubated at 37 °C and 200 rpm in an Innova incubator shaker until. The cells were harvested by centrifugation (10 min, 4 °C, 6000 rpm), washed with 20 mL PBS and resuspended in PBS to a theoretical OD₆₀₀ of 40. 200 µL of the bacterial suspension were then incubated with 2 µL of probe in DMSO in varying concentrations for 1 h at room temperature. For competitive experiments competitor was added for 30 min before probe was added for 1h. In case of UV-crosslinking cells were diluted 1:10 in PBS after incubation and transferred onto a 6-well plate, applying one condition to each well. Cells in suspension were irradiated for 10 min at 365 nm in case of diazirine containing compounds. After centrifugation (10 min, 4 °C, 6000 rpm), the bacterial cells were washed with 800 µL PBS and lysed by sonication (3 x 20 sec, 85% max. intensity, on ice). Soluble and insoluble fractions were separated by centrifugation (30 min, 13.000 rpm, 4 °C) and the insoluble fraction was washed additionally with 800 µL PBS. The click reaction was carried out with 50 µL of obtained proteome by addition of 1 µL 1 x RhN₃, 3 µL 1 x TBTA ligand and 1 µL TCEP solution were added to the cells. After gently vortexing the samples, the cycloaddition reaction was initiated by adding 1 µL CuSO₄ solution. The reaction was incubated for 1 h at room temperature and stopped by addition of 50 µL 2 x SDS loading buffer.

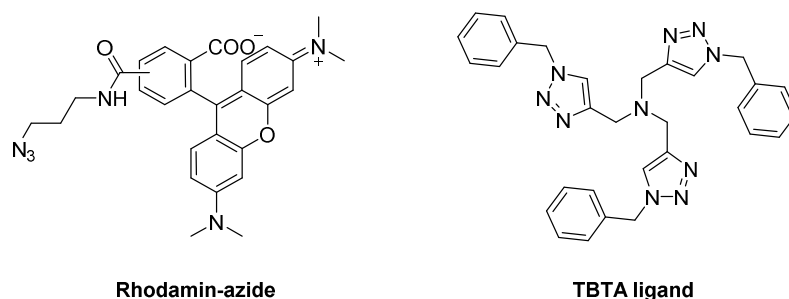


Fig. 5.1: Molecular structure of fluorescent dye Rhodamine-azide (RhN₃) and CuAAC ligand tris[(1-benzyl-1H-1,2,3-triazol-4-yl)methyl]amine (TBTA).

Preparative *in-situ* labeling and click reaction

For preparative *in situ* labeling, 300 mL of the respective cultivation media were inoculated with 30 mL of an overnight culture of the desired bacterial strain (1:10 v/v) in a 1000 mL flask and incubated at 37 °C and 200 rpm in an Innova incubator shaker until mid-exponential phase was reached. The cells were harvested by centrifugation (10 min, 6000 rpm, 4 °C), washed with 20 mL PBS and resuspended in PBS to a theoretical OD₆₀₀ of 40. 1000 µL of the bacterial suspension were then incubated with 10 µL of probe in DMSO in

varying concentrations (see probe stocks) for 1 h at room temperature. A DMSO control containing no probe was additionally added to each experiment to compare the results of the biotin-avidin enriched samples with the background of unspecific protein binding on avidin-agarose beads. After centrifugation (10 min, 6000 rpm, 4 °C), the bacterial cells were washed twice with 1 mL PBS, resuspended in 500 μ L PBS and lysed by sonication (5 x 20 sec, 85% max. intensity, on ice). Membrane and cytosol fraction were separated by centrifugation (45 min, 13.000 rpm, 4 °C), the membrane fraction was additionally washed with 1 mL PBS and resuspended in 700 μ L PBS. For the Click reaction 3 μ L 1 x trifunctional linker, followed by 30 μ L 1 x TBTA ligand and 10 μ L TCEP solution were subsequently added to each sample. After gently vortexing the probes, the click-reaction was initiated by adding 10 μ L CuSO₄ solution. The reaction was incubated for 1 h at room temperature after which the proteins were precipitated over night at -20 °C by adding 4 mL chilled acetone and pelletized by centrifugation (10 min, 8000 rpm, 4 °C). The supernatant was discarded and the pellet was washed two times with 500 μ L chilled MeOH (resuspension by sonication, 1 x 10 sec, 10% max. intensity). After centrifugation (10 min, 13000 rpm, 4 °C), the pellet was resuspended in 1 mL 0.4% SDS by sonication (4 x 10 sec, 10% max. intensity) and incubated under gentle mixing with 50 μ L pre washed avidin-agarose beads (3 x 1 mL 0.4% SDS solution, centrifugation was performed at 2500 rpm for 5 min at RT) for 1 h at room temperature. The beads were washed three times with 1 mL 0.4% SDS, twice with 1 mL 6 M urea and again three times with 1 mL PBS. All supernatants were discarded carefully and 50 μ L 2 x SDS loading buffer was added to the beads. The proteins were released for preparative SDS-PAGE by incubation for 6 min at 96 °C and 350 rpm in an eppi shaker. After centrifugation (2 min, 13000 rpm, RT), the supernatant was isolated and applied on a preparative SDS gel, which was developed for 4 - 5h (300 V). Bands were then visualized by fluorescent scanning (see chapter 3.1.3). The enriched bands as well as the DMSO control were cut out, dismembered into small pieces using a razor blade and stored at -20 °C until further usage.

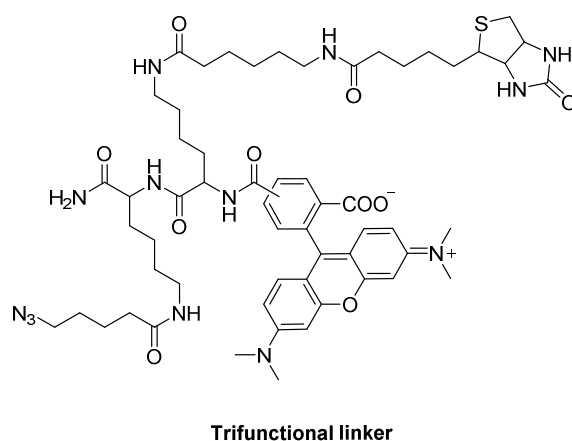


Fig. 5.2: Molecular structure of the trifunctional linker containing a rhodamine fluorophore, a biotin and an alkyl azide moiety.

5.2.3.2.2 SDS-Polyacrylamide gel electrophoresis (SDS-PAGE)

Gels for sodium dodecyl sulfate polyacrylamide gel electrophoresis (SDS-PAGE) were produced in two steps. First, the respective resolving gel mixture was carefully added between two glass plates in a gel chamber until complete polymerization occurred. Second, the stacking gel solution was filled on top of the resolving gel, a gel comb was plunged into the solution and the mixture was allowed to solidify. Before the samples were applied the gel chamber was filled with 1 x SDS running buffer and the comb was removed. Protein standards for coomassie staining and fluorescence analysis were combined and applied to a single well. Samples were loaded in amounts of 30 – 95 μL per well and 2 x SDS loading buffer was filled into remaining pockets. Separation by gel electrophoresis occurred for 2 – 3 h at 150 V for small gels and 4 – 5 h at 300 V for large gels in a EV261 or EC265 Electrophoresis Power Supply (Consort BVAB) under continuous cooling with water. Fluorescence scans were performed with a Fujifilm Las-4000 luminescent image analyzer equipped with a Fujinon VRF43LMD3 lens or a Fujifilm Las-3000 fluorescence darkbox equipped with a Fujinon VRF43LMD3 lens, 605DF40 filter and 520 nm EPI excitation wavelengths. Printouts of fluorescence gels were used to localize and cut the bands in preparative labeling experiments. After the fluorescence scans the gels were washed with ddH₂O and incubated in a Coomassie Brilliant Blue G-250 dye at room temperature overnight. After the stain was removed, the gels were washed with water and then covered with a Coomassie-destainer, which was changed several times until proteins became visible as blue bands.

5.2.3.2.3 In-gel digest

The gel pieces of the preparative labeling experiment stored at -20 °C were washed with ddH₂O (100 μL , 15 min, 550 rpm, RT), MeCN/50 mM ABC (200 μL , 15 min, 550 rpm, RT) and MeCN (100 μL , 10 min, 550 rpm, RT). Then, 100 μL 50 mM ABC was added to the gel pieces followed after 5 min at 550 rpm by additional MeCN (100 μL , 15 min, 550 rpm, RT). The supernatant was removed; the gel pieces were again washed with MeCN (100 μL , 15 min, 550 rpm, RT) and then dried under vacuum in a centrifugal evaporator (15 min, 1 mbar, RT). The proteins were reduced by adding DTT solution (100 μL , 45 min, 550 rpm, 56 °C) to the gel pieces, washed with MeCN (100 μL , 10 min, 550 rpm, RT) and then alkylated by the addition of IAA solution (100 μL , 30 min covered, 550 rpm, RT). After washing three times with MeCN/50 mM ABC (100 μL , 15 min, 550 rpm, RT) and MeCN (100 μL , 10 min, 550 rpm, RT), the gel pieces were again dried under vacuum in a centrifugal evaporator (15 min, 1 mbar, RT). Trypsin digest solution (100 μL , overnight, 300 rpm, 37 °C) was added and the next day the supernatant was transferred into a LoBind Eppendorf cup and 25 mM ABC solution (100 μL , 15 min, sonication, RT) was given to the gel pieces. MeCN (100 μL , 15 min, sonication, RT) was additionally added to the gel pieces and the supernatant was again

transferred into the LoBind Eppendorf cup. The gel pieces were discarded and the solvent of the digested proteins was removed under vacuum in a centrifugal evaporator (5 h, 1 mbar, RT). The remaining peptides were stored at -80 °C until further use.

5.2.3.2.4 Gel free protein profiling

For gel-free studies, cells were labeled in preparative scale as described above. For Click reaction the trifunctional linker was replaced by addition of 20 µL of a bifunctional Biotin-PEG-N₃ linker, followed by 30 µL 1 x TBTA ligand and 10 µL TCEP solution to the proteome samples. After gently vortexing the samples, the cycloaddition reaction was initiated by adding 10 µL CuSO₄ solution. The reaction was incubated for 1 h at room temperature after which the proteins were precipitated over night at -20 °C by adding 4 mL chilled acetone and pelletized by centrifugation (10 min, 8000 rpm, 4 °C). The supernatant was discarded and the pellet was washed two times with 500 µL chilled MeOH (resuspension by sonication, 1 x 10 sec, 10% max. intensity). After centrifugation (10 min, 13000 rpm, 4 °C), the pellet was resuspended in 1 mL 0.4% SDS by sonication (4 x 10 sec, 10% max. intensity) and incubated under gentle mixing with 50 µL pre washed avidin-agarose beads (3 x 1 mL 0.4% SDS solution, centrifugation was performed at 2500 rpm and RT for 5 min) for 1 h at room temperature. The beads were washed three times with 1 mL 0.4% SDS, twice with 1 mL 6 M urea and again three times with 1 mL PBS. After the last washing step, the supernatant was completely removed, digestion buffer (200 µL) was added to the beads and the proteins were reduced by adding DTT solution (1 M, 0.2 µL, 45 min, 450 rpm, RT). After alkylation with IAA solution (550 mM, 2 µL, 30 min in the dark, 450 rpm, RT), the reaction was quenched with DTT solution (1 M, 0.8 µL, 30 min, 450 rpm, RT) and the proteins were digested by adding LysC (0.5 µg/µL, 1 µL, 2 h, 450 rpm, RT). The samples were diluted with TEAB solution (600 µL) and further digested with Trypsin (0.5 µg/µL, 1.5 µL, overnight, 450 rpm, 37°C). To finally quench the reaction, FA (10 µL) was added to the samples which were further desalted using 50 mg Sep-Pak C18 Vac Cartridges (Waters).

5.2.3.2.5 Column-based dimethyl labeling

Column-based dimethyl labeling the cartridges had to be equilibrated with MeCN (1 x 1 mL), elution buffer (1 x 1 mL) and 0.5% FA (in ddH₂O, 3 x 1 mL). The samples (about 800 µL) were loaded to the column via gravity flow and washed with 0.5% FA (in ddH₂O, 5 x 1 mL) and then labeled with 5 mL of the respective dimethyl labeling solution (light (L): 30 mM NaBH₃CN, 0.2% CH₂O, 10 mM NaH₂PO₄, 35 mM Na₂HPO₄, pH 7.5; medium (M): 30 mM NaBH₃CN, 0.2% CD₂O, 10 mM NaH₂PO₄, 35 mM Na₂HPO₄, pH 7.5; heavy (H): 30 mM NaBD₃CN, 0.2% ¹³CD₂O, 10 mM NaH₂PO₄, 35 mM Na₂HPO₄, pH 7.5). The labeled peptides were eluted in a LoBind Eppendorf tube with elution buffer (3 x 250 µL), mixed via label switch, dried under vacuum in a lyophilizer (16 h, 1 mbar, -80°C) and stored at -80°C

5.2.3.2.6 Sample preparation and statistical evaluation

Lyophilized peptide samples were filtrated through centrifugal filters (VWR Centrifugal Filters, modified Nylon, 0.45 μm , low protein binding), which had to be pre-rinsed before usage: ddH₂O (2 \times 500 μL , 13000 rpm, 1 min, RT), aq. 0.05 M NaOH (2 \times 500 μL , 13000 rpm, 1 min, RT) and 1% FA (2 \times 500 μL , 13000 rpm, 1 min, RT). The peptides were dissolved in 1% FA (40 μL , 15 min sonication, RT) and then added to the pre-equilibrated filters (13000 rpm, 4 min, RT). The filtrate was transferred into a PP screw top vial and stored at -20 $^{\circ}\text{C}$ until the measurements were performed. Nano flow LC-MS/MS analysis was performed with an UltiMate 3000 Nano HPLC system (Thermo Scientific) coupled to a LTQ Orbitrap XL (Thermo Scientific) or an Orbitrap Fusion (Thermo Scientific). Peptides were loaded on a trap column (Acclaim C18 PepMap100 75 μm ID \times 2 cm) and washed for 10 min with 0.1% FA (5 $\mu\text{L}/\text{min}$ flow rate), then transferred to an analytical column (Acclaim C18 PepMap RSLC, 75 μm ID \times 15 cm). Raw files were analyzed using MaxQuant software (version 1.5.1.2) with Andromeda as search engine. The search included carbamidomethylation of cysteines as a fixed modification and oxidation of methionines as variable modifications. Trypsin was specified as the proteolytic enzyme with N-terminal cleavage to proline and two missed cleavages allowed. Precursor mass tolerance was set to 4.5 ppm (main search) and fragment mass tolerance to 0.5 Da. Searches were performed against the Uniprot database for the respective organism. The second peptide identification option was enabled. False discovery rate determination was carried out using a decoy database and thresholds were set to 1% both at peptide-spectrum match and at protein levels. “I = L”, “requantification” and “match between runs” (0.7 min match and 20 min alignment time windows) options were enabled. Label-free quantification was enabled with a minimum ratio count of 2. Quantification of dimethyl triplets was carried out based on unique peptides only using “DimethLys0,” and “DimethNter0” as “light”, “DimethLys4,” and “DimethNter4” as “medium” and “DimethLys8,” and “DimethNter8” as “heavy” isotope identifiers requiring a minimum ratio count of 2. In case of gel-based target identification, analysis of the resulting *proteingroups.txt*-table was performed with Perseus 1.5.2.6. Putative contaminants, reverse hits and proteins, that were identified by site only, were removed. Ratios were calculated by dividing the LFQ intensity signal of the excised band by the LFQ intensity of corresponding gel area for the untreated sample. Rows were filtered to contain seven valid values. Ratios were transformed using $\log_2(x)$ and normalized using z-score. *P*-values were obtained using a two sided one sample t-test. (Benjamini Hochberg FDR of 0.01). Statistical analysis of gel-free target identification was performed with Perseus 1.5.2.6. MaxQuant result table *proteingroups.txt* was used for further analysis. Putative contaminants, reverse hits and proteins, that were identified by site only, were removed. Dimethyl isotope ratios were $\log_2(x)$ -transformed, filtered to have six valid values per row (from three

replicates in total), and *z*-score-normalized. $-\text{Log}_{10}$ p-values were obtained by a two sided one sample t-test (Benjamini-Hochberg FDR of 0.01).

5.2.3.2.7 Overexpression and purification of recombinant proteins

The recombinant pDest007- and pET301-BL21 were grown in LB medium (1 L, inoculated 1:100 with an overnight culture) containing ampicillin (100 $\mu\text{g}/\text{mL}$) at 37 °C until an $\text{OD}_{600} = 0.6$ was reached. Afterwards the target gene expression was induced with IPTG solution (concentration adjusted to expression behavior). The cultures were further incubated at 16 °C for 16 h and a not-induced control was added in case of test-overexpressions. The cells were harvested (6000 rpm, 4 °C, 10min), washed with PBS (25 mL) and resuspended in storage buffer. The bacterial pellets were lysed by sonication (20 min, 80% max. intensity, under ice cooling) and the soluble fractions were separated via centrifugation (40 min, 18000 rpm, 4 °C). Purification was performed by an ÄKTA system (GE Healthcare) using a HisTrap™ HP 5 mL column (GE Healthcare). After washing with the binding buffers, the proteins were eluted with the respective elution buffers and suitable fractions were concentrated with an Amicon filter unit (MWCO 10 kDa, Millipore). Dialysis was performed to remove residual imidazol in storage buffer. Finally, the enzymes were purified via size exclusion with an ÄKTA system over a HiLoad 16/60 Superdex 200 prep grade column (GE Healthcare), concentrated again and stored at -80 °C in storage buffer.

5.2.3.2.8 In-situ labeling

For recombinant protein expression LB medium were inoculated with of overnight culture of *E. coli* BL21 (1:100) carrying the expression vector at 37 °C. Expression was induced at an OD_{600} of 0.6 by addition of isopropyl- β -D-thiogalactopyranosid (IPTG; final concentration: 0.20 mM) and carried out 20 h at 16°C. After centrifugation (5 min, 6200 xG, 4°C) and removal of the supernatant bacteria were resuspended in PBS to get an OD_{600} of 40. To 1 mL of this suspension in a microcentrifuge tube probe or DMSO as a control were added. After 30 min incubation at RT in the dark the microcentrifuge tube was again mixed by vortexing and incubated for another 30 min at RT in the dark. After centrifugation (6200 xG, 2 min, 4°C) the supernatant was removed and the pellets were stored at -80°C. Pellets were resuspended in 1 mL PBS (4°C) and transferred to a 'Precellys Glass/Ceramic Kit SK38 2.0 mL' tube. Tubes were cooled on ice for about 5 min or longer and cells were lysed with the Precellys Homogeniser using two times lysis program 3 (5400 rpm, run number: 1, run time: 20 sec, pause: 5 sec). After each lysis run the tubes were cooled on ice for 5 min. The ball mill tubes were centrifuged (16200 xG, 10 min, 4°C) and 86 μL of supernatant were transferred to new 1.5 mL microcentrifuge tubes and treated with 10 μL gel-based ABPP Mix (2 μL RhN₃ (Tetramethylrhodamine (TAMRA) Azide (Tetramethylrhodamine 5-Carboxamido-(6-Azido)hexanyl)), 5-isomer (life technologies, T10182); 5 mM in DMSO), 2 μL fresh TCEP (50 mM in ddH₂O), 6 μL TBTA Ligand (1.667 mM in 80 % tBuOH and 20 % DMSO)). The final concentrations were: 100 μM RhN₃, 1.0 mM TCEP and 100 μM TBTA Ligand. The lysates were mixed by vortexing and 2 μL CuSO₄ solution (50 mM in ddH₂O) were added. The lysates were again mixed by vortexing and incubated for 1h at RT in the dark. Then 80 μL 2x Laemmli

Sample Buffer were added, samples were mixed in a thermomixer (300 rpm, 3 min, 96°C) and analyzed via SDS PAGE (10 % agarose gel (PEQLAB Biotechnologie GmbH, Erlangen, PerfectBlue Dual Gel System, the gel was prepared according to the manual), 3.5 h, 300 V, 8 µL fluorescent protein standard) and fluorescence imaging (GE Healthcare, ImageQuant LAS-4000). After fluorescence scanning the gel was coomassie stained.

5.2.3.2.9 *Western Blot*

A culture of approximately 10 mL was grown to exponential growth phase and harvested by centrifugation at 6000x g and 4 °C for 10 min. The supernatant was discarded and the remaining pellet was resuspended in 300 µL of TBS buffer including protease inhibitor mix by Roche®. The cell suspension was transferred into a screw cap vial containing glass beads and lysed by beating four times for 30 sec. with ice cooling between runs. The turbid solution is transferred into a fresh vial and layers are separated by centrifugation at 15000x g and 4 °C for 30 min. The clear supernatant was transferred into a fresh vial and the protein concentration was determined and normalized for all samples. (Protein concentration should exceed 5 mg/mL) 3 µL of 6x Laemmli buffer were added to 15 µL of protein solution and mixed. 15 µL of the previous mix are separated by SDS-PAGE. Two slices of thick blotting paper were wet in WTB and one was placed on the bottom of transfer apparatus. A piece of polyvinylidene fluoride membrane was washed with MeOH and WTB and added on top of the blotting paper. The run gel was added to the sandwich and topped by the wet second blotting paper. Proteins were blotted by electrophoresis for 40 min. at 15 V. The membrane was blocked for 30 min. in TTBS with 5 % milk powder at r.t. The antibody was applied as a 1:1000 to 1:5000 dilution in TBS buffer for 1 h at r.t. and continuous shaking. The blot was washed three to five times with TTBS before the secondary antibody was applied for 1 h at r.t. After washing the gel several times with TTBS 500 µL of each Super Signal West Femto Luminol Enhancer and Peroxid Buffer were added. The gel was developed for 30 sec to 10 min.

Chapter 6 Appendix

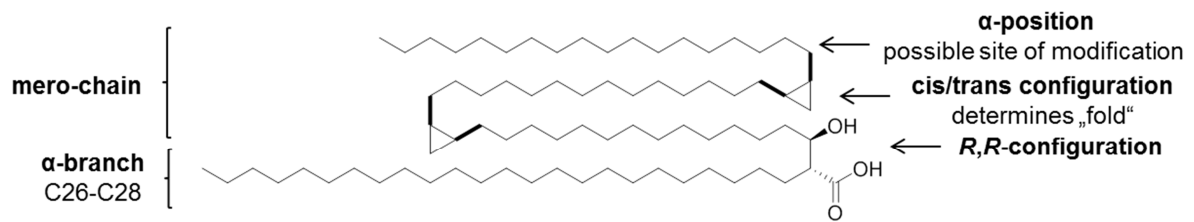


Fig. 6.1: Schematic structure of Mtb MA.

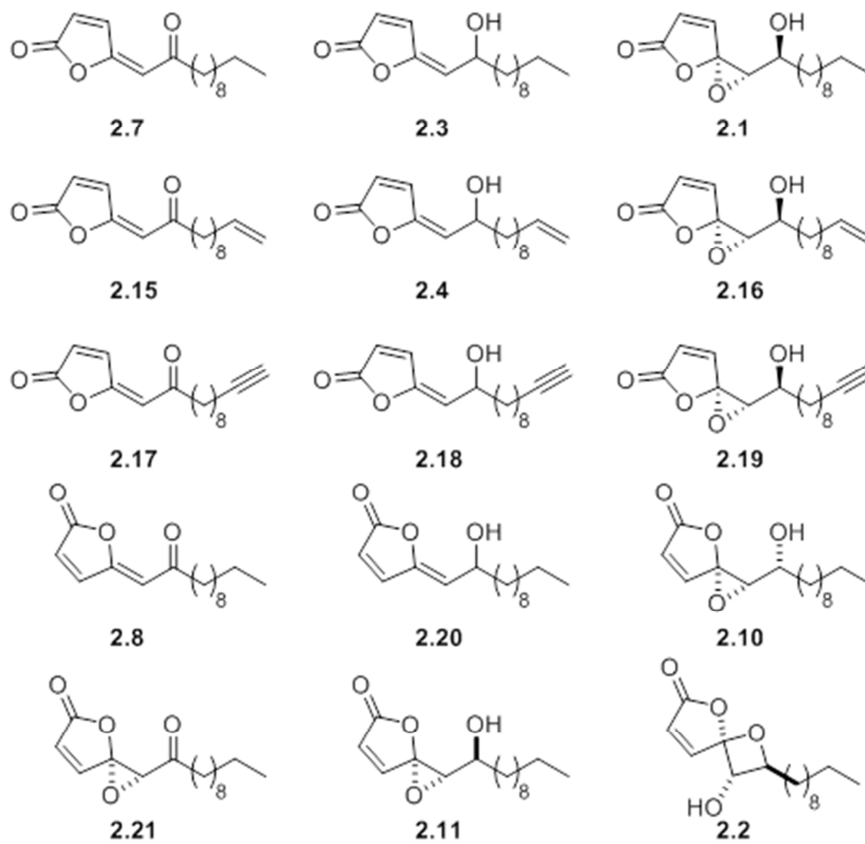


Fig. 6.2: Overview of synthesized ramariolide-molecules and -derivatives.

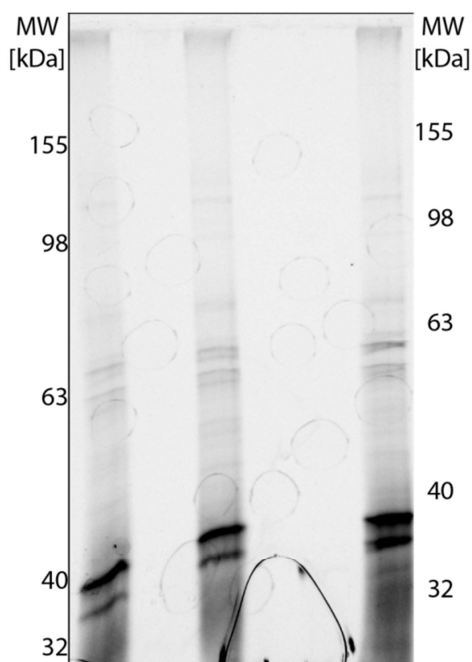


Fig. 6.3: Preparative gel-based labeling of Msmeg insoluble fraction using 50 μ M **EZ120P** in biological triplicates.

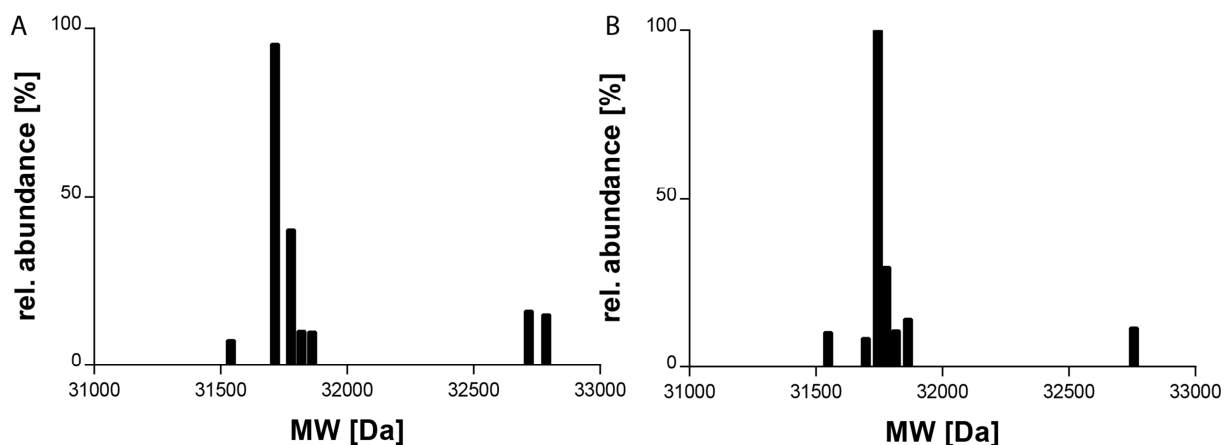


Fig. 6.4: Intact MS spectra of wt-Pks13TE domain with tenfold excess of **A.** D3 lactone and **B.** La-0.

Table 6.1: Protein hits without essential function for mycobacterial growth identified using probe 2.23. Entries 1-4 were found for UV-irradiated enrichment; 5-9 were found for enrichment without UV-irradiation.

entry	Gene name	Uniprot accession number
1	Msmeg_1028	A0QR89
2	Msmeg_1305	A0QS07
3	Msmeg_0309	A0QP86
4	Msmeg_0067	A0QNJ7
5	devR	A0R2V2
6	suhB	A0QW04
7	gspA	A0QUZ5
8	Msmeg_4686	A0R1A8
9	Msmeg_4272	A0R061

Chapter 7 References

1. M. Daffe and P. Draper, *Advances in microbial physiology*, 1998, **39**, 131-203.
2. L. Y. Gao, F. Laval, E. H. Lawson, R. K. Groger, A. Woodruff, J. H. Morisaki, J. S. Cox, M. Daffe and E. J. Brown, *Molecular microbiology*, 2003, **49**, 1547-1563.
3. C. L. Silva, S. M. Ekizlerian and R. A. Fazioli, *The American journal of pathology*, 1985, **118**, 238-247.
4. H. Noll, H. Bloch, J. Asselineau and E. Lederer, *Biochimica et biophysica acta*, 1956, **20**, 299-309.
5. J. C. Camus, M. J. Pryor, C. Medigue and S. T. Cole, *Microbiology*, 2002, **148**, 2967-2973.
6. WHO, 2015.
7. R. Koch, *Berliner Klinische Wochenschrift*, 1882, **19**, 221-230.
8. WHO, 2016, **20**.
9. M. Gengenbacher and S. H. Kaufmann, *FEMS microbiology reviews*, 2012, **36**, 514-532.
10. *MMWR. Morbidity and mortality weekly report*, 2006, **55**, 301-305.
11. A. Bhatt, V. Molle, G. S. Besra, W. R. Jacobs, Jr. and L. Kremer, *Molecular microbiology*, 2007, **64**, 1442-1454.
12. A. H. Diacon, A. Pym, M. Grobusch, R. Patientia, R. Rustomjee, L. Page-Shipp, C. Pistorius, R. Krause, M. Bogoshi, G. Churchyard, A. Venter, J. Allen, J. C. Palomino, T. De Marez, R. P. van Heeswijk, N. Lounis, P. Meyvisch, J. Verbeeck, W. Parys, K. de Beule, K. Andries and D. F. Mc Neeley, *The New England journal of medicine*, 2009, **360**, 2397-2405.
13. R. Mahajan, *International journal of applied & basic medical research*, 2013, **3**, 1-2.
14. P. A. Lambert, *Journal of applied microbiology*, 2002, **92 Suppl**, 46S-54S.
15. A. Koul, E. Arnoult, N. Lounis, J. Guillemont and K. Andries, *Nature*, 2011, **469**, 483-490.
16. R. E. Gordon and M. M. Smith, *Journal of bacteriology*, 1953, **66**, 41-48.
17. J. M. Reyrat and D. Kahn, *Trends in microbiology*, 2001, **9**, 472-474.
18. P. J. Brennan, *Tuberculosis*, 2003, **83**, 91-97.
19. A. Ortalo-Magne, A. Lemassu, M. A. Laneelle, F. Bardou, G. Silve, P. Gounon, G. Marchal and M. Daffe, *Journal of bacteriology*, 1996, **178**, 456-461.
20. R. L. Hunter, M. R. Olsen, C. Jagannath and J. K. Actor, *Annals of clinical and laboratory science*, 2006, **36**, 371-386.
21. J. Asselineau and E. Lederer, *Nature*, 1950, **166**, 782-783.
22. H. Marrakchi, M. A. Laneelle and M. Daffe, *Chem Biol*, 2014, **21**, 67-85.
23. E. Lederer, *Quarterly Reviews, Chemical Society*, 1969, **23**, 453-481.
24. D. Portevin, C. De Sousa-D'Auria, C. Houssin, C. Grimaldi, M. Chami, M. Daffe and C. Guilhot, *Proceedings of the National Academy of Sciences of the United States of America*, 2004, **101**, 314-319.
25. D. J. Lea-Smith, J. S. Pyke, D. Tull, M. J. McConville, R. L. Coppel and P. K. Crellin, *The Journal of biological chemistry*, 2007, **282**, 11000-11008.
26. A. E. Grzegorzewicz, H. Pham, V. A. Gundi, M. S. Scherman, E. J. North, T. Hess, V. Jones, V. Gruppo, S. E. Born, J. Kordulakova, S. S. Chavadi, C. Morisseau, A. J. Lenaerts, R. E. Lee, M. R. McNeil and M. Jackson, *Nature chemical biology*, 2012, **8**, 334-341.
27. A. Ahibo-Coffy, H. Aurelle, C. Lacave, J. C. Prome, G. Puzo and A. Savagnac, *Chemistry and physics of lipids*, 1978, **22**, 185-195.
28. J. T. Belisle, V. D. Vissa, T. Sievert, K. Takayama, P. J. Brennan and G. S. Besra, *Science (New York, N.Y.)*, 1997, **276**, 1420-1422.
29. K. Tahlan, R. Wilson, D. B. Kastrinsky, K. Arora, V. Nair, E. Fischer, S. W. Barnes, J. R. Walker, D. Alland, C. E. Barry, 3rd and H. I. Boshoff, *Antimicrobial agents and chemotherapy*, 2012, **56**, 1797-1809.
30. D. J. Newman and G. M. Cragg, *Journal of natural products*, 2007, **70**, 461-477.
31. D. J. Newman, G. M. Cragg and K. M. Snader, *Natural product reports*, 2000, **17**, 215-234.

32. G. M. Cragg and D. J. Newman, *Biochimica et Biophysica Acta (BBA) - General Subjects*, 2013, **1830**, 3670-3695.
33. C. A. Lipinski, *Drug discovery today. Technologies*, 2004, **1**, 337-341.
34. R. Mah, J. R. Thomas and C. M. Shafer, *Bioorganic & Medicinal Chemistry Letters*, 2014, **24**, 33-39.
35. J. Singh, R. C. Petter, T. A. Baillie and A. Whitty, *Nat Rev Drug Discov*, 2011, **10**, 307-317.
36. M. Gersch, J. Kreuzer and S. A. Sieber, *Natural product reports*, 2012, **29**, 659-682.
37. D. E. Hague, J. R. Idle, S. C. Mitchell and R. L. Smith, *Xenobiotica; the fate of foreign compounds in biological systems*, 2011, **41**, 837-843.
38. P. Y. Yang, K. Liu, M. H. Ngai, M. J. Lear, M. R. Wenk and S. Q. Yao, *Journal of the American Chemical Society*, 2010, **132**, 656-666.
39. N. L. Harvey, J. Krysiak, S. Chamni, S. W. Cho, S. A. Sieber and D. Romo, *Chemistry (Weinheim an der Bergstrasse, Germany)*, 2015, **21**, 1425-1428.
40. M. Jouanneau, B. McClary, J. C. Reyes, R. Chen, Y. Chen, W. Plunkett, X. Cheng, A. Z. Milinichik, E. F. Albone, J. O. Liu and D. Romo, *Bioorg Med Chem Lett*, 2016, **26**, 2092-2097.
41. K. Harmrolfs, L. Mancuso, B. Drung, F. Sasse and A. Kirschning, *Beilstein journal of organic chemistry*, 2014, **10**, 535-543.
42. J. Hermene, I. Bulyszko, S. Eichner, F. Sasse, W. Collisi, A. Poso, E. Schax, J.-G. Walter, T. Scheper, K. Kock, C. Herrmann, P. Aliuos, G. Reuter, C. Zeilinger and A. Kirschning, *ChemBioChem*, 2015, **16**, 302-311.
43. I. Bulyszko, G. Drager, A. Klenge and A. Kirschning, *Chemistry (Weinheim an der Bergstrasse, Germany)*, 2015, **21**, 19231-19242.
44. A. A. Brakhage, J. Schuemann, S. Bergmann, K. Scherlach, V. Schroeckh and C. Hertweck, *Progress in drug research. Fortschritte der Arzneimittelforschung. Progres des recherches pharmaceutiques*, 2008, **66**, 1, 3-12.
45. K. Scherlach and C. Hertweck, *Org Biomol Chem*, 2009, **7**, 1753-1760.
46. C. P. Hart, *Drug Discovery Today*, 2005, **10**, 513-519.
47. U. Rajcevic, S. P. Niclou and C. R. Jimenez, *Frontiers in bioscience (Landmark edition)*, 2009, **14**, 3292-3303.
48. B. Lomenick, R. Hao, N. Jonai, R. M. Chin, M. Aghajan, S. Warburton, J. Wang, R. P. Wu, F. Gomez, J. A. Loo, J. A. Wohlschlegel, T. M. Vondriska, J. Pelletier, H. R. Herschman, J. Clardy, C. F. Clarke and J. Huang, *Proceedings of the National Academy of Sciences*, 2009, **106**, 21984-21989.
49. B. Lomenick, R. W. Olsen and J. Huang, *ACS chemical biology*, 2011, **6**, 34-46.
50. G. C. Adam, B. F. Cravatt and E. J. Sorensen, *Chem. Biol.*, 2001, **8**, 81-95.
51. B. F. Cravatt, A. T. Wright and J. W. Kozarich, *Annu Rev Biochem*, 2008, **77**, 383-414.
52. K. T. Barglow and B. F. Cravatt, *Nature methods*, 2007, **4**, 822-827.
53. S. A. Sieber and B. F. Cravatt, *Chemical communications (Cambridge, England)*, 2006, 2311-2319.
54. T. Böttcher, M. Pitscheider and S. A. Sieber, *Angewandte Chemie (International ed. in English)*, 2010, **49**, 2680-2698.
55. E. Saxon and C. R. Bertozzi, *Science (New York, N.Y.)*, 2000, **287**, 2007-2010.
56. H. Staudinger and J. Meyer, *Helvetica Chimica Acta*, 1919, **2**, 635-646.
57. H.-W. Shih, D. N. Kamber and J. A. Prescher, *Current Opinion in Chemical Biology*, 2014, **21**, 103-111.
58. Craig S. McKay and M. G. Finn, *Chemistry & Biology*, 2014, **21**, 1075-1101.
59. D. M. Patterson, L. A. Nazarova and J. A. Prescher, *ACS chemical biology*, 2014, **9**, 592-605.
60. R. Huisgen, *Proc. Chem. Soc.*, 1961, 357-396.
61. R. Huisgen, *1,3 Dipolar Cylcoaddition Chemistry*, Wiley, New York, 1984.
62. V. V. Rostovtsev, L. G. Green, V. V. Fokin and K. B. Sharpless, *Angewandte Chemie (International ed. in English)*, 2002, **41**, 2596-2599.
63. C. W. Tornøe, C. Christensen and M. Meldal, *J Org Chem*, 2002, **67**, 3057-3064.
64. R. Berg and B. F. Straub, *Beilstein journal of organic chemistry*, 2013, **9**, 2715-2750.

65. J. Lehmann, M. H. Wright and S. A. Sieber, *Chemistry (Weinheim an der Bergstrasse, Germany)*, 2016, **22**, 4666-4678.
66. A. L. MacKinnon, J. L. Garrison, R. S. Hegde and J. Taunton, *Journal of the American Chemical Society*, 2007, **129**, 14560-14561.
67. L. Meng, R. Mohan, B. H. Kwok, M. Elofsson, N. Sin and C. M. Crews, *Proceedings of the National Academy of Sciences of the United States of America*, 1999, **96**, 10403-10408.
68. J. Eirich, J. L. Burkhardt, A. Ullrich, G. C. Rudolf, A. Vollmar, S. Zahler, U. Kazmaier and S. A. Sieber, *Mol Biosyst*, 2012, **8**, 2067-2075.
69. E. J. Corey and P. L. Fuchs, *Tetrahedron Letters*, 1972, **13**, 3769-3772.
70. E. W. Colvin and B. J. Hamill, *Journal of the Chemical Society, Chemical Communications*, 1973, 151-152.
71. S. Ohira, *Synthetic Communications*, 1989, **19**, 561-564.
72. T. Böttcher and S. A. Sieber, *Journal of the American Chemical Society*, 2010, **132**, 6964-6972.
73. E. Zeiler, N. Braun, T. Böttcher, A. Kastenmuller, S. Weinkauff and S. A. Sieber, *Angewandte Chemie (International ed. in English)*, 2011, **50**, 11001-11004.
74. R. M. Buey, E. Calvo, I. Barasoain, O. Pineda, M. C. Edler, R. Matesanz, G. Cerezo, C. D. Vanderwal, B. W. Day, E. J. Sorensen, J. A. Lopez, J. M. Andreu, E. Hamel and J. F. Diaz, *Nature chemical biology*, 2007, **3**, 117-125.
75. T. Usui, H. Watanabe, H. Nakayama, Y. Tada, N. Kanoh, M. Kondoh, T. Asao, K. Takio, H. Watanabe, K. Nishikawa, T. Kitahara and H. Osada, *Chem Biol*, 2004, **11**, 799-806.
76. L. Li, C.-W. Zhang, J. Ge, L. Qian, B.-H. Chai, Q. Zhu, J.-S. Lee, K.-L. Lim and S. Q. Yao, *Angewandte Chemie International Edition*, 2015, **54**, 10821-10825.
77. R. A. G. Smith and J. R. Knowles, *Journal of the American Chemical Society*, 1973, **95**, 5072-5073.
78. B. F. Cravatt, G. M. Simon and J. R. Yates, 3rd, *Nature*, 2007, **450**, 991-1000.
79. R. M. Centko, S. Ramon-Garcia, T. Taylor, B. O. Patrick, C. J. Thompson, V. P. Miao and R. J. Andersen, *Journal of natural products*, 2012, **75**, 2178-2182.
80. T. Böttcher and S. A. Sieber, *Angewandte Chemie (International ed. in English)*, 2008, **47**, 4600-4603.
81. T. Böttcher and S. A. Sieber, *Chembiochem*, 2009, **10**, 663-666.
82. E. Zeiler, V. S. Korotkov, K. Lorenz-Baath, T. Böttcher and S. A. Sieber, *Bioorg Med Chem*, 2011, **20**, 583-591.
83. B. Borgstrom, *Biochimica et biophysica acta*, 1988, **962**, 308-316.
84. M. S. Ravindran, S. P. Rao, X. Cheng, A. Shukla, A. Cazenave-Gassiot, S. Q. Yao and M. R. Wenk, *Molecular & cellular proteomics : MCP*, 2014, **13**, 435-448.
85. H. Ren and W. D. Wulff, *Org Lett*, 2010, **12**, 4908-4911.
86. L. Wang, C. Cherian, S. K. Desmoulin, L. Polin, Y. Deng, J. Wu, Z. Hou, K. White, J. Kushner, L. H. Matherly and A. Gangjee, *Journal of medicinal chemistry*, 2010, **53**, 1306-1318.
87. D. W. Knight and G. Pattenden, *Journal of the Chemical Society, Perkin Transactions 1*, 1979, 62-69.
88. D. M. Bradley, R. Mapitse, N. M. Thomson and C. J. Hayes, *J Org Chem*, 2002, **67**, 7613-7617.
89. J. S. Fowler and S. Seltzer, *The Journal of Organic Chemistry*, 1970, **35**, 3529-3532.
90. G. Struve and S. Seltzer, *The Journal of Organic Chemistry*, 1982, **47**, 2109-2113.
91. T. Katsuki and K. B. Sharpless, *Journal of the American Chemical Society*, 1980, **102**, 5974-5976.
92. N. S. Kim, J. R. Choi and J. K. Cha, *The Journal of Organic Chemistry*, 1993, **58**, 7096-7099.
93. W. H. Pirkle and P. L. Rinaldi, *The Journal of Organic Chemistry*, 1979, **44**, 1025-1028.
94. G. B. Payne, *The Journal of Organic Chemistry*, 1962, **27**, 3819-3822.
95. R. Cambie, N. Renner, P. Rutledge and P. Woodgate, *Australian Journal of Chemistry*, 1991, **44**, 61-75.
96. J. Chen, P. Gao, F. Yu, Y. Yang, S. Zhu and H. Zhai, *Angewandte Chemie (International ed. in English)*, 2012, **51**, 5897-5899.

97. Z. Li, P. Hao, L. Li, C. Y. Tan, X. Cheng, G. Y. Chen, S. K. Sze, H. M. Shen and S. Q. Yao, *Angewandte Chemie (International ed. in English)*, 2013, **52**, 8551-8556.
98. M. H. Wright and S. A. Sieber, *Natural product reports*, 2016, **33**, 681-708.
99. P. J. Boersema, R. Raijmakers, S. Lemeer, S. Mohammed and A. J. Heck, *Nature protocols*, 2009, **4**, 484-494.
100. C. M. Sasseti, D. H. Boyd and E. J. Rubin, *Proceedings of the National Academy of Sciences of the United States of America*, 2001, **98**, 12712-12717.
101. D. Mellacheruvu, Z. Wright, A. L. Couzens, J. P. Lambert, N. A. St-Denis, T. Li, Y. V. Miteva, S. Hauri, M. E. Sardi, T. Y. Low, V. A. Halim, R. D. Bagshaw, N. C. Hubner, A. Al-Hakim, A. Bouchard, D. Faubert, D. Fermin, W. H. Dunham, M. Goudreault, Z. Y. Lin, B. G. Badillo, T. Pawson, D. Durocher, B. Coulombe, R. Aebersold, G. Superti-Furga, J. Colinge, A. J. Heck, H. Choi, M. Gstaiger, S. Mohammed, I. M. Cristea, K. L. Bennett, M. P. Washburn, B. Raught, R. M. Ewing, A. C. Gingras and A. I. Nesvizhskii, *Nature methods*, 2013, **10**, 730-736.
102. J. Leodolter, J. Warweg and E. Weber-Ban, *PloS one*, 2015, **10**, e0125345.
103. K. R. Schmitz and R. T. Sauer, *Molecular microbiology*, 2014, **93**, 617-628.
104. D. Frees, K. Sorensen and H. Ingmer, *Infection and immunity*, 2005, **73**, 8100-8108.
105. V. Sritharan, P. R. Wheeler and C. Ratledge, *European journal of biochemistry / FEBS*, 1989, **180**, 587-593.
106. J. D. Cirillo, T. R. Weisbrod, L. Pascopella, B. R. Bloom and W. R. Jacobs, Jr., *Molecular microbiology*, 1994, **11**, 629-639.
107. R. H. Felting, G. O. Buchanan, T. J. Mincer, C. A. Kauffman, P. R. Jensen and W. Fenical, *Angewandte Chemie (International ed. in English)*, 2003, **42**, 355-357.
108. E. Tonew, M. Tonew, U. Grafe and P. Zopel, *Acta virologica*, 1992, **36**, 166-172.
109. M. Groll and B. C. Potts, *Current topics in medicinal chemistry*, 2011, **11**, 2850-2878.
110. P. Hadvary, W. Sidler, W. Meister, W. Vetter and H. Wolfer, *The Journal of biological chemistry*, 1991, **266**, 2021-2027.
111. M. Bogyo and E. W. Wang, *Curr. Top. Microbiol. Immunol.*, 2002, **268**, 184-208.
112. E. J. Corey and W. D. Li, *Chem Pharm Bull (Tokyo)*, 1999, **47**, 1-10.
113. M. Groll, E. P. Balskus and E. N. Jacobsen, *Journal of the American Chemical Society*, 2008, **130**, 14981-14983.
114. M. Groll, R. Huber and B. C. Potts, *Journal of the American Chemical Society*, 2006, **128**, 5136-5141.
115. T. Böttcher and S. A. Sieber, *Journal of the American Chemical Society*, 2008, **130**, 14400-14401.
116. R. L. Danheiser, Nowick, J. S., *J. Org. Chem.*, 1991, **56**, 1176-1185.
117. M. Gersch, F. Gut, V. S. Korotkov, J. Lehmann, T. Böttcher, M. Rusch, C. Hedberg, H. Waldmann, G. Klebe and S. A. Sieber, *Angewandte Chemie (International ed. in English)*, 2013, **52**, 3009-3014.
118. D. Frees, J. H. Andersen, L. Hemmingsen, K. Koskenniemi, K. T. Baek, M. K. Muhammed, D. D. Gudeta, T. A. Nyman, A. Sukura, P. Varmanen and K. Savijoki, *Journal of proteome research*, 2012, **11**, 95-108.
119. D. Frees, S. N. Qazi, P. J. Hill and H. Ingmer, *Molecular microbiology*, 2003, **48**, 1565-1578.
120. C. L. Compton, K. R. Schmitz, R. T. Sauer and J. K. Sello, *ACS chemical biology*, 2013, **8**, 2669-2677.
121. J. Cox, M. Y. Hein, C. A. Luber, I. Paron, N. Nagaraj and M. Mann, *Molecular & cellular proteomics : MCP*, 2014, **13**, 2513-2526.
122. J. M. Asara, H. R. Christofk, L. M. Freemark and L. C. Cantley, *Proteomics*, 2008, **8**, 994-999.
123. D. A. Bachovchin, T. Ji, W. Li, G. M. Simon, J. L. Blankman, A. Adibekian, H. Hoover, S. Niessen and B. F. Cravatt, *Proceedings of the National Academy of Sciences of the United States of America*, 2010, **107**, 20941-20946.
124. V. Puech, C. Guilhot, E. Perez, M. Tropis, L. Y. Armitige, B. Gicquel and M. Daffe, *Molecular microbiology*, 2002, **44**, 1109-1122.

125. S. Gavalda, F. Bardou, F. Laval, C. Bon, W. Malaga, C. Chalut, C. Guilhot, L. Mourey, M. Daffe and A. Quemard, *Chem Biol*, 2014, **21**, 1660-1669.
126. B. S. Kim, T. A. Cropp, B. J. Beck, D. H. Sherman and K. A. Reynolds, *The Journal of biological chemistry*, 2002, **277**, 48028-48034.
127. A. I. Rosenbaum, C. C. Cosner, C. J. Mariani, F. R. Maxfield, O. Wiest and P. Helquist, *Journal of medicinal chemistry*, 2010, **53**, 5281-5289.
128. L. Kremer, W. N. Maughan, R. A. Wilson, L. G. Dover and G. S. Besra, *Letters in applied microbiology*, 2002, **34**, 233-237.
129. I. Matsunaga, T. Naka, R. S. Talekar, M. J. McConnell, K. Katoh, H. Nakao, A. Otsuka, S. M. Behar, I. Yano, D. B. Moody and M. Sugita, *The Journal of biological chemistry*, 2008, **283**, 28835-28841.
130. D. R. Ronning, V. Vissa, G. S. Besra, J. T. Belisle and J. C. Sacchettini, *The Journal of biological chemistry*, 2004, **279**, 36771-36777.
131. L. Y. Armitige, C. Jagannath, A. R. Wanger and S. J. Norris, *Infection and immunity*, 2000, **68**, 767-778.
132. T. Warriar, M. Tropis, J. Werngren, A. Diehl, M. Gengenbacher, B. Schlegel, M. Schade, H. Oschkinat, M. Daffe, S. Hoffner, A. N. Eddine and S. H. E. Kaufmann, *Antimicrobial agents and chemotherapy*, 2012, **56**, 1735-1743.
133. L. Favrot, A. E. Grzegorzewicz, D. H. Lajiness, R. K. Marvin, J. Boucau, D. Isailovic, M. Jackson and D. R. Ronning, *Nature communications*, 2013, **4**, 2748.
134. L. Favrot, D. H. Lajiness and D. R. Ronning, *The Journal of biological chemistry*, 2014, **289**, 25031-25040.
135. K. R. Caleffi-Ferracioli, F. G. Maltempe, V. L. Siqueira and R. F. Cardoso, *Tuberculosis*, 2013, **93**, 660-663.
136. D. F. Bruhn, M. S. Scherman, J. Liu, D. Scherbakov, B. Meibohm, E. C. Bottger, A. J. Lenaerts and R. E. Lee, *Sci Rep*, 2015, **5**, 13985.
137. B. G. Schroeder and C. E. Barry, 3rd, *Bioorganic chemistry*, 2001, **29**, 164-177.
138. N. J. Garton, H. Christensen, D. E. Minnikin, R. A. Adegbola and M. R. Barer, *Microbiology*, 2002, **148**, 2951-2958.
139. G. Singh, G. Singh, D. Jadeja and J. Kaur, *Critical reviews in microbiology*, 2010, **36**, 259-269.
140. H. Christensen, N. J. Garton, R. W. Horobin, D. E. Minnikin and M. R. Barer, *Molecular microbiology*, 1999, **31**, 1561-1572.
141. J. Daniel, H. Maamar, C. Deb, T. D. Sirakova and P. E. Kolattukudy, *PLoS pathogens*, 2011, **7**, e1002093.
142. C. Deb, C. M. Lee, V. S. Dubey, J. Daniel, B. Abomoelak, T. D. Sirakova, S. Pawar, L. Rogers and P. E. Kolattukudy, *PloS one*, 2009, **4**, e6077.
143. H. Bloch and W. Segal, *Journal of bacteriology*, 1956, **72**, 132-141.
144. D. G. Russell, P. J. Cardona, M. J. Kim, S. Allain and F. Altare, *Nature immunology*, 2009, **10**, 943-948.
145. P. Peyron, J. Vaubourgeix, Y. Poquet, F. Levillain, C. Botanch, F. Bardou, M. Daffe, J. F. Emile, B. Marchou, P. J. Cardona, C. de Chastellier and F. Altare, *PLoS pathogens*, 2008, **4**, e1000204.
146. G. Dodson and A. Wlodawer, *Trends in biochemical sciences*, 1998, **23**, 347-352.
147. L.-N. Zhang, J. Vincelette, D. Chen, R. D. Gless, S.-K. Anandan, G. M. Rubanyi, H. K. Webb, D. E. MacIntyre and Y.-X. Wang, *European Journal of Pharmacology*, 2011, **654**, 68-74.
148. W. Li, J. L. Blankman and B. F. Cravatt, *Journal of the American Chemical Society*, 2007, **129**, 9594-9595.
149. C. W. t. Pemble, L. C. Johnson, S. J. Kridel and W. T. Lowther, *Nat Struct Mol Biol*, 2007, **14**, 704-709.
150. M. H. Ngai, P. Y. Yang, K. Liu, Y. Shen, M. R. Wenk, S. Q. Yao and M. J. Lear, *Chemical communications (Cambridge, England)*, 2010, **46**, 8335-8337.
151. E. K. Weibel, P. Hadvary, E. Hochuli, E. Kupfer and H. Lengsfeld, *The Journal of antibiotics*, 1987, **40**, 1081-1085.

152. H. S. Hoover, J. L. Blankman, S. Niessen and B. F. Cravatt, *Bioorg Med Chem Lett*, 2008, **18**, 5838-5841.
153. S. T. Cole, R. Brosch, J. Parkhill, T. Garnier, C. Churcher, D. Harris, S. V. Gordon, K. Eiglmeier, S. Gas, C. E. Barry, 3rd, F. Tekaiia, K. Badcock, D. Basham, D. Brown, T. Chillingworth, R. Connor, R. Davies, K. Devlin, T. Feltwell, S. Gentles, N. Hamlin, S. Holroyd, T. Hornsby, K. Jagels, A. Krogh, J. McLean, S. Moule, L. Murphy, K. Oliver, J. Osborne, M. A. Quail, M. A. Rajandream, J. Rogers, S. Rutter, K. Seeger, J. Skelton, R. Squares, S. Squares, J. E. Sulston, K. Taylor, S. Whitehead and B. G. Barrell, *Nature*, 1998, **393**, 537-544.
154. L. Dedieu, C. Serveau-Avesque, L. Kremer and S. Canaan, *Biochimie*, 2013, **95**, 66-73.
155. L. Kremer, C. de Chastellier, G. Dobson, K. J. Gibson, P. Bifani, S. Balor, J. P. Gorvel, C. Loch, D. E. Minnikin and G. S. Besra, *Molecular microbiology*, 2005, **57**, 1113-1126.
156. A. C. Braisted, J. D. Oslob, W. L. Delano, J. Hyde, R. S. McDowell, N. Waal, C. Yu, M. R. Arkin and B. C. Raimundo, *Journal of the American Chemical Society*, 2003, **125**, 3714-3715.
157. A. Michelucci, T. Cordes, J. Ghelfi, A. Pailot, N. Reiling, O. Goldmann, T. Binz, A. Wegner, A. Tallam, A. Rausell, M. Buttini, C. L. Linster, E. Medina, R. Balling and K. Hiller, *Proceedings of the National Academy of Sciences of the United States of America*, 2013, **110**, 7820-7825.
158. N. Reiling, S. Homolka, K. Walter, J. Brandenburg, L. Niwinski, M. Ernst, C. Herzmann, C. Lange, R. Diel, S. Ehlers and S. Niemann, *mBio*, 2013, **4**.
159. N. Reiling, A. Blumenthal, H. D. Flad, M. Ernst and S. Ehlers, *Journal of immunology (Baltimore, Md. : 1950)*, 2001, **167**, 3339-3345.